UNIVERSITÀ
DEGLI STUDI
DI PADOVA

UNIVERSITÀ DEGLI STUDI DI PADOVA

DIPARTIMENTO DI BIOLOGIA

SCUOLA DI DOTTORATO DI RICERCA IN BIOSCIENZE

Indirizzo: Biologia Evoluzionistica

Ciclo XXII

Tesi di Dottorato

NERVOUS SYSTEM DIFFERENTIATION IN THE COLONIAL ASCIDIAN *Botryllus schlosseri*: MOLECULAR AND CELLULAR ASPECTS AND EVOLUTIVE IMPLICATIONS

Direttore della Scuola: Ch.mo Prof. Tullio Pozzan

Coordinatore d'Indirizzo: Ch.mo Prof. Giorgio Casadoro

Supervisore: Ch.mo Prof. Paolo Burighel

Dottorando: Dott. Valentina Degasperi

1 Febbraio 2010

UNIVERSITÀ
DEGLI STUDI
DI PADOVA

Sede Amministrativa: Università degli Studi di Padova

Dipartimento di Biologia

SCUOLA DI DOTTORATO DI RICERCA IN BIOSCIENZE
INDIRIZZO: BIOLOGIA EVOLUZIONISTICA
CICLO XXII

NERVOUS SYSTEM DIFFERENTIATION IN THE COLONIAL ASCIDIAN *Botryllus schlosseri*: MOLECULAR AND CELLULAR ASPECTS AND EVOLUTIVE IMPLICATIONS

Direttore della Scuola: Ch.mo Prof. Tullio Pozzan
Coordinatore d'indirizzo: Ch.mo Prof. Giorgio Casadoro
Supervisore: Ch.mo Prof. Paolo Burighel

Dottorando: Dott. Valentina Degasperi

CONTENTS

ABSTRACT

In the last years, several studies are addressed to the investigation of mechanisms that permitted the appearance and evolution of those structures considered as extremely important in the vertebrates radiation. The rise of vertebrates was accompanied by the acquisition of a great complexity in the structural plan of the organisms that is related to the evolution of features associated with the nervous system, such as neural crests, cranial placodes and an elaborated brain.

The aim of the doctoral project is inserted in this line of research. Particularly, the attention is addressed to those characters, which in the non-vertebrate chordates can be interpreted as crucial for the subsequent evolution of the vertebrate body-plan. The starting point is represented by previous morphological studies that evidenced the presence, in the tunicate embryo, of transitory ectodermal and multipotential territories located at the neural plate border. Our research, carried out using different approaches, is focused on the characterisation and description of structures that differentiate from these domains. In this regard, it is investigated the organisation of the larval papillae and their formation from the rostral placode. These structures play a pivotal role in triggering the mechanisms and changes that characterise the metamorphosis, which in ascidians constitute the lost of the chordate body-plan of the larva and the begin of the sessile post-embryonic phase.

The analysis of the sensory components in ascidians, finalised to the identification of homologies with the structures that derive form the placodes in vertebrates, is also extended to the coronal organ. The coronal organ is recently discovered and possesses morphological, positional and ultrastructural features that, together with the presence of hair cells, are comparable to the lateral line and inner ear of vertebrates, which components derive from the acoustic-lateral placodes.

A substantial part of the work is dedicated to the investigation, with a molecular approach, of the presence of structures comparable to the neural placodes in ascidians. The attention is focused on the colonial ascidian *Botryllus schlosseri* that permits a comparative study on the mechanisms and genic networks involved in both embryogenetic and blastogenetic development. We characterised orthologues of placodal genes and constructed probes for *in situ* hybridisation experiments. During the stages of bud differentiation, we localised territories interested by expression of genes normally involved in the placodal induction and specification in vertebrates. These regions, for their position and differentiative potentialities, are comparable to other embryonic domains of *B. schlosseri* that are considered as homologues to the neural placodes.

The larva of ascidians possesses a striated symmetrical musculature sharing some features with that of vertebrates and it flanks the dorsal tube and the notochord, representing a peculiar propriety of chordates. The acquisition of this new locomotory system probably required the parallel appearance of a sophisticated control of the coordination. The nervous system established new interactions and differentiated sensory structures that permitted the rapid perception of the environment by the mobile organism. At metamorphosis, the larval musculature is reabsorbed, while the cardiac and unstriated muscle fibres differentiate *de novo* from circulating mesenchymal cells. This plasticity constitutes the source of the evolutive potentiality of ascidians and thus we investigate its molecular and morphological bases. We isolated and characterised transcripts coding for muscle-specific genes, analysing the expression during the blastogenetic cycle of *Botryllus*, from the bud appearance to the adult regression. The use of different methods allowed the description of the organisation and differentiation of the unstriated muscle, confirming its unique proprieties. Taking together, our results contribute to the understanding of the origin and development of structures that represent an important starting point in the evolution and radiation of vertebrates.

RIASSUNTO

Negli ultimi anni numerosi studi si sono rivolti all'approfondimento di quei meccanismi che hanno permesso la comparsa ed evoluzione di strutture ritenute di estrema importanza nella radiazione dei vertebrati. La comparsa dei vertebrati è stata accompagnata da un enorme balzo nella complessità del piano strutturale degli organismi, largamente ascrivibile all'evoluzione di strutture associate al sistema nervoso come le creste neurali, i placodi craniali ed un cervello elaborato.

La tematica trattata durante lo svolgimento del progetto di dottorato si inserisce in questa attuale linea di ricerca. In particolare, l'attenzione è stata rivolta a quei caratteri che nei cordati non-vertebrati possono essere letti come cruciali per la successiva evoluzione del piano strutturale dei vertebrati. Il punto di partenza è rappresentato da precedenti studi morfologici che hanno evidenziato la presenza, nell'embrione dei tunicati, di territori ectodermici transitori e multipotenti localizzati al confine con la piastra neurale. Il nostro studio, svolto mediante l'utilizzo di vari approcci metodologici, si è rivolto alla caratterizzazione e descrizione delle strutture che queste aree sono in grado di differenziare.

A questo proposito, è stata analizzata l'organizzazione delle papille larvali e la loro formazione a partire dal placode rostrale. Queste strutture giocano un ruolo primario nell'innescare i meccanismi e i cambiamenti che caratterizzano la metamorfosi, ovvero quel processo che nelle ascidie segna la perdita del piano corporeo da cordato della larva e il passaggio alla fase post-embrionale sessile. L'analisi riguardante strutture sensoriali presenti nelle ascidie, allo scopo di identificare eventuali omologie con le corrispondenti strutture derivanti dai placodi nei vertebrati, è stata poi estesa all'organo coronale. L'organo coronale è stato scoperto solo recentemente e presenta caratteristiche morfologiche generali, posizionali e ultrastrutturali tali, come la presenza di cellule capellute, che lo rendono comparabile alla linea laterale ed all'orecchio interno dei vertebrati, i cui componenti derivano dai placodi acustico-laterali.

Una parte consistente del lavoro è stata dedicata all'indagine, da un punto di vista molecolare, della presenza di strutture accomunabile ai placodi neurali nelle ascidie. L'attenzione è stata rivolta all'ascidia coloniale *Botryllus schlosseri*, che permette di svolgere uno studio comparativo sui meccanismi e reti geniche che intervengono sia durante lo sviluppo embriogenetico che blastogenetico. Abbiamo caratterizzato specifici geni e prodotto sonde utilizzate in esperimenti di ibridazione *in situ*. Durante le fasi di differenziamento della gemma sono stati individuati specifici territori caratterizzati da espressione di alcuni geni normalmente coinvolti nell'induzione e specificazione placodale nei vertebrati. Grazie alla loro posizione e potenzialità differenziativa, queste stesse regioni sono

apparse confrontabili con altri territori embrionali di *B. schlosseri* e di altre ascidie considerati omologhi a placodi neurali dei vertebrati.

La larva delle ascidie presenta una muscolatura simmetrica striata, con caratteri comuni a quella dei vertebrati, la quale fiancheggia il tubo dorsale e la notocorda e che rappresenta una proprietà peculiare dei cordati. L'acquisizione di questo nuovo sistema locomotorio ha verosimilmente richiesto la comparsa parallela di un sofisticato sistema di controllo della coordinazione. Il sistema nervoso ha stabilito nuove interazioni e differenziato strutture sensoriali che hanno permesso all'organismo mobile la rapida percezione dell'ambiente circostante. Alla metamorfosi, la muscolatura larvale viene completamente riassorbita, mentre le fibre muscolari non striate della parete del corpo e quelle cardiache si differenziano *de novo* da cellule mesenchimali circolanti. Questa plasticità sta alla base della potenzialità evolutiva delle ascidie e quindi ne abbiamo indagato le basi molecolari e morfologiche. Abbiamo quindi isolato e caratterizzato trascritti e geni muscolo-specifici, studiandone l'espressione durante il ciclo blastogenetico di *Botryllus*, dalla comparsa della gemma alla regressione dell'adulto. L'utilizzo di vari approcci ha permesso la descrizione dell'organizzazione e differenziamento della muscolatura non striata, confermandone le caratteristiche uniche. Nel complesso i diversi risultati rappresentano contributi significativi per la conoscenza delle origini e sviluppo quelle strutture che hanno rappresentato un punto di partenza importante nell'evoluzione e radiazione dei vertebrati.

INTRODUCTION

1. Chordates and the vertebrate innovations

Deuterostomes comprise five major clades: vertebrates, tunicates, cephalochordates, echinoderms and hemichordates. Typically, these organisms are characterised by a similar embryogenesis during which the blastopore becomes the anus (Chea *et al*., 2005). Because the group comprises also the vertebrates, the study of their invertebrate ancestor could help to better understand the development and evolution of structures that permitted the vertebrate radiation. At this regard, the extension of the genome sequencing projects to many non-model organisms allowed the improvement of the molecular phylogenetic analyses. Recent studies, that conjugated molecular methods with paleontological data, changed the historical vision and placed the tunicates as sister group of vertebrates (Delsuc *et al*., 2008; Swalla and Smith, 2008). These analyses bypassed the problems linked to the morphological-based phylogenesis, where the starting point is to identify and exclude the characters deriving from convergent evolution. The sequences comparison brought together the molecular and morphological features, allowing to follow the morphological innovations in parallel with the gene loss/acquisition pattern, in order to recognise the molecular bases underlying the development and evolution of the chordate body plan (Cañestro *et al.*, 2007). The common features shared by all the chordates comprise a dorsal and tubular nervous system, located above an axial notochord flanked by symmetrical musculature, endostyle and slit pharynx (Berrill, 1955; Katz, 1983, Satoh, 1994; 2003). Differently from vertebrates, tunicates possess a compact and simple genome: for example, the *Ciona intestinalis* haploid genome is formed by ~155 Mbp and contains 15852 protein-coding genes (Dehal *et al*., 2002). Of these, only a small set is essential for the chordate body plan establishment, so it makes easier to reconstruct the situation of the vertebrate ancestor, before the genome duplication events (Holland *et al*., 1994).

The rise of vertebrates is characterised by the appearance of motile organisms with a remarkable complexity of structures, a large part of which is ascribed to features shared by all chordates. These modifications are largely due to the evolution and development of structures associated to the nervous system, in particular the neural crests, placodes, an elaborated segmented brain, but also the skeleton and acquisition of new genes (Shimeld and Holland, 2000). Nervous systems of non-chordate metazoans is characterised by series of ganglia, a ventral nerve cord or a diffuse nerve net. As described above, chordates display an inverted pattern, where a dorsal nerve cord is associated with a notochord. On the origin of neural tube in chordates two main theories have been proposed, both

based on the derivation of chordates from organisms with direct development. The first scenario predicts that the central nervous system arose by the rolling up and coalescence of a hemichordate epidermal nerve net. The alternative and more likely hypothesis explains the neural tube origin from the ciliary bands of an echinoderm dipleura-like larva (see Hall, 2009).

In cephalochordates, the most basal group of chordates, the nervous system displays some homologous features with vertebrate rostral nervous system (brain), including an anterior expanded portion, presence of an eye spot, homologs of vertebrate sensory organs and expression of gene that specify the position of the neural plate border and midbrain-hindbrain (MHB) boundary. However, it lacks most placodes, neural crests (but possesses genes and regulatory pathways associated with both) and MHB organiser, even if displays ectodermal sensory neurons proposed as homologues to adenohypopyseal and olfactory placodes (Holland, 2009). Thus, amphioxus could represent the basal organisation from which these structures subsequently evolved. In contrast to the other chordates, tunicates are considered organisms subjected to rapid evolution and it can be difficult to distinguish between characters derived from a common ancestor or by convergent evolution. The ascidian larval central nervous system (CNS) is composed of 330 cells and subdivided in three parts: tubular nerve chord, visceral ganglion with motoneurons innervating the tail and a hollow anterior vesicle (Katz, 1983; Nicol and Meinertzhagen, 1991). Vertebrates and ascidians shared many processes in the CNS formation, consistent with a prevertebrate origin of neural induction, such as duplicated *Hox* genes regulated by retinoic acid, expression of *Brachyury* under the regulation of elements related to the vertebrate Notch pathway, expression of *Pax2/5/8* in a region homologous to MHB organiser and transcription factors in a region equivalent to the vertebrate hindbrain (Hall, 2009).

The interest in understanding the evolution and developmental mechanisms of these structures lies in the fact that they can differentiate tissues and cells that represent crucial steps of the vertebrate evolution. Neural crests are a population of cells delaminating from the neural plate and neural folds border, when the two rims become in contact and fuse. Subsequently, these cells migrate into head and trunk and differentiate into multiple cell types, such as sensory neurons, pigment cells, smooth muscle and connective cells, odontoblasts, cartilage- and bone producing cells that largely generate the vertebrate skull (Meulemans and Bronner-Fraser, 2004; Morales *et al*., 2005). The presence of neural crests in ascidians is debated. In *C. intestinalis*, cells of the trunk lateral mesenchyme, migrating into the oral siphon primordium and expressing markers such as *FoxD*, *Ap2*, *twist*-like genes, *c-myc*, *cadherin-2* and *rhoABC* are suggested as homologous to the neural crests (Jeffery *et al*., 2008). Although none of these genes are an exclusive marker for this cell type, the domain of their expression in

non-vertebrate chordates could help in specifying possible regions of neural complex precursors in the common ancestor. However, in *Ecteinascidia turbinata* presumptive homologues to the neural crests differentiate in migrating pigment cells (Jeffery *et al*., 2004). It was proposed that the ancestral neural crests acted as "proto-neural crest" with different functions in respect to those of vertebrates, co-opting genes and pathways from various tissues (Hall, 2009). The cranial placodes are specialised regions of the ectoderm localised at the neural plate border that give rise to cranial sense organs and represent a fundamental source of neural tissue, such as the central ganglia of the cranial nerves, but also the lateral line, neuromasts and mechanosensory system. Initially it was proposed that neural placodes possess a common evolutionary origin with the neural crests (Northcutt and Gans, 1983; Baker and Bronner-Fraser, 1997). Now, developmental studies revealed that, on a molecular point of view, placodes and neural crests are induced during a different time windows and under the influence of different signals. According with this, placodes develop as specialisation of the non-neural ectoderm and neural crests of neural ectoderm. These conclusions open the possibility of an independent evolutionary origin of both structures, where the neural plate border acted as region of potential innovation during the chordate evolution (Schlosser, 2008). In tunicates, some vertebrate placodal genes are expressed in the non-neural component of the neural plate border plus other ectodermal domains. These regions can differentiate sensory cells and, bringing together the morphological and molecular data, some authors proposed that tunicates could possess homologues to the vertebrate olfactory, adenohypophyseal, otic and lateral line placodes (Manni *et al*., 2004; Bassham and Postlethwait, 2005; Mazet *et al*., 2005). The noteworthy potential contained in both placodes and neural crests to differentiate a broad spectrum of structures can represent the starting point of the vertebrate evolution, permitting the arise of organs and cells that triggered the jump from filter-feeding to active organisms (Northcutt and Gans, 1983).

The expression of vertebrate placodal genes has been first studied in the solitary ascidian *C. intestinalis* where, during embryogenesis, they identified two domains, anterior and posterior to the brain, respectively (Mazet *et al*., 2005). Moreover, morphological studies extended to other ascidian species revealed that in the embryo four ectodermal territories are recognisable and capable to differ non-epidermal cells, throughout movement recalling the steps of placodal differentiation (Manni *et al*., 2004). The transitory thickenings include the atrial rudiments (atrial placodes), rostral epidermis (rostral placode), stomodeum (stomodeal placode) and neurohypophysial duct (neurohypophysial placode) (Manni and Burighel, 2006).

1.1. Neural placodes in ascidians

Our work is focused on the development and organisation of structures deriving from the transitory thickenings proposed as homologues to vertebrate placodes in the colonial ascidian *Botryllus schlosseri*. The study is also extended to other species, in order to contribute in the understanding the evolution of these ectodermal regions that represent a fundamental starting point for the achievement of vertebrate complexity.

Larval papillae. A first paper is centred on the origin and differentiation of the rostral papillae in the *B. schlosseri* (see contribution A in the present thesis, Caicci *et al*., 2010a). These structures play a pivotal role during the metamorphosis and derive from a thickening located in the anterior epidermis comparable, as organisation and fate, to vertebrate placodes. In particular, we examined the papillae differentiation in embryo and larva using a multi-level approach that includes confocal microscopy, *in vivo* observations and electron microscopy.

Papillae represent a key element in the spatio-temporal determination of metamorphosis onset, phenomenon that in ascidians marks the end of the free-swimming planktonic phase, the passage to the sessile life and the loss of the chordate body plan. We described the appearance, differentiation and regression of papillae during the larval development, the settlement on an adequate substrate and the metamorphic changes. Two principal types of sensory cells are recognisable: primary sensory neurons (papillary neurons) flanked by parietal cells and RTENs (Rostral Trunk Epidermal Neurons), that are distributed through the entire rostral epidermis and especially at the base of papillae. Their function is not yet well known and both molecular and physiological data are lacking. We propose, on ultrastructural characteristics, position and developmental changes, that the papillary neurons are capable to respond to mechanical stimuli, while the RTENs act as chemoceptors. Moreover, these cells differentiate from a thickening of the rostral epidermis (rostral placode), region that displays features comparable to the vertebrate olfactory placode and appears to possess, as the other ectodermal domains, a great multipotency.

Coronal organ. Tunicates are filter-feeding organisms with a sac-like body, provided with an oral and an atrial siphon. As described above, the siphons derive from thickened epidermal areas denominated as stomodeal and atrial placodes. Within the oral siphon, recent morphological studies revealed the presence of a coronal organ that shares morphological and positional features with the hair cells and the vertebrate lateral line, which derive from the acustico-lateralis placodes (Bone *et al*., 1995; Burighel *et al*., 2003). The coronal organ is located on the

velum, an epithelial evagination at the base of siphon, and is constituted of ciliated cells to form a row running both on the velum and on the border of each tentacle exposed to the entering water flow. These receptors are secondary sensory cells and neurophysiological studies evidenced their mechanoceptorial function. We addressed the study of the coronal organ also on a comparative level (see contribution B, Burighel *et al*., 2008 and contribution C, Caicci *et al*., 2010b), to investigate its presence and organisation in a number of ascidian species. The results showed that the coronal cells display some basic similarities in all the species and thus they can be considered as plesiomorphic features for ascidians. Other characteristics can vary between the orders: for example, the ascidians belonging to the Enterogona possess multiciliate coronal cells whereas the Pleurogona have cells with one or two cilia flanked by microvilli or stereovilli. This led to hypothesise that the diversity may represent the consequence of the long parallel evolution of the two orders and the appearance of different ability for the water flow monitoring.

Placodal genes expression during the blastogenesis. A relevant chapter of the research program is dedicated to investigate the presence of neural placodes in ascidians by isolating and characterising the expression pattern of orthologues to genes belonging to the genic network involved in the induction and specification of these structures (see contribution D, Degasperi *et al*., 2010). Previous papers have well characterised the development and differentiation of these multipotential ectodermal thickening during the embryogenesis of both the solitary ascidian *C. intestinalis* and the colonial *B. schlosseri* (Manni *et al*., 2004; Manni *et al*., 2005) and a first molecular study was conducted during the *C. intestinalis* embryogenesis (Mazet *et al.*, 2005). We chose to extend this type of analysis to *B. schlosseri*, an ascidian species that has the peculiarity to possess both sexual and asexual reproduction. The colonial propagation occurs through blastogenesis, with the formation of a double-walled vesicle that evaginates from the atrial chamber. Three synchronised generations co-exist in a colony, the filter-feeding adult, primary and secondary bud (Manni *et al*., 2007; contribution E, Degasperi *et al*., 2009 and contribution D, Degasperi *et al*., 2010). Thus, bud and embryo develop following different steps, as a consequence of the completely different starting point, that is the zygote in the embryogenesis and a somatic-derived vesicle in blastogenesis. Despite this, it common morphogenetic processes can be recognised in the two pathways and also for those structures that during development derive from thickened areas resembling the vertebrate placodes. Thus, *B. schlosseri* offers the opportunity to extend the analysis to the blastogenesis, in order to identify, in addition to overlapped morphologic steps of differentiation, if there is co-optation of gene networks.

We examined the expression of the vertebrate placodal genes *Six1/2*, *Six3/6*,

Eya and *FoxI* during the blastogenetic cycle of *B. schlosseri*. Sequences coding for these genes were isolated and characterised and then used to construct antisense probes for *in situ* hybridisation (ISH) experiments on bud sections of each differentiation stage. We observed that each transcript recognises structures and cells that are not only in active differentiation, but also subjected to morphological changes as evagination/invagination and delamination. The regions involved by the expression of these genes are comparable with the data obtained in *Ciona* embryo and larva. *Six1/2* and *Eya* display a pan-placodal domain in vertebrates and also in *Ciona* they marked the two anterior ectodermal regions. In buds, these genes are expressed in the primordium of both siphons and the peribranchial epithelium during their differentiation, regions that during embryogenesis derive respectively from the two placodal-like areas. *Six3/6* marks the oral siphon and neural complex of the primary bud, showing a profile partially overlapped to *Pitx* and in line with its expression limited to the adenohypophyseal and olfactory placodes. *FoxI* expression appears early during the bud formation, when it begins to evaginate from the parental wall. In the later stages, the transcript is confined to the differentiating peribranchial epithelium, until the stigmata formation. These regions derive from the posterior embryo thickening that invaginates to form the atrial primordium, for which a homology with the otic placode, which expresses *FoxI* in vertebrates.

We interpreted our results in the light of expression of vertebrate placodal genes during the blastogenesis, in tissues and cells involved in active differentiation. Moreover, this analysis is discussed in reference to the recent findings on the evolution and development of structures considered the starting point that triggered the vertebrate radiation, such as the placodes and neural crests.

1.2. Plasticity of tunicate muscles and evolutive considerations

The appearance of symmetrical striated musculature flanking the notochord and the neural tube was a key event in the chordate evolution. Classically, the larval stage represents a dispersive moment of fundamental importance for the sessile organisms. The acquisition of a locomotion system not based on ciliary beating (*e.g.* as occurs in the planktonic larva of echinoderms) permitted to increase the mobility potential that strictly correlate with the feeding ability, the possibility to escape from predators, the research of an adequate substrate for the metamorphosis and finally, as consequence, the improving of the total life-span.

The muscle coordination requires a complex control apparatus, implying a parallel evolution of the peripheral nervous system. It has been proposed that with the emergence of the muscle-based locomotion, the dorsal nerve acquired the control, freeing the epidermal nerve cells for other functions (Hall, 2009). The

dorsal nerve, or neural tube, increases the complexity establishing new interactions and differentiating a sensorial apparatus to perceive the surrounding environment. Ascidian larval musculature is striated and resembles the vertebrate sarcomeric muscle, even if it differs for some features (Ceresa Castellani *et al*., 1972; Schiaffino *et al*., 1974; 1976). During the metamorphosis, there are radical changes in the internal organisation: the larval muscles are reabsorbed and begin to differentiate two muscle types, cardiac and unstriated fibres that constitute the body-wall musculature. The latter possesses intermediate characteristics with the striated muscle of vertebrates, such as multinucleated cells, contractions regulated by the troponin/tropomyosin system and other both morphologic and physiologic aspects (Toyota *et al*., 1979; Endo and Obinata, 1981; Shinohara and Konishi, 1982; Nevitt and Gilly, 1986; Terakado and Obinata, 1987; Meedel and Hastings, 1993). This great muscular plasticity permitted tunicates to reach various adaptive motory solutions: doliolids and salps show unusual muscle fibres enveloping their body and in particular the doliolids possess obliquely striated muscles that permit extremely rapid movements (Bone and Ryan, 1974). The differences in muscle types are based on modifications regarding a variety of molecular and morpho-physiological aspects that required a parallel reorganisation of the nervous system and merit to be investigated.

Our aim is to extend the study of those structures playing a pivotal role in the chordates evolution. As described above, we have focused the attention on ectodermal territories displaying a strictly relation with the vertebrate placodes which, in association with the neural crests, are proposed as key features that permitted the vertebrate radiation. In consideration of the great adaptive potentiality of the musculature for larval and adult movement of tunicates, we planned to characterise its organisation, molecular expression of some main muscular genes involved in muscle differentiation and its relationships with evolution of nervous system.

Muscle differentiation. Previous both molecular and morphological studies were addressed on the larval musculature of solitary ascidians. We chose to investigate the organisation and differentiation of the unstriated muscle during the blastogenetic cycle of the colonial ascidian *B. schlosseri* (see contribution E, Degasperi *et al*., 2009). Moreover, we followed gene expression of muscle actin and troponin T in the larva and during the development of blastozooids, beginning from the early bud stage to adult and regression stage. We isolated and characterised two transcripts from colonies that resulted homologous to muscle genes of solitary ascidians. Phylogenetic analyses performed with the deduced amino acid sequences showed a close relationship between urochordates and vertebrates muscle genes. The genomic sequences were compared in the exon-intron organisation with other muscle and cytoplasmic–type actin genes of both

invertebrates and vertebrates. Our data revealed that intron positions are conserved in ascidians and in the other deuterostomes.

We detected the expression of the two genes by *in situ* hybridisation on section (ISH) throughout the blastogenetic cycle of *B. schlosseri*. Thus, all the phases of muscle development and regression were documented by an integrated study showing the close correspondence of *in situ* expression of *BsMA2* and *BsTnT-c*, phalloidin signal and ultrastructure.

RESULTS

In the following pages, the lines of the above presented work are illustrated in detail, referring to previous literature, experimental plan and results, as appeared in international journals or in manuscript prepared for the submission to journal.

In order, the subsequent articles are presented:

Larval papillae

- Contribution A:

Caicci F., Zaniolo G., Burighel P., **Degasperi V.**, Gasparini F., Manni L. 2010a. Differentiation of papillae and rostral sensory neurons in the larva of the ascidian *Botryllus schlosseri* (Tunicata). *J. Comp. Neurol.* 518: 547-566.

Coronal organ

- Contribution B:

Burighel P., Caicci F., Zaniolo G.,Gasparini F., **Degasperi V.**, Manni L. 2008. Does hair cell differentiation predate the vertebrate appearance? *Brain Res. Bull.* 75: 331-334.

- Contribution C:

Caicci F., **Degasperi V.**, Gasparini F., Zaniolo G., Del Favero M., Burighel P., Manni L. 2010b. Variabilty of hair cells in the coronal organ of ascidians (Chordata, Tunicata). *Can. J. Zool.* Submitted.

Placodal genes expression during the blastogenesis

- Contribution D:

Degasperi V., Shimeld S.M., Gasparini F., Burighel P., Manni L. 2010. Expression analysis of placodal genes during the blastogenetic cycle of the colonial ascidian *Botryllus schlosseri*. In preparation.

Muscle differentiation

- Contribution E:

Degasperi V., Gasparini F., Shimeld S.M., Sinigaglia C., Burighel P., Manni L. 2009. Muscle differentiation in a colonial ascidian: organisation, gene expression and evolutionary considerations. *BMC Dev. Biol.* 9: 48.

CONTRIBUTION A

Caicci F., Zaniolo G., Burighel P., Degasperi V., Gasparini F., Manni L. 2010a

Differentiation of papillae and rostral sensory neurons in the larva of the ascidian *Botryllus schlosseri* (Tunicata)

J. Comp. Neurol. 518: 547-566

Differentiation of Papillae and Rostral Sensory Neurons in the Larva of the Ascidian *Botryllus schlosseri* (Tunicata)

Federico Caicci, Giovanna Zaniolo, Paolo Burighel, Valentina Degasperi, Fabio Gasparini,* and Lucia Manni
Dipartimento di Biologia, Università degli Studi di Padova, I-35121 Padova, Italy

ABSTRACT

During the metamorphosis of tunicate ascidians, the swimming larva uses its three anterior papillae to detect the substrate for settlement, reabsorbs its chordate-like tail, and becomes a sessile oozooid. In view of the crucial role played by the anterior structures and their nerve relations, we applied electron microscopy and immunocytochemistry to study the larva of the colonial ascidian *Botryllus schlosseri*, following differentiation of the anterior epidermis during late embryogenesis, the larval stage, and the onset of metamorphosis. Rudiments of the papillae appear in the early tail-bud stage as ectodermic protrusions, the apexes of which differentiate into central and peripheral bipolar neurons. Axons fasciculate into two nerves direct to the brain. Distally, the long, rod-like dendritic terminations extend during the larval stage, becoming exposed to sea water. After the larva selects and adheres to the substrate, these neurons retract and regress. Adjacent to the papillae, other scattered neurons insinuate dendrites into the tunic and form the net of rostral trunk epidermal neurons (RTENs) which fasciculate together with the papillary neurons. Our data indicate that the papillae are simple and coniform, the papillary neurons are mechanoreceptors, and the RTENs are chemoreceptors. The interpapillary epidermal area, by means of an apocrine secretion, provides sticky material for temporary adhesion of the larva to the substrate. J. Comp. Neurol. 518:547–566, 2010.

INDEXING TERMS: metamorphosis; palps; neurogenic placodes; peripheral nervous system; sensory cells; Urochordata

Metamorphosis generally refers to a postembryonic developmental stage characterized by intense changes at morphological, biochemical, and ecological levels (Bishop et al., 2006). It concerns most metazoan phyla and, in particular, all the subphyla of the Chordata (cephalochordates, tunicates, and vertebrates), although with striking diversity. For example, in amphibians, metamorphosis transforms a swimming fish-like larva into a tetrapod, whereas in tunicate ascidians, the tadpole-like swimming larva is transformed into a sessile individual. Ascidian metamorphosis arouses much developmental and ecological interest, because it involves dramatic body remodeling, with loss of the larval chordate-like *Bauplan* and the formation of a "sac-like" organism while, at the same time, settlement arrests the dispersal phase of the life cycle. Thus, both developmental and evolutionary biologists are interested in knowing which mechanisms regulate metamorphosis in these nonvertebrate chordates, which are now considered the sister group of vertebrates (Delsuc et al., 2008). Unlike amphibians, events regulating metamorphosis in ascidians are largely unknown, although the main metamorphic changes have been described for some species (Cloney, 1978; Cloney and Torrence, 1984; Burighel and Cloney, 1997) and a number of factors are known to influence them (Nakayama-Ishimura et al., 2009).

Metamorphosis involves participation of the anterior area of the ascidian larva, which contains special sensory structures (the papillae, or palps), used for exploring and/or adhering to the substrate; a net of sensory rostral trunk epidermal neurons (RTENs) has also been indentified in some species (Takamura, 1998), also by green fluorescent protein (Imai and Meinerthagen, 2007). When the larva contacts the substrate, by means of a series of rapid touches, papillae projecting from the anterior epidermis probably act as a control center for the initiation of metamorphosis. Recent molecular reports on ascidian meta-

Grant sponsor: Ministero della Università e Ricerca Scientifica e Tecnologica (to L.M. and P.B.); Grant sponsor: Università di Padova (to L.M. and P.B.).

*CORRESPONDENCE TO: Fabio Gasparini, Dipartimento di Biologia, Università degli Studi di Padova, Via U. Bassi 58/B, I-35121 Padova, Italy. E-mail: fabio.gasparini@unipd.it

Received 14 June 2009; Revised 14 August 2009; 2 September 2009
DOI 10.1002/cne.22222
Published online September 16, 2009 in Wiley InterScience (www.interscience.wiley.com).

morphosis indicate that: 1) a diffusing epidermal growth factor (EGF)-like protein called Hemps, located in the papillae and anterior epidermis of the *Herdmania curvata* larva, may act as an inducer for metamorphosis (Eri et al., 1999); 2) various genes, some of them expressed in the papillae, which are up- and downregulated during metamorphosis, can be identified in *Ciona intestinalis* (Nakayama et al, 2001., 2002); 3) the characteristics of the bacterial biofilm may induce settlement of *Boltenia villosa* larvae (Zeng et al., 2006; Roberts et al., 2007); 4) several neurotransmitters can be recognized in papillary neurons, such as serotonine, dopamine (Pennati et al., 2001, 2007; Zega et al., 2005), acetylcholine, glutamate, γ-aminobutyric acid (GABA) (Coniglio et al., 1998; Horie et al., 2008; Zega et al., 2008), adrenaline, and noradrenaline (Kimura et al., 2003), and some of them are considered capable of inducing or modulating metamorphic events; and 5) studies of *C. intestinalis* metamorphosis, by using larvae with their papillae removed and analysis of mutants (Nakayama-Ishimura et al., 2009), also suggest that papilla-cut larvae cannot initiate a series of metamorphic events. All these studies support the importance of papillae and the anterior larval epidermis in triggering the events of metamorphosis.

Papillae and RTENs form from a thickened ectodermal area, called the rostral placode, due to its embryological origin and the ability to form sensory structures (Manni et al., 2004). The idea of neurogenic placodes in ascidians is of evolutionary interest, because it bypasses the classic concept that neural crests and placodes are exclusive to vertebrates (Northcutt and Gans, 1983) and stimulates study of the origin and extension of these derivatives in basal chordates.

The morphology of papillae has been studied in a number of swimming larvae. Ascidian larvae commonly bear three papillae in a typical triangular arrangement, with the morphology varying among species. Two main types are distinguished (Burighel and Cloney, 1997): not eversible and eversible papillae. The former, typical of solitary and a few colonial species (such as *Botryllus schlosseri*), are simple and conic; the latter, typical of colonial species, are complex and capable of rapid eversion, to expose sticky mucus (Cloney, 1977, 1979). The adhesive papillae often contain elongated secreting cells and sensory neurons, the axons of which form the papillary nerves that fasciculate with axons of RTENs and terminate in the central nervous system (Burighel and Cloney, 1997; Takamura, 1998; Imai and Meinertzhagen, 2007). At the moment, there is no unequivocal evidence about the nature of neurons, which were once considered mechanoreceptors or chemoreceptors (Burighel and Cloney, 1997; Hinman and Degnan, 1998; Groppelli et al., 2003).

Although the ultrastructure of papillae has been described in a number of swimming larvae, the cytodifferentiation and complete cycle of changes undergone by the papillary cells has not yet been examined in detail. We therefore approached this problem in *Botryllus schlosseri* larvae by studying the characteristics and developmental changes of the anterior ectoderm.

Grave (1934) and Grave and Riley (1935) described the papillae in this species as "ganglionated," because sensory cells sink below the epidermis to form a sort of "papillary ganglion," while maintaining relationships and tight junctions with epidermic cells (Torrence, 1983). Apically, the sensory cells develop specializations, called *receptor end-organs*, emerging from the tips of papillae and extending into the tunic. In the absence of glandular cells, Grave (1934) argued that a "holdfast mechanism" involves the whole papillary area: the concavity between three papillae acts as a sucker, in which a partial vacuum is created when the anterior area is pressed against a smooth surface. The mechanism for temporary attachment has not been re-examined in this species but, in the closely related *Botryl-loides leachi*, a glandular organ, formed of secreting cells clustering in the interpapillary area, has been presumed to attach the larva to the substrate by means of adhesive secretion (Pennati et al., 2007). Thus, it should be of interest to verify whether two closely related species use two different systems to attach their larva to the substrate.

In this work, by means of in vivo observations, serial section reconstructions, and transmission electron and confocal microscopy, we examined the development of the anterior ectoderm of *B. schlosseri* larvae, in order to clarify the differentiation and nature of RTEN and papillary sensory cells, the dynamic formation and fate of both the "papillary ganglia" and the interpapillary area, and their involvement in the selection of substrate and mechanism of settlement at the onset of metamorphosis.

MATERIALS AND METHODS

Colonies of *Botryllus schlosseri* are composed of a large number of small blastozooids embedded in a common thin tunic and arranged in star-shaped systems. They were cultured on glass in the laboratory at 18°C following Sabbadin's (1955) technique. They have internal fertilization and are ovoviviparous. The transparency of the colonies allowed us to follow the daily in vivo development of embryos under the stereomicroscope and select them at appropriate stages. Larvae develop in a week and, after a short period of swimming life, undergo metamorphosis, giving rise to sessile oozooids, which reproduce asexually by budding. After some blastogenetic generations, the blastozooids reach maturity and can reproduce sexually, producing new larvae. Embryos were dissected from their parents with a thin tungsten needle; free swimming and

metamorphosing larvae were directly pipetted into the fixative liquid.

Definition of the developmental phases of the embryo was based on correlations between the developmental stage of the colony and embryogenesis and on gross anatomical features (Manni et al., 2007). As the embryos possess a tail, which grows below the follicle cells and encircles the trunk 1.5 times at its maximum extension, we defined embryos with tails making a three-quarter turn around the trunk (about 3 days before hatching) as *early tail-bud* embryos, ones with tails making one whole turn around the trunk (about 2 days before hatching) as *mid-tail-bud* embryos, and those with tails making 1.5 turns around the trunk (about 1 day before hatching) as *late tail-bud* embryos. Embryonic development occurs in the atrial chamber of the adult during the period of filtering activity and, at a temperature of 18°C, takes about 5 days. The mature larva is released from the colony through the cloacal siphon, just before the parent closes its siphons and contracts, beginning its regression. The larva swims freely in the water (swimming larva phase), showing positive, indifferent, and negative responses to light in sequence (Grave and Woodbridge, 1924). After a variable period (on average 2 hours), it begins to touch the substrate repeatedly (late swimming phase), until it attaches itself permanently to the substrate and begins to metamorphose.

Whole-mount preparations

Larvae at various stages were anesthetized with 0.02 % MS222, fixed in 4% paraformaldehyde in 0.1 M phosphate-buffered saline (PBS), pH 7.6, for 1–3 hours, washed in 50% ethyl alcohol, rehydrated, and stained with Mayer's hematoxylin. After washing in distilled water, they were dehydrated in alcohol and mounted in balsam.

Light and transmission electron microscopy

Embryos and larvae were fixed in 1.5% glutaraldehyde buffered with 0.2 M sodium cacodylate, pH 7.4, plus 1.6 % NaCl. After washing in buffer and postfixation in 1% OsO_4 in 0.2 M cacodylate buffer, specimens were dehydrated and embedded in Epon Araldite. Sagittal serial sections (1 μm) were counterstained with toluidine blue; thin sections (90 nm) were given contrast by staining with uranyl acetate and lead citrate. Micrographs were taken with a Hitachi H-600 electron microscope operating at 75 kV. All photos were acquired with an Epson Perfections Scanner 1200S and were collected and typeset in Corel Draw X3.

Scanning electron microscopy

Larvae were fixed as described for transmission electron microscopy. After dehydration, they were critical-point-dried, sputter-coated with gold-palladium, and observed under a Cambridge Stereoscan 260. All photos were acquired with a Duoscan (Agfa), with adjusted levels, and were collected and formatted in Corel Draw X3.

Confocal microscopy

Specimens were anesthetized with 0.02 % MS222 at 4°C and fixed in 4% paraformaldehyde in 0.1 M PBS, pH 7.6, for 1–3 hours, washed in buffer solution, and placed in NH_4Cl 50 mM for 3 hours, and then in Triton X 0.5 in 0.1% sodium citrate overnight.

Specimens were then incubated again overnight with monoclonal mouse anti α-tubulin primary antibodies (a mouse IgG1 isotype produced with purified chick tubulin that recognizes an epitope located at the C-terminal end of the α-tubulin isoform [amino acids 426 – 430] and reactive against chicken, human, bovine, rat, mouse, amphibian, yeast, and fungi; Sigma, St. Louis, MO, T6199) and then with goat anti-mouse IgG H&L chain-specific fluorescein-conjugated secondary antibodies (Calbiochem, San Diego, CA, 401234). After rinsing with PBS, specimens were mounted in glycerol and observed under a Bio-Rad (Hercules, CA) Radiance 2000 confocal system, mounted on a Nikon Eclipse 600 microscope.

RESULTS

We followed the development of the sensory rostral structures in the embryo, and their modifications in the swimming larval phase and at onset of metamorphosis in *Botryllus schlosseri*. In vivo observations also allowed us to compare changes in the behavior of larvae and to select specific stages for ultrastructural study.

The swimming larva (Fig. 1A) is normally about 1.2 mm long, with an oval trunk about 0.4 mm long. Its trunk (or cephalenteron) contains both larval (transitory) and prospective juvenile (oozooid) organs. Its general organization has been reported previously (Manni et al., 1999) and is shown in Figure 1A and B. The anterior region of the larva—the area of main interest for this investigation—contains the ring of eight epidermal vascular ampullae and, most anteriorly, the three apical sensory papillae. A wide blood lacuna extends between these rostral epidermal structures and the anterior endodermal wall of the pharynx. The latter is asymmetrically deformed, due to the presence of the visceral ganglion and the large sensory vesicle emerging on the right of the ganglion itself and containing the pigmented photolith (Fig. 1A), which, in contrast to other ascidians, combines the ocellus and otolith functions (Sorrentino et al., 2000). The entire larval body is enveloped by the outer cuticular layer and the outer compartment of the tunic, which constitute the larval fin and are lost at metamorphosis. In addition, the trunk region is enveloped by two layers, the inner cuticle and inner compartment of the

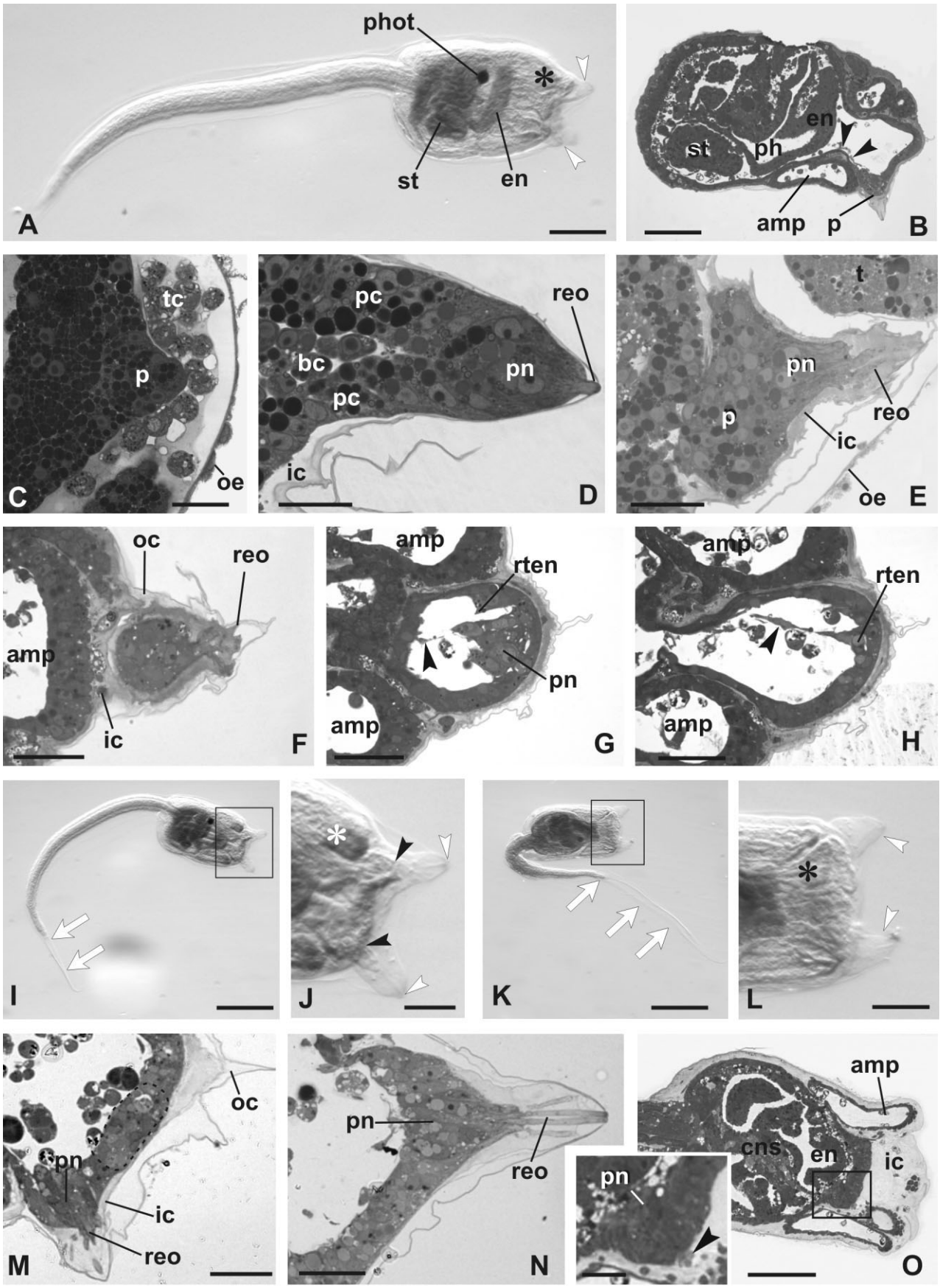
phot
st
en
A
en
st
ph
amp
p
B
tc
p
oe
C
pc
reo
bc
pn
pc
ic
D
t
pn
p
reo
ic
oe
E
oc
reo
amp
ic
F
amp
rten
pn
amp
G
amp
rten
amp
H
I
J
K
L
oc
pn
ic
reo
M
pn
reo
N
amp
cns
en
ic
pn
O

Figure 1

tunic, representing the definitive tunic of the adult; the inner cuticle displays a great number of small protrusions (Milanesi et al., 1978) (here called "micropapillae," to avoid confusion with the sensory papillae). The micropapillae are absent in the tunic area defined by the papillae. The inner compartment is populated by tunic cells, derived from blood cells in the hemocoel (Burighel and Cloney, 1997).

The general anatomy of embryos at these stages has been reported previously (Manni et al., 1999). The early tail-bud stage concerns embryos with a spherical trunk, in which all the rudiments of organs are visible, particularly the sensory papillae, the pharynx, with its wings laterally extended toward the atrial chamber, the visceral ganglion, and the sensory vesicle with the first granules of pigment deposited in the photolith. In the following stages, the rudimentary organs progressively acquire their definitive shape, while the tail grows, encircling the trunk. Younger embryos have been studied at the histological level, but their anatomy is not considered here, because the papillary rudiments cannot be identified.

Embryonic development and regression of papillae

The sequence of events characterizing papillary development is shown in Figure 1 and is summarized as follows: in the early tail-bud embryo, the rudiments of sensory papillae are visible as three simple, epidermal protrusions (two dorsal and one ventral, arranged at the vertexes of an equilateral triangle), in continuity with the trunk epidermis (Fig. 1C). The papillae are composed of a layer of columnar cells, with nuclei in the apical region, and rich in yolk granules. There is a remarkable concentration of tunic cells in the perivitelline space close to the papillae.

In the mid-tail-bud embryo, the papillae extend, becoming digitiform, and the papillary hemocoel becomes occupied by blood cells (Fig. 1D). We distinguished two kinds of papillary cells: apical, which are primary sensory neurons (papillary neurons) characterized by a few small yolk granules, and parietal, which are typical epidermal cells very rich in yolk. The papillary apexes are pointed, due to the extension of cytoplasmic dendritic protrusions from sensory neurons; they extend for a short distance into the tunic as *receptor end-organs* (Grave and Riley, 1935). Proximally, thin axons emerging from basal regions of papillary neurons can be seen. The latter are therefore bipolar.

In the late tail-bud embryo, the papillae are more extended and dome-shaped; they are often bent to one side, being compressed by the tail and egg envelopes (Fig. 1E). The receptor end-organs are very extended and lie in the inner tunic compartment, which forms a cupola. The papillary neurons, although maintaining their dendritic apex extending into the tunic, now sink their basal portion into the papillary hemocoel, forming the "papillary ganglion" of Grave and Riley (1935) and Torrence (1983). The axon extends from the basal portion of each neuron soma toward the central nervous system; the cluster of axons forming the papillary nerve branches, ultimately constituting the two papillary nerves connected to the visceral ganglion. At this stage, only at the ultrastructural level is it possible to distinguish the presence of some scattered neurons (RTENs; see below). The epidermal region, located at the center of the papillary triangle (interpapillary region) is distinguished from the remaining epidermis by being composed of columnar cells, forming a slowly thickening area.

In the swimming larva, cells possess small yolk granules; the papillary region is encircled by the ring of eight blood ampullae, which now expand, because they are no longer compressed by the tail or egg envelopes (Fig. 1A,F–H). In addition to the papillary neurons and the epidermal parietal cells, scattered peripheral sensory cells, the axons

Figure 1. Anterior area development in *B. schlosseri* embryos and larvae. **A:** Whole-mounted early swimming larva of *B. schlosseri* showing, in the trunk, photolith (phot) in sensory vesicle, endostyle (en), and stomach (st), components of digestive tract of future sessile oozooid, and sensory papillae (white arrows) emerging forward of area occupied by ampullae (asterisk). **B:** Sagittal section of trunk of a swimming larva (right: anterior; top: dorsal), showing relationships among pharynx (ph), endostyle (en), and stomach (st). Anterior epidermis protrudes into blood ampullae (amp) and papillae (p). Arrowheads: papillary nerve in blood lacuna; toluidine blue. **C–E:** Details of a papilla during development. Papilla (p) is in form of epidermal protrusion in early tail-bud embryo (C), digitiform in mid-tail-bud embryo (D), and dome-shaped in late tail-bud embryo (E). bc, blood cell; ic, inner tunic compartment; oe, ovular envelopes, pc, parietal cells; pn, papillary neurons; reo, receptor end-organ; tc, test cells. Toluidine blue. **F–H:** Three sagittal sections (from right to left of trunk) selected from a complete series of a swimming larva, to show morphology of a papilla. Each papillary neuron (pn) has a dendrite, receptor end-organ (reo), projecting into tunic. Papillary neuron axons (arrowheads) fasciculate together with those emerging from RTENs (rten). amp, blood ampulla; ic, inner tunic compartment; oc, outer tunic compartment. Toluidine blue. **I–L:** Whole-mounted larvae to show modifications of rostral region at onset of metamorphosis (compare also with A). I–J: Late swimming larva. K–L: Larva at onset of metamorphosis. J and L are enlargements of boxed areas of I and K, respectively. At onset of metamorphosis, ampullae (asterisks) grow with respect to papillae (black arrowheads), which are retracted. White arrowheads: tunic at apex of papillae; white arrows: tunic remaining in situ after tail retraction. Hematoxylin. **M,N:** Two sagittal sections from a complete series of a late swimming larva. Cluster of papillary neuron (pn) is incorporated in epidermis, and receptor end-organs are rod-like. Note thick interpapillary region (dotted line in M). Toluidine blue. **O:** Sagittal section of a larva at onset of metamorphosis. Boxed area is enlarged in inset. Ampullae (amp) now protrude, whereas remaining anterior epidermis is retracted; a papilla is notable for presence of papillary neuronal cluster (pn) sunk in hemocoel. Arrowhead: retracted receptor end-organ; cns, central nervous system; en, endostyle; ic, inner tunic compartment. Toluidine blue. Scale bar = 100 μm in A; 50 μm in B,G,I,O; 20 μm in C–E, inset of O; 200 μm in F,H; 25 μm in J–L; 30 μm in M,N.

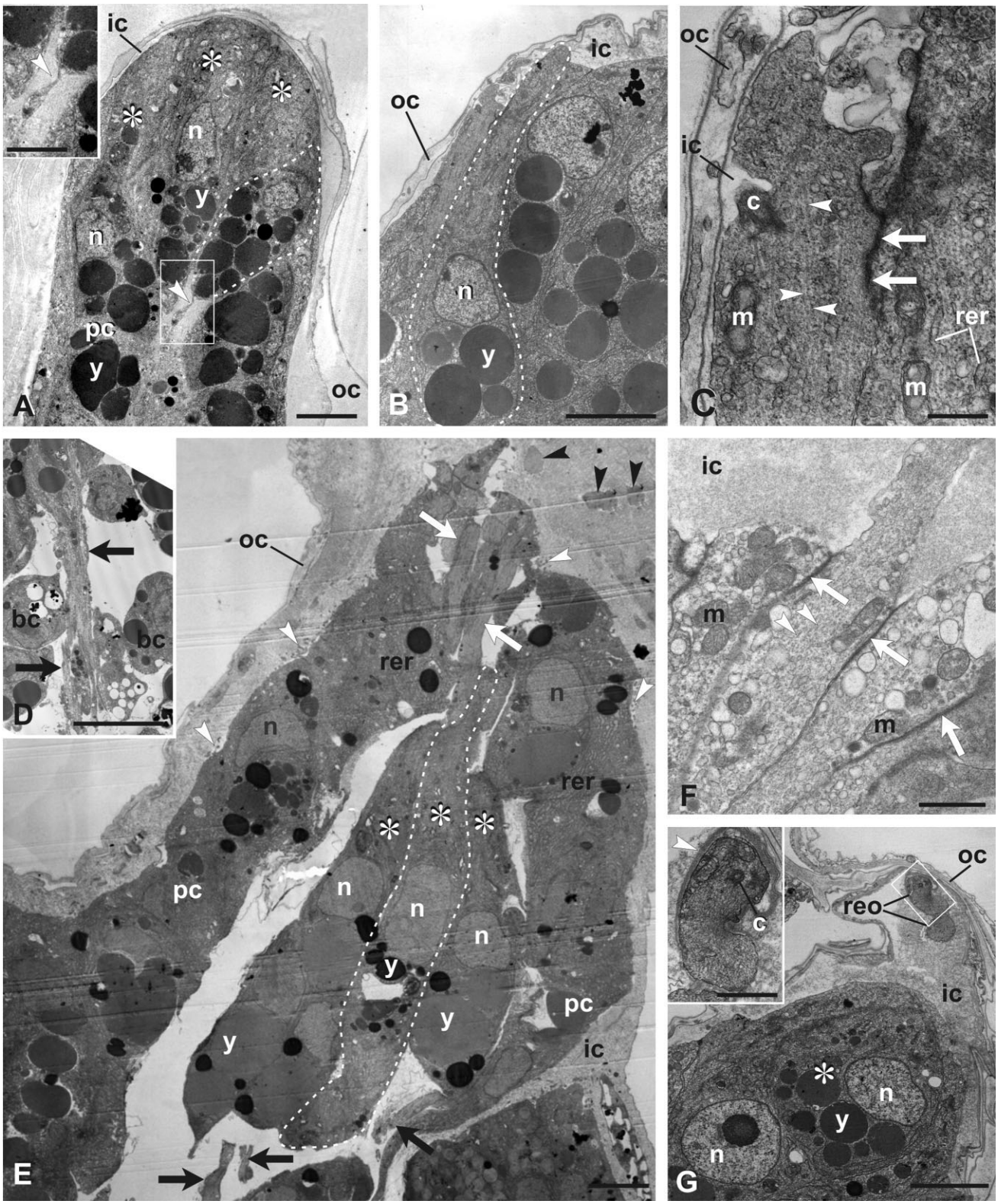
A
ic
n
y
n
pc
y
oc
B
ic
oc
n
y
C
oc
ic
c
m
rer
m
D
bc
bc
E
oc
rer
n
n
rer
pc
n
n
n
y
y
y
pc
ic
F
ic
m
m
G
c
oc
reo
ic
n
y
n

Figure 2

of which fasciculate with axons belonging to papillary neurons, now become clearly visible in thick sections. These scattered sensory cells are abundant in the rostral epidermis of the larva: in histological sections, they are especially frequent, not only at the base of and around the papillae, but also in the interpapillary region and in the epidermis outside the papillary region (Fig. 1G,H). Due to their location, and the anatomical relation of their axons with the papillary axons, we consider them as corresponding to the RTENs described in *C. intestinalis* (Takamura, 1998; Imai and Meinertzhagen, 2007). The cells of the interpapillary region remain distinguishable, due to their columnar shape.

When the swimming larva tests the substrate for permanent adhesion (late swimming phase) (Fig. 1I,J,M,N), the rostral area changes morphology: the receptor end-organs become long and rod-like and, emerging from the tunic at the tips of the papillae, are exposed to sea water; the tunic fenestrates at the papillary apices, and the two cuticular layers (inner and outer) fuse together; the papillary neuronal clusters become incorporated in the epidermal layer; the interpapillary region rises, and the underlying blood lacuna becomes wider, so that a specific papillary hemocoel is no longer identifiable; the thickened interpapillary area becomes more prominent and extended; and the definitive tunic facing it is thin and not bounded by a typical cuticular layer displaying micropapillae.

Figure 2. Differentiation of papillary sensory neurons. Transmission electron microscopy. **A:** Mid-tail-bud embryo. Papillary neurons (asterisks) are polarized, having a central nucleus (n), yolk granules (y) in basal cytoplasm, and other organelles concentrated in apical cytoplasm. A thin axon (arrowhead) emerges from their base. Boxed area is enlarged in inset. ic, inner tunic compartment; oc, outer tunic compartment; pc, parietal cell. B,C: Late tail-bud embryo. **B:** Note tapering supranuclear region of papillary neuron (dotted line), representing differentiating dendrite. **C:** Detail of a dendrite at tight junction level (arrows). Dendrite is rich in microtubules (arrowheads), mitochondria (m), and reticulum endoplasmic cisternae (rer). c, centriole; ic, inner tunic compartment; n, nucleus; oc, outer tunic compartment; y, yolk granule. D–G: Swimming larva. **D:** Detail of papillary axons (arrows) fasciculated in a bundle. **E:** Papillary neurons (asterisks) sunk in hemocoel, constitute papillary neuronal cluster. Note long dendritic processes (white arrows) and axons (black arrows) in hemocoel. Dotted line borders a papillary neuron. Microvilli (white arrowheads) and dendrites (black arrowheads) belonging to RTENs are recognizable. **F:** Detail of papillary neuron dendrites at level of tight junctions (arrows). White arrowheads: microtubules. **G:** Papillary apex, showing a papillary neuron (asterisk) cut at level of nucleus (n); receptor end-organs (reo) in inner tunic compartment (ic). Boxed area is enlarged in inset, to show a centriole (c) in receptor end-organ. Arrowhead: tunic fibers adhering to receptor end-organ plasmalemma. bc, blood cells. m, mitochondrium; oc, outer tunic compartment; pc parietal cells; y, yolk granules. Scale bar = 5 μm in A,C; 2.5 μm in F, inset of A; 10 μm in B; 2 μm in D; 4 μm in E,G; 1 μm in inset of G.

At the onset of metamorphosis, when tail resorption is advanced (Fig. 1K,L,O), the whole rostral larval area assumes the role of a zone of permanent adhesion to the substrate. The eight blood ampullae extend to adhere to the substrate. They are rich in blood cells and very prominent with respect to the remaining anterior epidermis, which is retracted and not directly in contact with the substrate; the tunic facing the retracted epidermis is very thick. The papillary and interpapillary epidermis is represented by rostral thickening, defined by the crown of the ampullae (Fig. 1O); the papillae are now very close to each other, but are identified by the presence of a prominent papillary neuronal cluster, now sunk into the hemocoel facing the endostyle. The receptor end-organs are completely embedded in the tunic and retracted. The interpapillary region is now involved in apocrine secretion.

Differentiation papillary sensory neurons

Papillary sensory neurons were identified in mid-tail-bud embryos, due to their location at the papillary apex, soma shape, and polarity (Fig. 2). Parietal cells are cylindrical, have an apical nucleus, and are rich in yolk granules scattered in the cytoplasm, whereas papillary neurons are elongated, with nuclei in a central position, and yolk granules concentrated in the basal cytoplasm; all the cellular organelles, such as mitochondria, long rough endoplasmic reticulum, (RER) cisternae, and Golgi apparatus, are in the tapering sopranuclear region (Fig. 2A,B). This region represents the differentiating dendrites of the sensory neurons, the presumptive receptor end-organ. While the dendrites remain joined by means of tight junctions to contiguous cells, they begin to extend their apical regions into the tunic over the junctions (Fig. 2C); a section of the basal body of a very short cilium is occasionally visible. Each apical termination contains many parallel microtubules extending along the main cell axis, and a few mitochondria and RER cisternae. At the base of the papillary neurons, thin axons emerge and extend into the narrow papillary hemocoel (Fig. 2A). The axons contain many granules, mitochondria, and endoplasmic vesicles. In the hemocoel at the papillary base, the axons fasciculate tightly; a fibrous sheet enveloping the nerve bundle, as described for nerves in the blastozooid of *B. schlosseri* (Zaniolo et al., 2002), was not observed. Blood cells, such as granulocytes and precocious morula cells, are sometimes seen to associate closely with the bundle (Fig. 2D).

Later, as the entire papilla elongates, the papillary neurons extend most of their soma into the papillary hemocoel, although they remain joined to each other and to parietal cells with tight junctions at the base of their thin dendritic processes. In the swimming larva, the cluster of neuron somata is clearly recognizable as a mass occupying the apical papillary hemocoel (Fig. 2E). The neuron soma

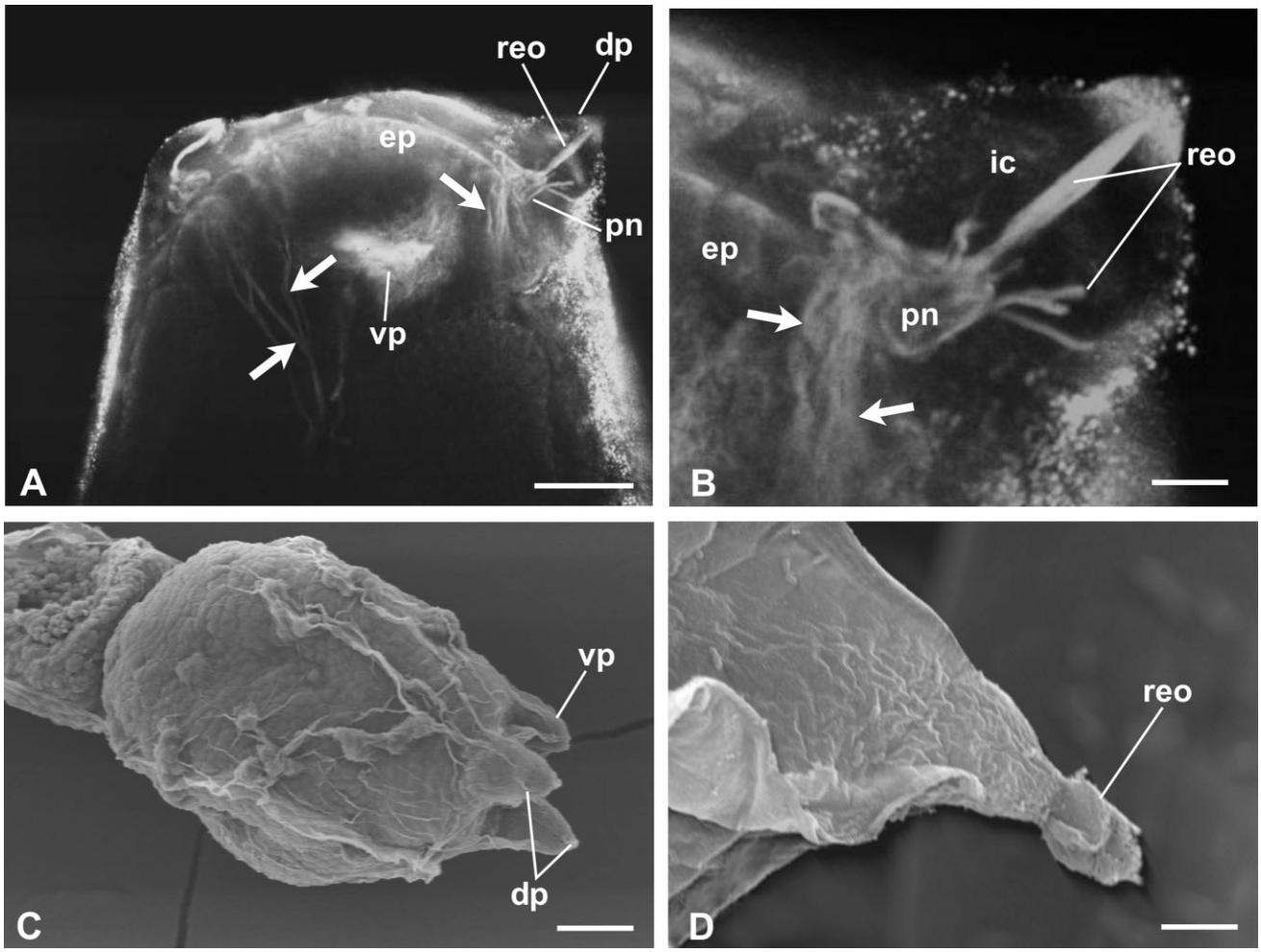

Figure 3. Larval papillary morphology. **A,B:** α-Tubulin labeling at confocal microscopy, to show nerve fibers (arrows) emerging from papillary neuronal clusters (pn), directed to central nervous system. Note central and peripheral receptor end-organs (reo). dp, dorsal papilla; ep, epidermis; ic, inner tunic compartment; vp, ventral papilla. **C,D:** Scanning electron microscopy to show larval papillae; receptor end-organs (reo) form a tuft emerging from tunic fenestration. dp, dorsal papillae; vp, ventral papilla. Scale bar = 20 μm in A; 6 μm in B; 25 μm in C; 5 μm in D.

contains the round nucleus, most cytoplasmic organelles, and a few yolk granules. Apically, the long dendrite (receptor end-organ), filled with many parallel microtubules, extends into the tunic and has occasional sections of centrioles at its base (Fig. 2F,G). The receptor end-organs of the sensory neurons emerge together from the papillary epithelium, forming a tuft. At this stage, the central and peripheral terminations are visible: the central ones are long and tightly packed with respect to the peripheral ones, which form a corolla of shorter terminations. Many axonal fibers are seen in the area at the base of each papilla and in the interpapillary region.

When the swimming larva begins to adhere to the substrate (late swimming stage), the papillary apex undergoes major changes: the receptor end-organs differentiate into rod-like structures (about 26 μm long and 2.2 μm in diameter), crossing the papillary tunic and protruding into the external environment through an apical fenestration in the tunic (Figs. 3, 4). Confocal microscopy confirmed the presence in the tunic of a tuft of rod-like receptor end-organs labeled by an anti-α-tubulin antibody (Fig. 3A,B). Labeling was also visible in the tunic near the apices of the receptor end-organs. The tunic fenestration is bounded by the outer and inner tunic cuticles, fused together, and the inner tunic cuticle appears to be particularly rich in fibers in the region near the fenestration (Fig. 4A–C). The inner tunic compartment forms a sort of "hyaline cap" and does not adhere to the inner cuticle, so that a wide space is created between them. The cap is bounded by a fibrous matrix, which lies on the edges of the terminations and then joins the inner tunic cuticle.

At the onset of metamorphosis, in the interpapillary region, the retracted epidermal cells are cylindrical and form a button-like structure defined by the crown of ampullae.

The papillae are still recognizable as three slight protrusions, with the papillary neuronal cluster in the form of a spherical mass sunk in the hemocoel (Fig. 4D–F). The neuron somata are dissociated from one another, maintaining only a few points of adhesion; they exhibit various signs of involution, such as large, electron-dense lysosomal vacuoles and nuclei with irregular profiles. Each papilla maintains a tuft of retracted, sensory terminations protruding into the tunic. These terminations are no longer rod-like, but irregular and slack, and contain variously oriented microtubules and often a small cilium, visible at their apex (Fig. 4E). Owing to the general contraction, the whole anterior epidermal area approaches the endostyle, while the papillary nerves bend in the restricted hemocoel.

Differentiation of rostral trunk sensory neurons

In late tail-bud embryos, scattered sensory cells, called RTENs following Takamura (1998) and Imai and Meinertzhagen (2007), are found among the rostral epidermal cells, especially at the base of the papillae (Fig. 5A,B). These sensory cells are elongated and exhibit central nuclei, basal yolk granules, apical Golgi fields, and scattered RER cisternae. They possess modified cilia protruding into the tunic, with conventional 9+2 microtubular arrangements but with irregular profiles of cytoplasmic area accompaning the axonema. The cilia have a dense, short, basal body connected to poorly developed ciliary rootlets.

In the swimming larva, RTENs were more differentiated and thus more easily identifiable among the epidermis or papillary parietal cells (Fig. 5C–E). They are numerous and tapered, often in small clusters, and their base, from which a thin axon emerges, protrudes into the papillary hemocoel. Axons from different RTENs fasciculate both together and with axons from papillary neurons. Apically, they extend their dendrites, deriving from modifications of the cilia, into the tunic: the dendrites are long, thin, frayed, and serpentiform. In an area like that shown in Figure 5C, a number of dendrite sections are visible, including sections of receptor end-organs, either isolated or grouped and joined by tight junctions, because they were cut close to the point of their emergence from the papillary neuron somata. Unlike parietal cells and papillary neurons, RTENs are characterized by short microvilli, which represent markers distinguishing these sensory cells.

At the onset of metamorphosis, the RTENs, owing to displacement of the anterior retracted epidermis and papillary nerves, begin to show signs of involution.

Differentiation of interpapillary region

In the late tail-bud stage, the central interpapillary region presents distinctive features with respect to the epidermal cells exterior to the papillary triangle (Fig. 6A–C). The latter are typically cylindrical, with central nuclei and many yolk granules, in both basal and apical cytoplasm. The epidermis is covered by the two tunic compartments, the inner one possessing the cuticle furnished with micropapillae. The interpapillary region is formed of polarized cells: in sequence, from base to apex, are yolk granules, long and large RER cisternae with homogeneous content, round nuclei with nucleoli, and Golgi fields composed of stacks of cisternae budding many small vesicles. Small vesicles also lie close to the apical cell membrane, and aspects of secretion, perhaps involved in tunic formation, are visible. A few yolk granules may occur in the apical cell region. The apical plasmalemma rises in short microvillar protrusions covered by a thin layer of inner tunic, with a smooth cuticle. Mitochondria are scattered.

The distinctive features of the interpapillary region become more accentuated in the following developmental phases (Fig. 6D,E). In the larva touching the substrate, typical epidermal cells still possess large yolk granules, whereas interpapillary cells undergo a reduction in yolk granules; some of them are accompanied by large vacuoles in the apical cytoplasm. The cytoplasm is filled with elongated RER cisternae; there are always many Golgi fields, and budded vesicles are concentrated in the subplasmalemmal cytoplasm; signs of secretion are visible. The inner tunic compartment facing the interpapillary region is expanded and characterized by a dense matrix; the inner and outer compartments are fused together, so that the inner cuticle is no longer clearly recognizable.

When the larva has definitively adhered to the substrate and the eight ampullae are expanded, the whole interpapillary region is retracted, together with the papillae (Fig. 6F,G). Histological sections of this area at the onset of metamorphosis show that the central secretive region is still present and active, composed of cells very rich in RER cisterns, with their apical regions protruding, defining labyrinthic spaces. Large vacuoles, filled with a homogeneous content accumulating in the cytoplasm, often form large bubbles protruding into the tunic. These features are indicative of the transfer of substances by means of apocrine secretion from the epidermal cells toward the tunic.

Figure 7 shows the main steps of differentiation of papillae and the interpapillary region.

DISCUSSION

Peripheral nervous system in the larval anterior region

In recent years, attention has been particularly directed toward elucidating the role of the larval anterior region (containing the papillae, interpapillary region, and scattered RTENs) in triggering and regulating metamorphic

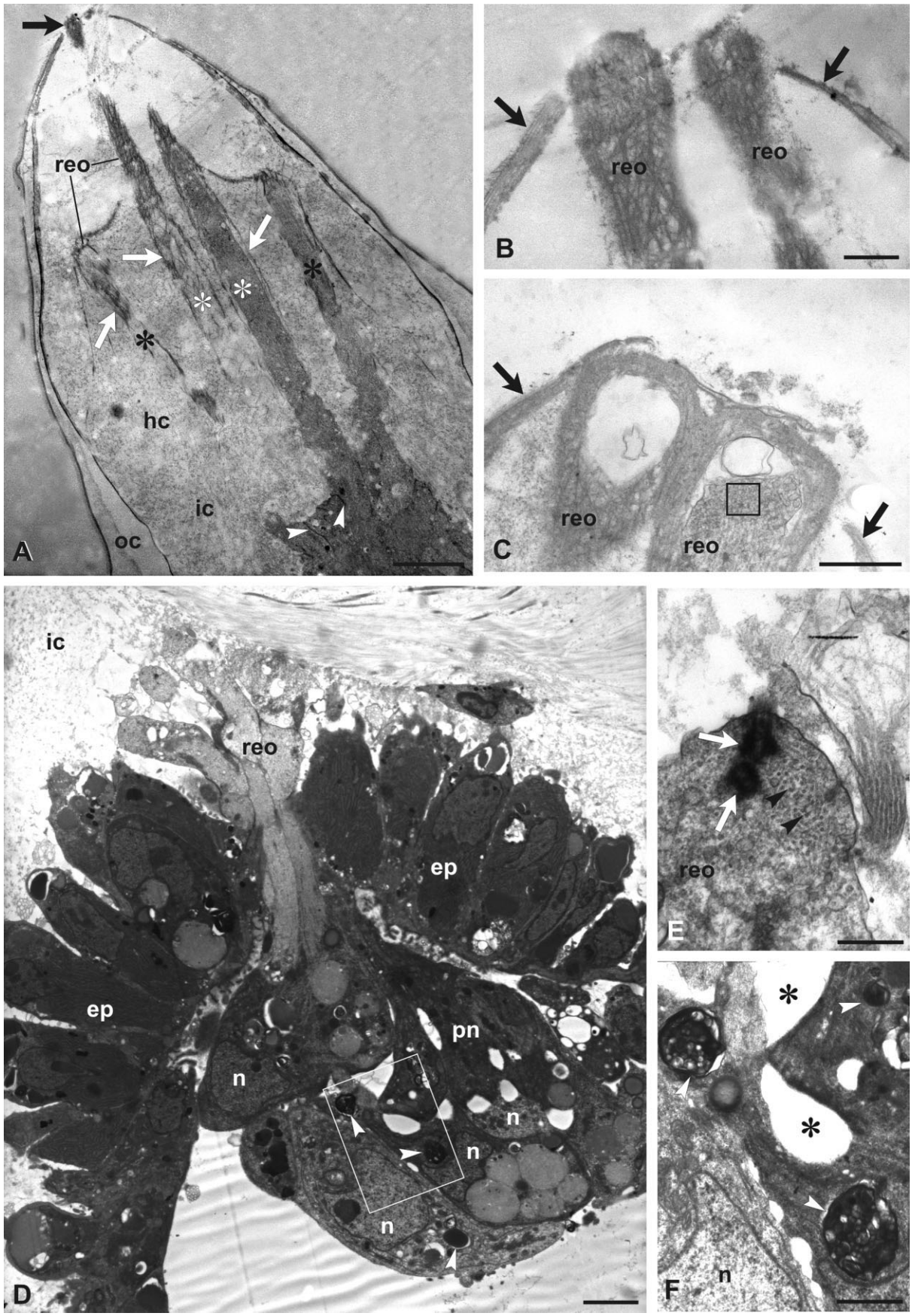

Figure 4

events in ascidians. We now know the anterior ectoderm cell lineage and that some developmental factors (Wada et al., 1999; Ohtsuka et al., 2001a,b; Yagi and Makabe, 2002) are responsible for specification of the anterior components. We also know about the structure of the papillae in restricted stages of swimming larvae of several species. However, based on our data, the information is limited, because the papillae do not retain the same structural features throughout the swimming phase, but change their morphology as metamorphosis approaches. The literature lacks detailed information on the changes that the anterior larval area undergoes during larval differentiation and metamorphosis, or is only limited to a few reports. Our data now present a coherent description of the ultrastructural aspects and changes that occur during differentiation, the physiological activity and alteration of anterior components during embryonic development, the life course, and settlement of the larva of one ascidian, *Botryllus schlosseri*. Our data show how and when the papillae (with their papillary neurons), the RTEN sensory cells, and the interpapillary area form, organize themselves, and are activated; in addition, thanks to ultrastructural studies, we now have evidence of the activity of these components and of the role they play during metamorphic events.

In the course of our study, we addressed the question of the presence of "ganglia" connected to the papillary system in *B. schlosseri*, as first reported by Grave and Riley (1935). This is now of current importance for biologists interested in the presence of true peripheral ganglia in ascidians, perhaps deriving from neural crest/placodal ectodermic areas. Based on their histological study, Grave and Riley (1935) defined the papillae of *B. schlosseri* as "ganglionated," due to the presence of "papillary ganglia" below the epidermis, a report later confirmed through the ultrastructural observations of Torrence (1983), who also defined the sensory nature of the papillae and the absence of secretory cells in other species (Cloney, 1978). Our data are in line with these previous reports; in addition, we add information about the characteristics of these "ganglia" that induces us to classify them as nonhomologous to vertebrate peripheral ganglia (see below), as well as information revealing the presence of RTEN sensory elements in *B. schlosseri*.

In vertebrates, most sensory neurons originate from the neural crest and neurogenic placodes, two specialized ectodermal derivatives, commonly thought to be vertebrate innovations. However, recent studies have shown that ascidians maintain neural crest/placodal-like elements probably inherited from the common ancestor of chordates (Manni et al., 2004; Jeffery et al., 2004; Mazet and Shimeld, 2005; Hall, 2009). In this context, some authors believe that the papillae are homologous to the cement and hatching glands of vertebrates because they share the ventral position with respect to the mouth (i.e., the oral siphon) and some developmental genes (Katz, 1983; Miya et al., 1996; De Bernardi, 2002; Groppelli et al., 2001, 2003). However, the vertebrate cement and hatching glands may not be placodal derivatives in a strict sense, because they do not share a common developmental origin with placodes (reviewed in Schlosser, 2005). The adhesive papillae have also been thought to derive from embryonic territories homologous to the vertebrate olfactory placode, on the basis of developmental gene expression (Mazet et al., 2005). At present, any direct homology with neurogenic placodes of vertebrates is difficult to establish, although the papillae derive from blastomeres located in the most anterior region of the neural plate (Nishida, 1997; Yagi and Makabe, 2002), a region involved in the placode formation of vertebrates (Manni et al., 2004; Schlosser, 2008).

In this respect, the supposed presence in *B. schlosseri* of "papillary ganglia" calls attention due to their possible similarity to sensory ganglia derived from neural crest/placodal cells in vertebrates. However, the "papillary ganglia" are not exactly homologous to those of vertebrates, because, confirming the data of Torrence (1983), we have shown that they do not derive from aggregated neurons originating by delamination from an epithelium (like vertebrate ganglia), but from neurons, which maintain their original connection with contiguous cells by means of apicolateral tight junctions, while their somata grow and sink below the epidermis. Moreover, no synaptic interactions have been revealed among neuron somata, there is no a typical neuropil region, and the "ganglia" are transient structures during the larval stage. Therefore, we propose abandoning the designation "ganglion" for the cluster of

Figure 4. Differentiation of papillary sensory neurons. Transmission electron microscopy. A–C: Late swimming larva. **A:** Receptor end-organs (reo) are rod-like and diversified in a central group (white asterisks) of long terminations emerging from apical tunic fenestration (black arrow) and a peripheral group (black asterisks) of shorter terminations. Arrowheads: tight junctions joining dendrites to each other; ic, inner tunic compartment; hc, hyaline cap; oc, outer tunic compartment; white arrows: net of tunic fibers enveloping terminations. **B,C:** Details of papillary apex, showing receptor end-organs (reo) protruding from tunic fenestration. Note that tunic inner and outer cuticles are fused together (arrows); in B, terminations are cut tangentially, and a net of tunic fibers enveloping them is recognizable. **D–F:** Onset of metamorphosis. Papilla is retracted: papillary neurons (pn) are sunk in hemocoel, nuclei (n) have irregular profile, and empty spaces (asterisks) lie between neuron somata, which have dense lysosomes (white arrowheads); receptor end-organs (reo) are irregular. Box in D: area very close to that shown in F. Arrows: pair of centrioles at tip of termination; black arrowheads: microtubules in termination; ep, epidermis. Scale bar = 4 μm in A; 1 μm in B,C,E,F; 200 nm in inset of C; 2.5 μm in D.

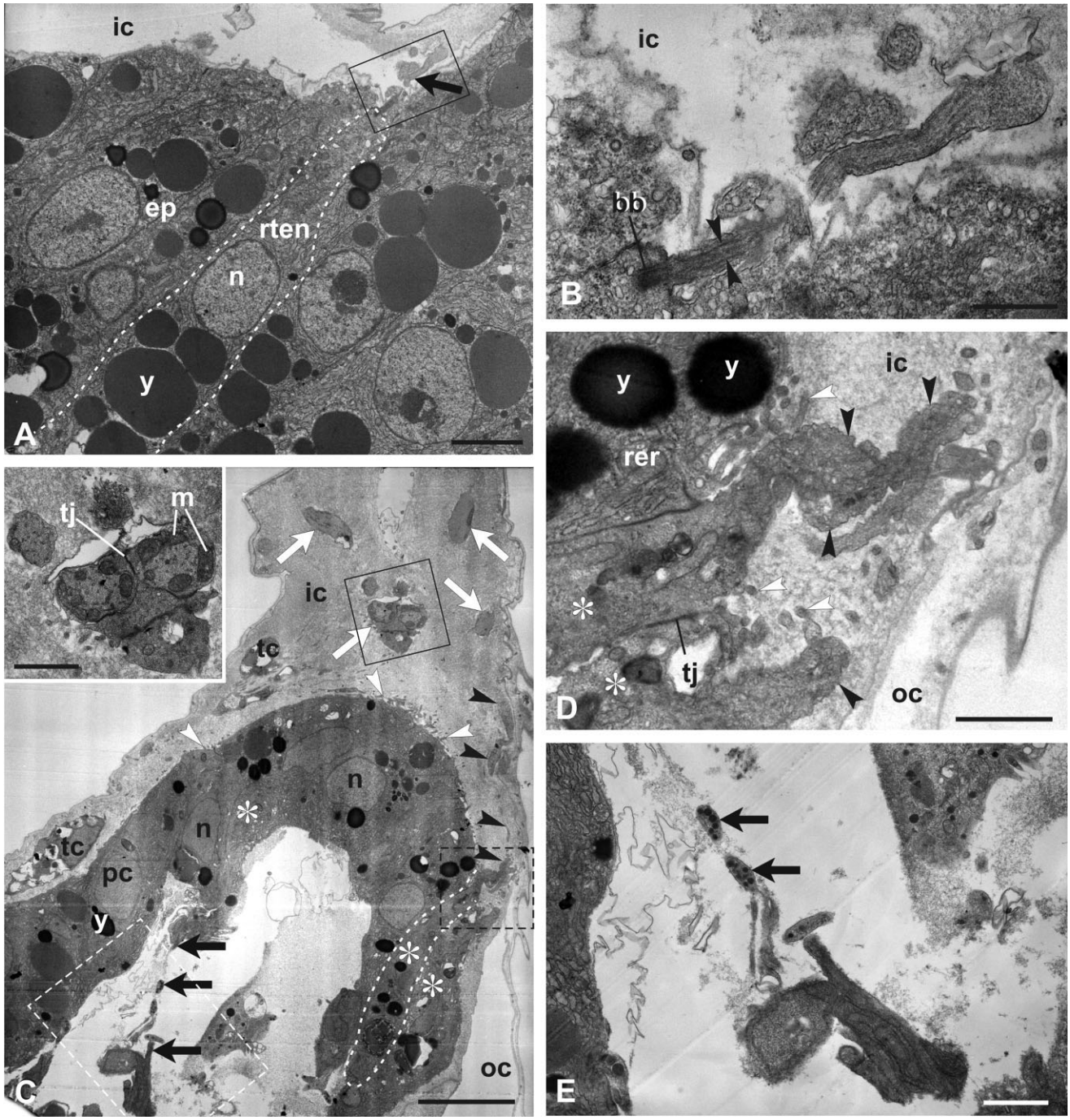

Figure 5. Differentiation of rostral trunk epidermal neurons. Transmission electron microscopy. A,B: Late tail-bud embryo. **A:** RTEN (dotted line) among epidermal cells (ep). Note modified cilium (arrow) protruding into inner tunic compartment (ic). **B:** Boxed area in A, enlarged. Black arrowheads: ciliary microtubules; bb, basal body of cilium; n, nucleus; y, yolk. C–E: Swimming larva. **C:** RTENs (asterisks) are extended and form small clusters among parietal cells (pc); RTENs are characterized by apical microvilli (white arrowheads), and a long, serpentiform dendrite (black arrowheads) and an axon emerge from their base (black arrows). Boxed area bordered by continuous black line is enlarged in inset, to show receptor end-organs (white arrows) belonging to papillary neurons cut close at level of tight junctions. **D:** Boxed area bordered by black dotted line in C, enlarged, to show apical side of RTEN bearing a dendrite and short microvilli. **E:** Boxed area bordered by white dotted line in C, enlarged, to show axons in hemocoel rich in electron-dense neurotransmitter vesicles. ic, inner tunic compartment; m, mitochondria; n, nucleus; oc, outer tunic compartment; rer, rough endoplasmic reticulum; tc, tunic cell; tj, tight junctions; y, yolk. Scale bar = 2.5 μm in A; 1 μm in B; 10 μm in C; 5 μm in inset of C; 2 μm in D,E.

papillary sensory somata. The papillae of *B. schlosseri* should be more properly classified as "simple coniform."

Besides papillary neurons, we found that each papilla is rich in other primary sensory neurons, similar to other scattered neurons in the epidermis. Their features and distribution indicate that they correspond to the RTENs described in other ascidians (Takamura, 1998; Imai and Meinertzhagen, 2007) as part of the larval peripheral nervous system extending into the trunk and tail. RTENs represent the most rostral system of neurons, distributed bilaterally-symmetrically, and may be a common constituent of the peripheral nervous system of ascidian larvae, because scattered anterior neurons have been observed in some species (see below) (Torrence, 1983; Vorontsova et al., 1997).

Both papillary neurons and RTENs are identified beginning from late tail-bud embryos, thanks to their spindle shape and the possession of a caudally projecting axon. Presumably, both share a common precursor with adjacent epidermal cells, as evidenced in the case of sensory and epidermal cells of the tail of *C. intestinalis* (Pasini et al., 2006).

Unlike Grave and Riley (1935), we were unable to identify the specific "hold-fast ganglia" described by the above authors, despite careful analysis of serial sections and the use of anti-α-tubulin antibodies. According to Grave and Riley, the "ganglia" are two conical neuronal aggregates with their bases attached to the epidermis, dorsal and lateral to the two dorsal papillae, involved in a hold-fast mechanism. It should be noted that Torrence (1983), who identified both a papillary cluster of neuron somata and some scattered sensory cells in *B. schlosseri*, did not report the presence of the "hold-fast ganglia." Thus, we are inclined to think that they represent particular aggregations of RTENs.

In *B. schlosseri*, axons from papillary neurons and RTENs fasciculate together, ultimately to form the two papillary nerves, connected to the central nervous system. Confocal microscopy confirmed the presence of many nervous system interconnections among sensory rostral structures, despite "background noise" in *B. schlosseri* larva due to the size of the trunk, the thick layer of autofluorescent tunic, and yolk globules. In accordance with Grave's (1934) observations, the right nerve contains mainly axons of the right dorsal and ventral papilla; the left nerve contains axons from the left dorsal and ventral papilla. Right and left nerves receive axons from RTENs on their side, and enter the visceral ganglion next to the sensory vesicle, on the right and left sides, respectively. Thus, the two nerves have symmetric distributions, although they emerge from the visceral ganglion at different levels, probably due to the asymmetric position and shape of the sensory vesicle. It is noteworthy that the peripheral nervous system of *C. intestinalis* (Imai and Meinertzhagen, 2007; Horie et al., 2008) has two papillary nerves, symmetric in their arrangements, both split into three main branches and each supplying a dorsal papilla, the ventral papilla, and peripheral neurons. Thus, although the larva of *B. schlosseri* is rather different from that of *C. intestinalis*, both in general anatomy and in papillary morphology (Manni et al., 2004), the rostral sensory system is similar in the two species. Also, rostral sensory nerves with similar courses occur in the ascidian *Molgula citrina*, which lacks papillae but possesses nerves originating from scattered sensory cells in the anterior epidermis (Vorontsova et al., 1997).

Morphogenesis and dynamic changes of papillae until onset of metamorphosis

Papillary rudiments in *B. schlosseri* are first recognizable in the early tail-bud embryo, i.e., when the first two spots of pigment in the statolith fuse (Sorrentino et al., 2000). The rudiments are not in the form of a solid mass, as reported by Grave and Riley (1935), but are composed of a single layer of cylindrical epidermal cells, in continuity with the adjacent epidermis, and defining a thin hemocoel filled with a dense extracellular matrix. For comparison, in the closely related *Halocynthia roretzi*, the papillae are morphologically identifiable after the middle tail-bud stage, whereas specific molecular markers label their position at the early tail-bud stage (Yagi and Makabe, 2002).

In *B. schlosseri*, dynamic changes occur in the rostral structures during late embryonic differentiation until the onset of metamorphosis. As the papillary rudiments appear, undifferentiated papillary neurons become distinguishable for their location at the apex of the papilla, their shape, and the thin axons extending caudally into the hemocoel. RTENs are identifiable in late tail-bud embryos, scattered among papillary parietal cells and in the rostral epidermis. As the papillae develop, their neurons differentiate apical dendritic extensions and progressively sink, to form the papillary cluster of neuron somata. At the same time, the cells of the interpapillary area acquire secretory features. In the natatory phase, the whole anterior area undergoes marked changes: the anterior hemocoel extends; the epidermis rises, incorporating the papillary cluster of neuron somata; the receptor end-organs of papillary neurons protrude into the environment, passing through small fenestrations in the tunic; and the cells of the interpapillary area release secretions that change the properties of the tunic layers. The final attachment of the larva to the substrate is accompanied by expansion of blood ampullae, regression of the papillae, production of new tunic, and apocrine secretion of adhesive material by interpapillary cells.

The possibility that apoptosis takes part in the involution of papillae is supported by a number of data. Apoptosis, proba-

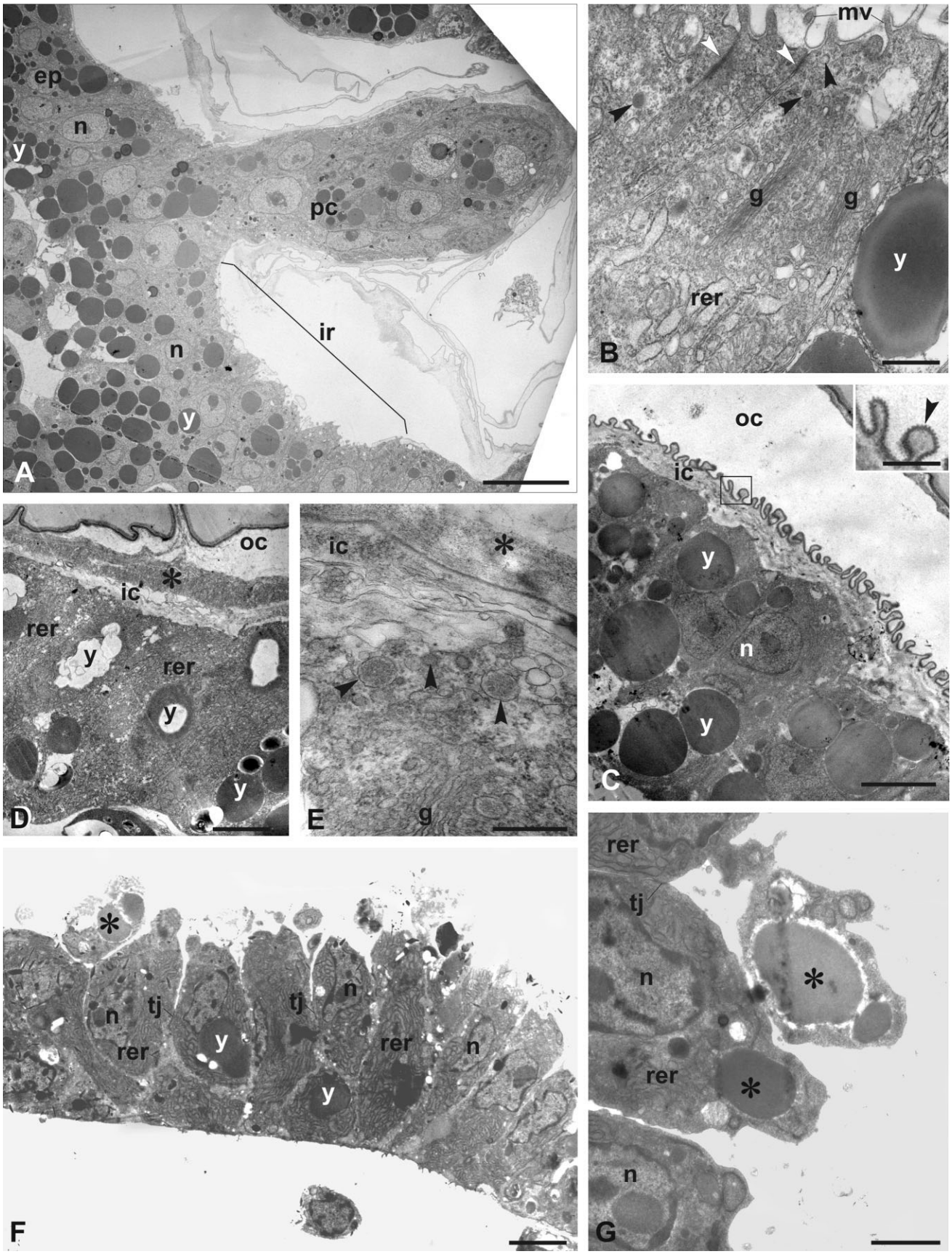
ep
n
y
pc
ir
n
y
A
mv
g
g
y
rer
B
oc
ic
y
n
y
C
oc
ic
*
rer
y
rer
y
y
D
ic
*
g
E
rer
tj
n
tj
n
rer
y
rer
n
y
F
rer
tj
n
*
rer
*
n
G

Figure 6

bly related to substrate adhesion, has also been signaled in the papillae of *C. intestinalis* larvae (Tarallo and Sordino, 2004; Chambon et al., 2007). Our data show that, in *B. schlosseri*, the signs of involution exhibited by the papillary neurons at the onset of metamorphosis (dissociation of neuron somata, presence of electrondense lysosomal vacuoles, nuclei with irregular profiles) may be morphological features of an initial apoptotic process: the alterations correspond to those described with cytological criteria for other adult tissues of *B. schlosseri* during the process of generational change, when all the adults of a colony are resorbed and replaced by their buds in filtering activity (Burighel and Schiavinato, 1984; Ballarin et al., 2008). Thus, on the whole, all the data show that apoptosis can coordinate papillary resorption during metamorphosis.

Differentiation of papillary sensory neurons and RTENs

The presence of sensory neurons in ascidian papillae is confirmed by observations in a number of species (Cloney, 1977; Torrence and Cloney, 1983; Sotgia et al., 1998; Takamura, 1998; Gianguzza et al., 1999; Imai and Meinertzhagen, 2007; Horie et al., 2008; Dolcemascolo et al., 2009), including two species of the genus *Clavelina* (Pennati et al., 2009), previously considered to possess papillae with only a secretory function (Turon, 1991).

In *B. schlosseri*, cytodifferentiation of papillary neurons is gradual. In the early tail-bud stage embryo, papillary neuroblasts can be distinguished from adjacent epidermal cells thanks to the polarized distribution of cytoplasmic components: yolk globules are concentrated in the basal region of the cells; Golgi fields and endoplasmic cisternae lie in the supranuclear region extended slightly into the tunic to form short dendrites (receptor end-organs); and thin axons extend from the basal plasmalemma. We suggest that dendritic sensory terminations derive from modified cilia, because a pair of centrioles has been identified.

In *B. schlosseri*, as yolk granules are reduced, the neuron somata extend in the hemocoel, so that the papillary neuronal cluster becomes recognizable, and the supranuclear region elongates and becomes enriched in parallel microtubules. Our ultrastructural studies clarify previous reports on receptor end-organs (Grave and Riley, 1935). In the swimming larva there are two kinds of end-organs: 1) rod-like, tightly packed central terminations, the ends of which touch the apex of the papilla; and 2) peripheral, cone-shaped, shorter terminations, which radiate from the common central point of origin and are embedded in a sort of "hyaline cap" formed by the inner tunic compartment. This cap becomes recognizable in the swimming larva as it begins to adhere to the substrate (late swimming larva), concomitantly with the appearance of the apical tunic fenestration, through which the central terminations are exposed to the outer environment. A similar situation has been described in *Ascidia malaca* and *Phallusia mammillata* (Sotgia et al., 1998; Gianguzza et al., 1999). In *B. schlosseri*, sea water entering the fenestration probably separates the inner cuticle from the inner tunic compartment, which remains collapsed on the peripheral terminations.

In *B. schlosseri*, RTEN differentiation occurs from neuroblasts in the late tail-bud embryo. These neuroblasts possess modified cilia protruding into the tunic, with a conventional 9+2 microtubular arrangement but with irregular profiles. The cilia progressively differentiate into long, serpentiform dendrites, which cover an extended sensory field in the tunic; short microvilli flank the dendrites in the larval stage. RTENs with complex dendritic arborization extending into the tunic have also been reported in *C. intestinalis* (Imai and Meinertzhagen, 2007). Although direct comparisons among scattered sensory neurons are difficult among ascidians, because of the different morphology of the larvae, all these data suggest that neurons like RTENs represent a common ascidian feature, irrespective of the morphology or absence of papillae. This would suggest that the rostral sensory nervous system originated from an ancestral larva with three symmetric papillae and the same basic pattern of nerve connection with the brain found today in extant species. Ascidians have evolved a surprising variety of papillary morphologies, as a convergent solution to the problem of choosing a suitable substrate on which to metamorphose (Burighel and Cloney, 1997): a common starting point for this variety of papillae is the use of scattered sensory cells, variously aggregated and specialized in different species.

Figure 6. Differentiation of interpapillary region. Transmission electron microscopy. A–C: Late tail-bud stage. **A,B:** Interpapillary region (ir) characterized by cells with central nucleus (n), basal yolk granules (y), apical RER cisternae (rer) and Golgi fields (g), and many budding vesicles (black arrowheads). Apical plasmalemma is raised in short microvillar protrusions (mv), covered by a thin inner tunic compartment. **C:** In contrast, the remaining embryonic epidermis is composed of cells rich in yolk granules and covered by a thick inner tunic compartment (ic) with a cuticle furnished with micropapillae (arrowhead in inset, corresponding to boxed area). ep, epidermis; pc, papillary parietal cells; white arrowheads: tight junctions. **D,E:** Late swimming larva. Cells of interpapillary region are involved in production and secretion of proteins toward tunic, as evidenced by many RER cisterns (rer) and Golgi fields (g); many secretion vesicles are close to apical plasmalemma (arrowheads). A dense matrix (asterisks) characterizes inner tunic compartment (ic) facing interpapillary region, so that inner cuticle is not clearly recognizable. oc, outer tunic compartment; y, yolk granules. **F,G:** Onset of metamorphosis. Interpapillary region cells are involved in apocrine secretion (asterisks): large vacuoles lie in cytoplasmic bubbles and discharge their contents toward tunic. Note labyrinthic spaces defined by apical cell protrusions. n, nucleus; rer, RER; tj, tight junctions; y, yolk granules. Scale bar = 10 μm in A; 1 μm in B,G, inset of C; 4 μm in C; 2.5 μm in D,F; 400 nm in E.

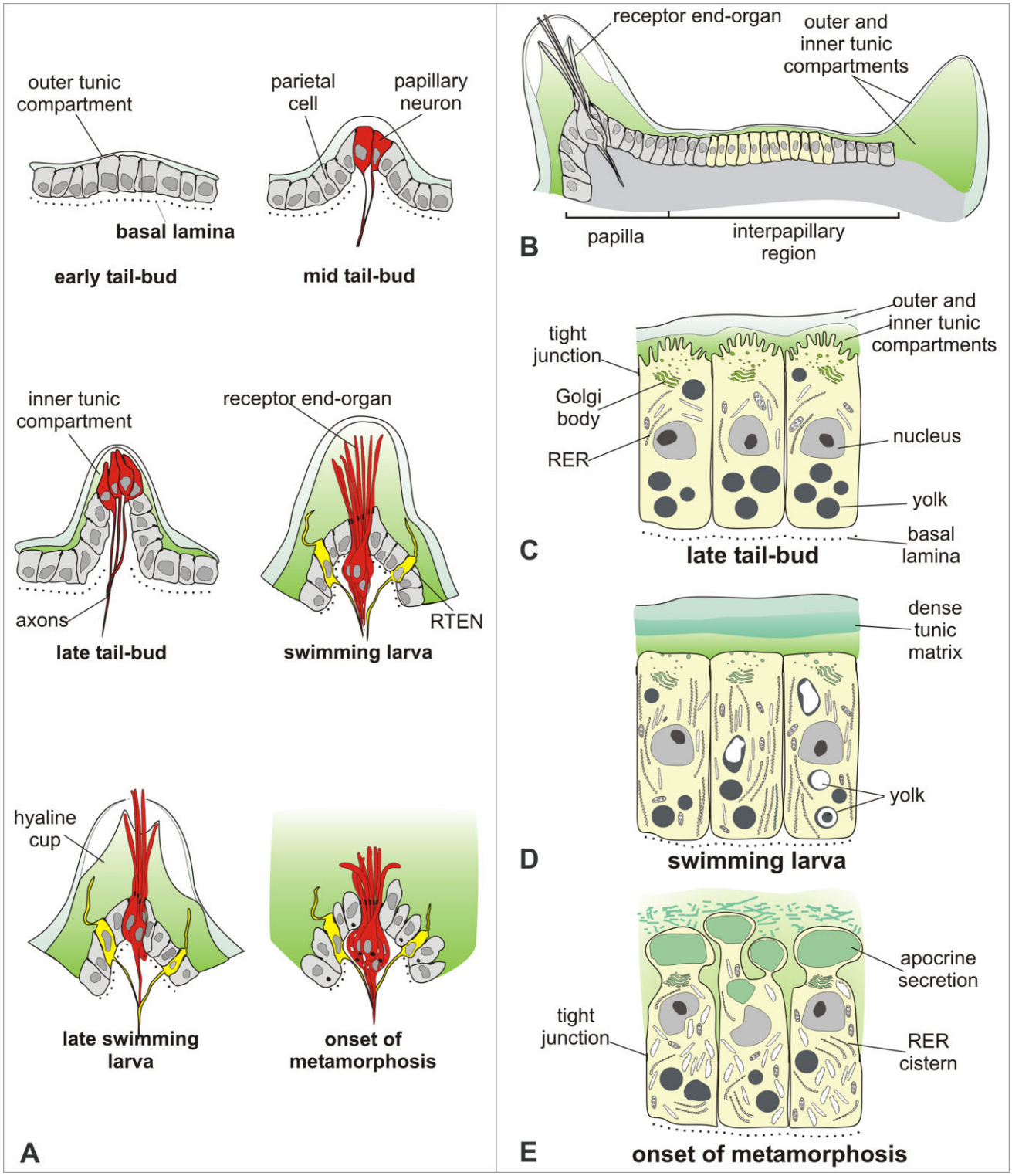

Figure 7. **A:** Sketch showing main events of papilla differentiation. While papilla rises, papillary neurons (red) extend and sink into hemocoel to constitute papillary cluster of sensory neurons (swimming larva stage). Their dendrites form receptor end-organs, which protrude into external environment when larva is ready to choose substrate on which to metamorphose (late swimming larva stage). Axons belonging to papillary neurons fasciculate together with RTEN axons (yellow). After larval adhesion, papillae degenerate (larva at onset of metamorphosis). B–E: Differentiation of interpapillary cells. **B:** Secretory region lies among papillae (interpapillary region). **C–E:** Here, cells undergo progressive changes, represented by increase in RER cisternae and Golgi activity, and secretion of homogeneous, dense matrix toward tunic. At onset of metamorphosis, secretion becomes apocrine, with discharge of large quantities of matrix from apical cytoplasmic bubbles. [Color figure can be viewed in the online issue, which is available at www.interscience.wiley.com.]

Role of papillary sensory neurons and RTENs

Although it is known that the papillae contain epidermal neurons probably involved in receiving and transmitting stimuli for metamorphosis to the posterior part of the body (Nakayama-Ishimura et al., 2009) and although several reports have shown that neurotransmitters induce the initiation of metamorphic events (Kimura et al., 2003; Zega et al., 2005), the actual sensory nature of the papillae has long been controversial. In the absence of direct physiological evidence, authors have so far based their deductions on the role of papillary sensory cells on indirect observations, supporting the idea that the papillae are chemoreceptor organs, or that they may possess both chemosensory and mechanosensory properties.

The chemosensory role is supported by evidence showing that a wide range of chemicals act as artificial inducers, shortening the time to onset of ascidian metamorphosis; these include trypsin, thyroxine, dimethylsulfoxide, acetylcholine, copper, dicapryloylglycerol, and NH_4+ (see Degnan et al., 1997, for a review). Moreover, in *Phallusia mammillata*, it has been shown that larvae can discriminate between different lithological substrates by "tasting" their silica content (Groppelli et al., 2003).

Torrence and Cloney (1983) proposed that the papillae of *Diplosoma macdonaldi* have both chemosensory and mechanosensory functions. When exposed to differing substrates (for example, glass or plastic), the larvae select the substrate according to its chemical nature, and not the texture of the surface. However, they can also distinguish surface contours when exposed to chemically identical substrates of differing textures (for example, rough or smooth glass surfaces). According to the authors, papillary basal cells have mechanosensory ability, because they exhibit morphological similarities with the tail epidermal sensory neurons, which are mechanoreceptors.

Some ascidians possess papillary sensory neurons that differ in neurotransmitter production, suggesting that they belong to diverse kinds of receptors and/or modulate sensory perception. In *Phallusia mammmillata* larva, dopamine and serotonin are located in adhesive papillae, where they modulate the onset of metamorphosis with opposite effects: dopamine signaling delays metamorphosis, whereas serotonin signaling triggers it (Pennati et al., 2001; Zega et al., 2005). Both *Phallusia mammillata* and *C. intestinalis* larvae have adhesive papillae with cholinergic neurons (Coniglio et al., 1998; Groppelli et al., 2001). The latter species has also GABAergic neurons in its papillae (Zega et al., 2008) together with glutamatergic papillary neurons and RTENs (Horie et al., 2008).

The adhesive papillae of *Botrylloides leachi* have recently been described according to immunohistochemical properties (Pennati et al., 2007). The species belongs to the same family as *B. schlosseri* (Botryllidae) and, like it, displays papillae with an exclusive sensory function. In *Botrylloides leachi*, the papillae have two kinds of sensory neurons in the papillary cluster of somata: 1) cells disposed in the center of the papilla, with a long distal process, which passes through the two layers of the tunic and emerges as small protrusions at the apex of the papilla (thus corresponding to the central terminations in *B. schlosseri*); and 2) cells with marginal disposition, having shorter cytoplasmic processes forming a ring (corresponding to the peripheral terminations in *B. schlosseri*). Only cells of the second type contain serotonin in their distal endings. Pennati et al. (2007) propose that the central neurons are the first to come into contact with the substrate during the exploratory period of the larva. The shorter terminal endings of the peripheral neurons do not make contact with the substrate during the series of quick touches by means of which the larva tests the substrate, but are stimulated only after it has firmly attached itself to a suitable substrate, so that these endings participate later in metamorphic events. The central and peripheral terminations in *B. schlosseri* may play a similar role, although this should be proved by specific physiological studies.

On the basis of their cytological features, we propose that all papillary neurons are mechanoreceptors, because they have very long, rod-like dendrites sustained by parallel microtubules, with a smooth plasmalemma. We also propose that RTENs in *B. schlosseri* are chemoreceptors: their dendrites are long and sinuous and possess a folded microvillar membrane, all features typically found in chemoreceptors (Altner and Prilinger, 1980). The fenestration of the cuticle may facilitate the diffusion of solutes into the tunic, improving the detection of chemicals in the substrate by the RTENs. A direct comparison between the sensory cells of *B. schlosseri* papillae and those of papillae of other species (e.g., basal cells or anchor cells in *Diplosoma macdonaldi*) is not simple, because of the great variability in papillary cell morphology. The possiblity cannot be excluded that the sensory neurons of the ascidian rostral epidermis have different functions in different species, but the co-presence of the two kinds of sensory cells may explain the variety of behavioral properties of larvae.

Differentiation of interpapillary region

Our data show that the interpapillary region is responsible for producing sticky molecules, which render the larval anterior tunic suitable for temporary attachment to the substrate before definitive adhesion. This region exhibits signs of secretion, which become more and more accentuated as metamorphosis approaches: starting from the late tail-bud stage, the interpapillary region is distin-

guished from the remaining epidermis by its columnar cells involved in protein synthesis and secretion of tunic components; the inner and outer tunic compartments facing them are fused together, so that the inner cuticle is not clearly recognizable; and the definitive tunic is thin, and not bounded by a typical cuticular layer displaying micropapillae. At the onset of metamorphosis, the interpapillary epidermis is represented by rostral thickening, involved in transferring substances by means of apocrine secretion toward the tunic. Therefore, the tunic shows progressive modifications, making it suitable for temporary adhesions. In *B. schlosseri*, definitive adhesion is in fact due to expansion of the eight peripheral blood ampullae, which extend into the tunic during metamorphosis but remain interconnected by means of the marginal vessel running along the periphery of the tunic (Burighel and Brunetti, 1971). The blood ampullae are used by colonies to adhere to the substrate; they multiply according to colony growth and facilitate colony displacement.

Our data furnish a cytological reinterpretation of the observations of Grave (1934) and Grave and Riley (1935), who described for *Botryllus* larvae (*B. schlosseri* and *B. niger*) a mechanism of attachment at the onset of metamorphosis operating on the principle of a sucker, in which a partial vacuum is created when the hold-fast portion is pressed against a smooth surface. We propose that the sticky tunic, not a vacuum, is responsible for adhesion.

In the interpapillary region of *Herdmania curvata*, Eri et al. (1999) identified a group of cells, called papillary-associated tissue (PAT), centered among the three papillae, which express the protein Hemps, a soluble factor controlling metamorphosis. These cells are released into the tunic at the time of development of a concentration gradient of Hemps along the anterior-posterior axis of tunic and epidermal cells. In *Boltenia villosa* settling larvae, the same PAT cells have also been seen to migrate through a tunnel in the juvenile tunic to the external environment (Davidson and Swalla, 2002; Roberts et al., 2007). The authors hypothesize that these cells are positioned to detect external settlement cues, and that the innate immune system is employed to detect and respond rapidly to environmental settlement cues. In *B. schlosseri*, the larval interpapillary region may contain PAT cells involved in producing soluble morphogens controlling metamorphosis or upregulating innate immunity transcripts. Our study shows that the tunic in *B. schlosseri* larva is rich in tunic cells, which colonize it starting from the late tail-bud stage, from the hemocoel (data not shown); this process also occurs commonly in colonies (Zaniolo, 1981). However, our analysis failed to show transepidermal migration across the anterior epidermis and tunic toward the external environment.

In the closely related *Botrylloides leachi*, histological analysis has recently revealed many secreting cells clustering in the triangular area among the three papillae and forming a glandular organ (Pennati et al., 2007). Burighel and Cloney (1997) also reported that the larvae of *Botrylloides* sp. are sticky both on and between the papillae, and suggested as a possible explanation the presence of glandular epidermal cells located within the triangle between the papillae. Thus, taking all the data into account, we may state that species of the Botryllidae family have evolved papillae with an exclusively sensory role (mechanosensory and chemosensory), whereas their adhesive ability is taken on by the interpapillary region, specializing in the production of sticky tunic.

ACKNOWLEDGMENTS

The authors thank Marcello Del Favero for help in providing and rearing *B. schlosseri* colonies.

LITERATURE CITED

Altner H, Prillinger L. 1980. Ultrastructure of invertebrate chemo-, thermo-, and hygroreceptors and its functional significance. Int Rev Cytol 67:69–139.

Ballarin L, Burighel P, Cima F. 2008. A tale of death and life: natural apoptosis in the colonial ascidian *Botryllus schlosseri* (Urochordata, Ascidiacea). Curr Pharm Des 14:138–147.

Bishop CD, Erezyilmaz DF, Flatt T, Georgiou CD, Hadfield MG, Heyland A, Hodin J, Jacobs MW, Maslakova SA, Pires A, Reitzel AM, Santagata S, Tanaka K, Youson JH. 2006. What is metamorphosis? Integr Comp Biol 46:655–661.

Burighel P, Brunetti R. 1971. The circulatory system in the blastozooid of the colonial ascidian *Botryllus schlosseri* (Pallas). Boll Zool 38:273–289.

Burighel P, Cloney RA. 1997. Urochordata: Ascidiacea. In: Harrison FW, Ruppert EE, editors. Microscopic anatomy of invertebrates, vol 15: Hemichordata, Chaetognatha, and the invertebrate chordates. New York: Wiley-Liss Inc.p 221–347.

Burighel P, Schiavinato A. 1984. Degenerative regression of digestive tract in the colonial ascidian *Botryllus schlosseri* (Pallas). Cell Tissue Res 235:309–318.

Chambon JP, Nakayama A, Takamura K, McDougall A, Satoh N. 2007. ERK- and JNK signalling regulate gene networks that stimulate metamorphosis and apoptosis in tail tissues of ascidian tadpoles. Development 134:1203–1219.

Cloney RA. 1977. Larval adhesive organs and metamorphosis in ascidians. I. Fine structure of the everting papillae of *Distaplia occidentalis*. Cell Tissue Res 183:423–444.

Cloney RA. 1978. Ascidian metamorphosis: review and analysis. In: Chia FS, Rice M, editors. Ascidian metamorphosis: review and analysis. Amsterdam: Elsevier North Holland Biochemical Press. p 255–282.

Cloney RA. 1979. Larval adhesive organs and metamorphosis in ascidians. II. The mechanism of eversion of the papillae of *Distaplia occidentalis*. Cell Tissue Res 200:453–473.

Cloney RA, Torrence SA. 1984. Ascidian larvae: structure and settlement. In: Costolow JD, Tipper RC, editors. Marine biodeterioration: interdisciplinary study, Annapolis, MD: Naval Institute Press. p 141–148.

Coniglio L, Morale A, Angelini C, Falugi C. 1998. Cholinergic activation of settlement in *Ciona intestinalis* metamorphosing larvae. J Exp Zool 280:314–320.

Davidson B, Swalla BJ. 2002. A molecular analysis of ascidian metamorphosis reveals activation of an innate immune response. Development 129:4739–4751.

De Bernardi F. 2002. Evoluzione degli organi adesivi larvali nei cordati. Ist Lomb Rend Sci B 134:19–33.

Degnan BM, Souter D, Degnan SM, Long SC. 1997. Induction of metamorphosis with potassium ions requires development of competence and an anterior signalling center in the ascidian *Herdmania momus*. Dev Genes Evol 206:370–376.

Delsuc F, Tsagkogeorga G, Lartillot N, Philippe H. 2008. Additional molecular support for the new chordate phylogeny. Genesis 46:592–604.

Dolcemascolo G, Pennati R, De Bernardi F, Damiani F, Gianguzza M. 2009. Ultrastructural comparative analysis on the adhesive papillae of the swimming larvae of three ascidian species. ISJ 6:S77–S86.

Eri R, Arnold JM, Hinman VF, Green KM., Jones MK, Degnan BM, Lavin MF 1999. Hemps, a novel EGF-like protein, plays a central role in ascidian metamorphosis. Development. 126: 5809–5818.

Gianguzza M, Dolcemascolo G, Fascio U, De Bernardi F. 1999. Adhesive papillae of *Ascidia malaca* swimming larvae: investigations on their sensory function. Invertebrate Reprod Dev 35:239–250.

Grave C. 1934. The *Botryllus* type of ascidian larva. Carnegie Inst Wash Publ 435:143–156.

Grave C, Riley G. 1935. Development of the sense organs of the larva of *Botryllus schlosseri*. J Morphol 57:185–211.

Grave C, Woodbridge, H. 1924. *Botryllus schlosseri* (Pallas): the behaviour and morphology of the free-swimming larva. J Morphol Physiol 39:207–247.

Groppelli S, Pennati R, Sotgia C, De Bernardi F. 2001. AchE localization in the adhesive papillae of the ascidian larvae: effects of citral, a retinoic acid synthesis inhibitor. Inv Reprod Dev 40:95–102.

Groppelli S, Pennati R, Scarı‘ G, Sotgia C, De Bernardi F. 2003. Observations on the settlement of *Phallusia mammillata* larvae: effects of different lithological substrata. Ital J Zool 70: 321–326.

Hall BK. 2009. The neural crest and neural crest cells in vertebrate development and evolution. New York: Springer.

Hinman VF, Degnan BM. 1998. Retinoic acid disrupts anterior ectodermal and endodermal development in ascidian larvae and postlarvae. Dev Genes Evol 208:336–345,

Horie T, Kusakabe T, Tsuda M, 2008. Glutamatergic networks in the *Ciona intestinalis* larva. J Comp Neurol 508:249–263.

Imai JH, Meinertzhagen IA. 2007. Neurons of the ascidian larval nervous system in *Ciona intestinalis*: II. Peripheral nervous system. J Comp Neurol 501:335–352.

Jeffery WR, Strickler AG, Yamamoto Y. 2004. Migratory neural crest-like cells form body pigmentation in a urochordate embryo. Nature 431:696–699.

Katz MJ. 1983. Comparative anatomy of the tunicate tadpole, *Ciona intestinalis*. Biol Bull 164:1–27.

Kimura Y, Yoshida M, Morisawa M. 2003. Interaction between noradrenaline or adrenaline and the β1-adrenergic receptor in the nervous system triggers early metamorphosis of larvae in the ascidian *Ciona savignyi*. Dev Biol 258:129–140.

Manni L, Lane NJ, Sorrentino M, Zaniolo G, Burighel P. 1999. Mechanism of neurogenesis during the embryonic development of a tunicate. J Comp Neurol 412:527–541.

Manni L, Lane NJ, Joly JS, Gasparini F, Tiozzo S, Caicci F, Zaniolo G, Burighel P. 2004. Neurogenic and non-neurogenic placodes in ascidians. J Exp Zool Part B (Mol Dev Evol) 302:483–504.

Manni L, Zaniolo G, Cima F, Burighel P, Ballarin L. 2007. *Botryllus schlosseri*: a model ascidian for the study of asexual reproduction. Dev Dyn 236:335–352.

Mazet F, Shimeld SM. 2005. Molecular evidence from ascidians for the evolutionary origin of vertebrate cranial sensory placodes. J Exp Zool B (Mol Dev Evol) 304:340–346.

Mazet F, Hutt JA, Milloz J, Millard J, Graham A, Shimeld SM. 2005. Molecular evidence from *Ciona intestinalis* for the evolutionary origin of vertebrate sensory placodes. Dev Biol 282:494–508.

Milanesi C, Burighel P, Zaniolo G, Sabbadin A. 1978. The structure and the fate of the test cuticle during the fusion-non fusion reaction in colonies of *Botryllus schlosseri* (Tunicata). Boll Zool 45:83–86.

Miya T, Morita K, Ueno N, Satoh N. 1996. An ascidian homologue of vertebrate BMPs-5-8 is expressed in the midline of the anterior neuroectoderm and in the midline of the ventral epidermis of the embryo. Mech Dev 57:181–190.

Nakayama A, Satou Y, Satoh N. 2001. Isolation and characterization of genes that are expressed during *Ciona intestinalis* metamorphosis. Dev Genes Evol 211:184–189.

Nakayama A, Satou Y, Satoh N. 2002. Further characterization of genes expressed during *Ciona intestinalis* metamorphosis. Differentiation 70:429–437

Nakayama-Ishimura A, Chambon JP Satoh N, Sasakura Y. 2009. Delineating metamorphic pathways in the ascidian *Ciona intestinalis*. Dev Biol 326:357–367.

Nishida H. 1997. Cell lineage and timing of fate restriction, determination and gene expression in ascidian embryos. Semin Cell Dev Biol 8:359–365.

Northcutt RG, Gans C. 1983. The genesis of neural crest and epidermal placodes: a reinterpretation of vertebrate origins. Q Rev Biol 58:1–28.

Ohtsuka Y, Obinata T, Okamura Y. 2001a. Induction of ascidian peripheral neuron by vegetal blastomeres. Dev Biol 239:107–117.

Ohtsuka Y, Okamura Y, Obinata T. 2001b. Changes in gelsolin expression during ascidian metamorphosis. Dev Genes Evol 211:252–256

Pasini A, Amiel A, Rothba U, Roure A, Lemaire P, Darras S. 2006. Formation of the ascidian epidermal sensory neurons: insights into the origin of the chordate peripheral nervous system. PLoS Biol 4:1173–1186.

Pennati R, Groppelli S, Sotgia C, Candiani S, Pestarino M, De Bernardi F. 2001. Serotonin localization in *Phallusia mammillata* larvae and effect of 5-HT antagonists during larval development. Dev Growth Differ 43:647–656.

Pennati R, Zega G, Groppelli S, De Bernardi F. 2007. Immunohistochemical analysis of the adhesive papillae of *Botrylloides leachi* (Chordata, Tunicata Ascidiacea): implications for their sensory function. Ital J Zool 74:1–5.

Pennati R, Groppelli S, De Bernardi F, Mastrototaro F, Zega G. 2009. Immunohistochemical analysis of adhesive papillae of *Clavelina lepadiformis* (Muller, 1976) and *Clavelina phlegrea* (Salfi, 1929) (Tunicata, Ascidiacea). Eur J Histochem 53:25–34.

Roberts B, Davidson B, MacMaster G, Lockhart V, Ma E, Wallace SS, Swalla BJ. 2007. A complement response may activate metamorphosis in the ascidian *Boltenia villosa*. Dev Genes Evol 217:449–458.

Sabbadin A. 1955. Osservazioni sullo sviluppo, l’accrescimento e la riproduzione di *Botryllus schlosseri* (Pallas), in condizioni di laboratorio. Boll Zool 22:243–263.

Schlosser G. 2005. Evolutionary origins of vertebrate placodes: insights from developmental studies and from comparisons with other deuterostomes. J Exp Zool (Mol Dev Evol) 304B:1–53.

Schlosser G. 2008. Do vertebrate neural crest and cranial placodes have a common evolutionary origin? BioEssays 30: 659–672.

Sorrentino M, Manni L, Lane JN, Burighel P. 2000. Evolution of cerebral vescicles and their sensory organs in an ascidian larva. Acta Zool (Stockholm) 81:243–258.

Sotgia C, Fascio U, Melone G, De Bernardi F. 1998. Adhesive papillae of *Phallusia mamillata* larvae: morphology and innervation. Zool sci 15:363–370.

Takamura K. 1998. Nervous network in larvae of the ascidian *Ciona intestinalis*. Dev Genes Evol 208:1–8.

Tarallo R, Sordino P. 2004. Time course of programmed cell death in *Ciona intestinalis* in relation to mitotic activity and MAPK signaling. Dev Dyn 230:251–262, 2004.

Torrence SA. 1983. Ascidian larval nervous system: anatomy, ultrastructure and metamorphosis. Doctoral thesis, University of Washington. p 1–77.

Torrence SA, Cloney RA. 1983. Ascidian larval nervous system: primary sensory neurons in adhesive papillae. Zoomorphology 102:111–123.

Turon X. 1991. Morphology of the adhesive papillae of some ascidian laevae. Cah Biol Mar 32:295–309.

Vorontsova MN, Nezlin LP, Meinertzhagen IA. 1997. Nervous system of the larva of the ascidian *Molgula citrina* (Alder and Hancock, 1848). Acta Zool 78:177–185.

Wada S, Katsuyama Y, Saiga H. 1999. Anteroposterior patterning of the epidermis by inductive influences from the vegetal hemisphere cells in the ascidian embryo. Development 126: 4955–4963.

Yagi K, Makabe KW. 2002. Retinoic acid differently affects the formation of palps and surrounding neurons in the ascidian tadpole. Dev Genes Evol 212:288–292.

Zaniolo G. 1981. Histology of the ascidian *Botryllus schlosseri* tunic: in particular, the test cells. Boll Zool 48:169–178.

Zaniolo G, Lane JN, Burighel P, Manni L. 2002. Development of the motor nervous system in ascidians. J Comp Neurol 443: 124–135.

Zega G, Pennati R, Groppelli S, Sotgia C, De Bernardi F. 2005. Dopamine and serotonin modulate the onset of metamorphosis in the ascidian *Phallusia mammillata*. Dev Biol 282:246–256.

Zega G, Biggiogero M, Groppelli S, Candiani S, Oliveri D, Parodi M, Pestarino M, De Bernardi F, Pennati R. 2008. Developmental expression of glutamic acid decarboxylase and of gamma-aminobutyric acid type B receptors in the ascidian *Ciona intestinalis*. J Comp Neurol 506:489–505.

Zeng L, Jacobs MW, Swalla BJ. 2006. Coloniality has evolved once in Stolidobranch ascidians. Integr Comp Biol 46:255–268

CONTRIBUTION B

Burighel P., Caicci F., Zaniolo G.,Gasparini F., Degasperi V., Manni L.
2008

Does hair cell differentiation predate the vertebrate appearance?

Brain Res. Bull. 75: 331-334

ELSEVIER

Brain Research Bulletin 75 (2008) 331–334

BRAIN RESEARCH BULLETIN

www.elsevier.com/locate/brainresbull

Research report

Does hair cell differentiation predate the vertebrate appearance?

Paolo Burighel *, Federico Caicci, Giovanna Zaniolo, Fabio Gasparini, Valentina Degasperi, Lucia Manni

Department of Biology, University of Padova, Via U. Bassi 58/B 35131, Italy

Received 7 September 2007; accepted 17 October 2007
Available online 20 November 2007

Abstract

It is generally accepted that the three main chordate groups (tunicates, cephalochordates and vertebrates) originated from a common ancestor having the basic features of the chordate body plan, i.e. a neural tube and a notochord flanked by striated musculature. There is now increasing evidence that tunicates, rather than cephalochordates, are the vertebrate sister-group. Correlated with this, tunicates have sensory structures similar to those derived from placodes or neural crest in vertebrates. In this context, we discuss here whether the precursors of vertebrate hair cells, which are placodal in origin, were present in ancestral chordates. The ascidian tunicates possess a coronal organ, consisting of a row of mechanosensory cells that runs around the base of the oral siphon. Its function is to monitor the incoming water flow. The cells are secondary sensory cells, i.e. they lack axons and synapse with neurons whose somata lie in the cerebral ganglion. They are accompanied by supporting cells and, as in vertebrates, have varying morphologies in the species so far examined: in one order (Enterogona), they are multiciliate; in the other (Pleurogona), they may possess an apical apparatus, consisting of one or two cilia accompanied by stereovilli, that are graded in length. Coronal cells thus resemble vertebrate hair cells closely in their morphology, embryonic origin and arrangement, which suggests they originated early in ancestral chordates. We are continuing our study of the coronal organ in other ascidian species, and report new data here on *Botrylloides leachi*, which conforms with the pattern of Pleurogona and, in particular, with previously published results on other botryllid ascidians.

Keywords: Ascidians; Coronal organ; Neural placodes; Oral siphon; Sensory system

1. Introduction

The two non-vertebrate chordate groups, cephalochordates and tunicates, are reference animals for studying the origin of vertebrates, since their anatomy is relatively simple and they occupy a strategic phylogenetic position. Some aspects of the latter are still unresolved, however. Traditionally, amphioxus has been viewed as the closest living relative to vertebrates, but this has recently been questioned on both morphological [8,12,13] and molecular grounds [2,7]. Among the former is the presence of placode-like structures and neural crest-like cells in tunicates, and their apparent absence in amphioxus, which supports the idea that tunicates are the true vertebrate sister group. It is thus possible that sensory placodes did not arise *de novo* in vertebrates, but evolved from pre-existing specialised areas of the ectoderm in the common chordate ancestor. The study of selected sensory structures in tunicates is very relevant here, since corresponding structures arise from the neural crest or placodes in vertebrates.

Tunicates are filter-feeding animals, mainly represented by the ascidians, which are grouped into two orders, Pleurogona and Enterogona. They have a swimming chordate-like larva, whereas the adults have a sac-like body, provided with an oral (incurrent) and an atrial (excurrent) siphon. At the base of the oral siphon, there is typically a laminar epithelial extroflection, called the velum, from which a ring of tentacles arises. This is the location also of the coronal organ, a sensory organ composed of parallel rows of ciliate receptor cells, accompanied by supporting cells that run along the entire margin of the velum and the tentacles. The receptor cells are secondary sensory cells, i.e. they lack axons, but have both afferent and efferent synapses at their bases with neurites whose somata lie in the cerebral ganglion. Neurophysiological studies have shown that the coronal cells are mechanoreceptors, since they can detect large particles entering the siphon with inflowing water [11]. The morphology of the coronal organ varies: species belonging to Enterogona

* Corresponding author. Tel.: +39 0498276185; fax: +39 0498276199.
E-mail address: paolo.burighel@unipd.it (P. Burighel).

0361-9230/$ – see front matter © 2007 Elsevier Inc. All rights reserved.
doi:10.1016/j.brainresbull.2007.10.012

have multiciliate coronal cells; those belonging to Pleurogona have cells with one or two cilia, sometimes accompanied by microvilli or stereovilli. The stereovilli are of equal length in some species, but are graded in length from one side of the array to the other in other species, as in typical vertebrate hair cells [6,13]. Because of this, and because of other embryonic and molecular similarities, it has been suggested that ascidian and vertebrate hair cells share a common origin in ancestral chordates [4,5,12,13].

In order to widen our knowledge of hair cells in ascidians, we have extended our studies to include *Botrylloides leachi* (order Pleurogona), which forms colonies of numerous clonal zooids embedded in a common tunic and produced by synchronised asexual reproduction (blastogenesis). Three blastogenetic generations coexist in each colony: filtering adults, their buds, and the youngest buds produced by the latter. Zooids are hermaphroditic, and eggs develop into chordate-like tadpole larvae, which escape from the colony, adhere to the substrate, reabsorb their larval organs, and metamorphose into sessile filtering zooids (oozooids). These represent the founders of new colonies, whose growth occurs by blastogenesis. The oozooids and blastozooids derived from it are genetically identical and similar in morphology. Data presented in this paper refer mainly to blastozooids.

2. Materials and methods

Colonies of *Botrylloides leachi* (family Styelidae, order Pleurogona) were collected from the Lagoon of Venice (Italy) and maintained in seawater aquaria. For transmission electron microscopy (TEM), zooids were anaesthetised with 0.02% ethyl 3-aminobenzoate methanesulfonate salt (MS 222) at 4 °C. After complete relaxation of the siphons, specimens were fixed in 1.5% glutaraldehyde, buffered with 0.2 M sodium cacodylate, pH 7.4, plus 1.7% NaCl. After washing in buffer, and post-fixation in 1% OsO_4 in 0.2 M cacodylate buffer, they were dehydrated and embedded in Epon Araldite 812. Thick sections (1 μm) were counterstained with toluidine blue; thin sections (70 nm) were given contrast by staining with uranyl acetate and lead citrate. Micrographs were taken with a Hitachi H-600 transmission electron microscope operating at 75 kV. For scanning electron microscopy (SEM), specimens were fixed as described for TEM. After dehydration, they were critical-point dried, sputter-coated with gold, and observed under a Cambridge Stereoscan 260 scanning electron microscope. Micrographs both from TEM and SEM were acquired and typeset in Corel Draw 11.

3. Results

The coronal organ was found only in the inner side of the oral siphon, in the area completely exposed to incurrent seawater, whereas no trace of it or of other mechanosensory organs was found in the excurrent atrial siphon. As in other ascidians, the inner side of the oral siphon comprises the area between the external rim of the siphon and the region of velum with the ring of tentacles. This area is covered by tunic, the thin limit of which reaches the base of the velum and tentacles. In *Botrylloides leachi*, the crown of tentacles is formed of a series of four symmetrical tentacles that alternate regularly with shorter tentacles. When the tentacles are raised, they extend on the plane of the velum to form a sort of filter, for more efficient monitoring of the incurrent flow; when they are relaxed, they bend down towards the branchial chamber. As they lack internal musculature, their movements depend on a combination of factors, such as blood pressure and the activity of siphon muscles.

The coronal organ forms a continuous row along the margin of the velum, the lateral borders, and the tips of the tentacles (Fig. 1A). In cross-section, the two sensory areas lie on the lateral upper borders of the tentacles and are thicker than the remaining epithelium. The entire epithelium is simple, with cells interconnected apico-laterally by tight junctions, resting on a thick basal lamina bathed by blood. Several haemocytes and nervous fibres, but no muscle, lie inside the tentacles. Most of the epithelial cells are seen by SEM to bear a single cilium but no microvilli, unlike

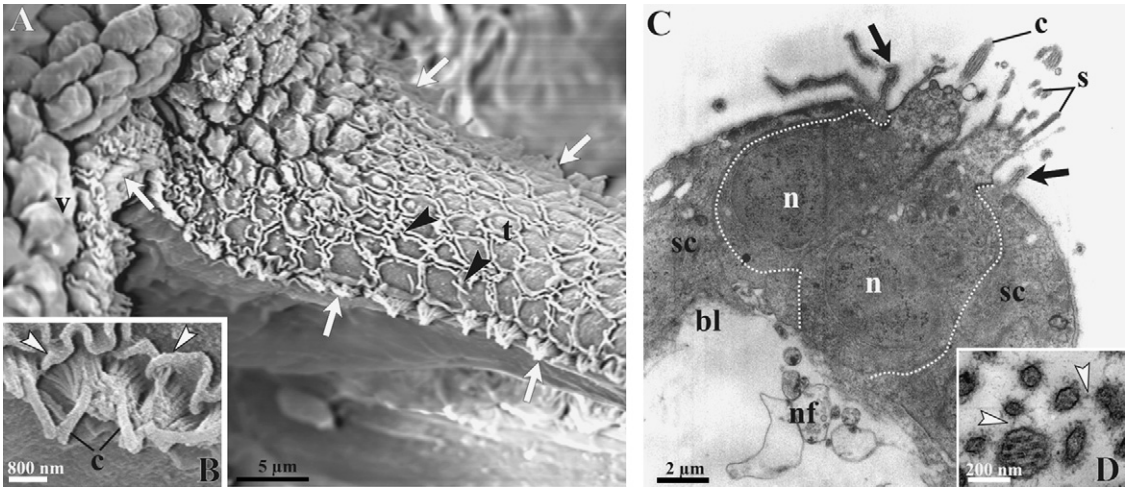

Fig. 1. Hair cells in *Botrylloides leachi*. (A and B) Scanning electron microscopy. (A) Coronal organ is formed of hair cells (white arrows), running in a continuous row along the border of tentacle (t) and velum (v). Black arrowheads: isolated cilia of epithelial cells. (B) Apices of coronal cells to show one cilium (c) per cell emerging among corolla of stereovilli. Sensory area appears as a groove limited by cytoplasmic extensions of supporting cells (white arrowheads). (C and D) Transmission electron microscopy. (C) Coronal cells (white spots) are flanked by supporting cells (sc), whose protrusions (arrows) define apical area of sensory cells. Sections of cilia (c) are recognizable among stereovilli (s). Several nerve fibres (nf) run in close proximity to the base of sensory cells. bl: basal lamina; n: sensory cell nucleus. (D) Cilium and stereovilli are interconnected by thin microfibillar bridges (white arrowheads).

the coronal cells, all of which bear a cilium emerging at the centre or side of a tuft of stereovilli (Fig. 1B). The nervous fibres closely approach only the sensory cells. Supporting cells flank the sensory cells; on both sides of the sensory row, they extend the plasmalemma to form a lamina which defines the groove hosting the apical apparatus of the sensory cells (Fig. 1B and C).

Coronal cells are cylindrical, slightly restricted at apex and base, in such a way that the supporting cells become C-shaped by adhering to them. Often two sensory cells are visible in the cross-section of the same row (Fig. 1C). They have nuclei in the basal region, glycogen granules, scattered mitochondria, and RER cisternae. The single cilium has the classical microtubular arrangement, 9 + 2, and the basal body has attached striated rootlets. It is accompanied by stereovilli, about half the length of the cilium itself. Numerous fibrils extend radially from the plasmalemma of the stereovilli and cilium, interconnecting all the apical components (Fig. 1D). On the opposite side, the plasmalemma is closely associated to bundles of neurites, probably coming from, or directed to, the cerebral ganglion, where the somata are presumably located. No coronal cell was seen to send axonal extensions towards the centre, as primary sensory cells typically do. Clusters of small vesicles, occasionally seen close to thick apposing plasmalemmata of neurites and sensory cells, were indicative of synapses, as reported for other ascidians [10].

4. Discussion

Because variability was found in the previously examined ascidians, analysis of new species, such as *Botrylloides leachi* can help to better define the characteristics of coronal organs in these animals and, in general, our understanding of the evolutionary pattern of coronal cells. The species has a coronal organ with two kinds of sensory cells: one with a cilium at the centre of a corolla of stereovilli, and one with a cilium by the side of a group of stereovilli; a pattern found also in other botryllids [4]. Sensory cells are flanked by supporting cells, which extend their plasmalemma to form the groove hosting the hair bundles. As in the majority of ascidians so far investigated, coronal cells establish synapses with neurites. Thus the data on *B. leachi* support the idea that species within the Pleurogona have more complex coronal organs than those in the Enterogona [13], both in terms of having several kinds of sensory cells and in the presence and arrangement of the stereovilli. Coronal cells are able to detect particles entering the oral siphon with inflowing water and trigger a 'crossed response' (i.e. contraction of the atrial siphon) or squirting, and some degree of particle rejection [11]. Their role, as mechanoreceptors, reveals a functional similarity with vertebrate hair cells.

Hair cells are the sensory component in a variety of vertebrate mechanoreceptor organs, and are used for sensing disturbances in water, head rotation, gravity, and hearing. They are secondary sensory cells which make direct contact with the axons of the nearby ganglion neurons which feed information to brain centres. Both hair cells and neurons originate from neural placodes. Although hair cells have been intensively analysed in vertebrates, their ancestry and phylogeny are not fully understood. For this, the non-vertebrate chordates are the appropriate reference. Cephalopod molluscs also have secondary sensory cells, but these are not considered homologous to vertebrate hair cells [6]. The presence of hair cells in ascidians [4], and their obvious morphological similarity to vertebrate hair cells, have stimulated renewed debate concerning the early evolution of this type of receptor. Ascidian coronal cells vary in morphology between species, in some way parallelling the variability seen among vertebrates. This suggests that, as in vertebrates [6], there are differences between species in how these organs respond to differing stimuli and in the physiological response that results.

There is nevertheless a case to be made for the idea of a common origin for essentially similar secondary sensory cells in vertebrates and ascidians. Comparative studies show that coronal cells have fundamental similarities in all ascidian species so far investigated (seven from the Enterogona and five from the Pleurogona), suggesting that they represent a plesiomorphic condition for ascidians. They are located around the mouth, and find counterparts in both appendicularian tunicates [3] and cephalochordates [9]. Among vertebrates, secondary sensory cells are found in the ears, lateral line and derived electroreceptor organs, and extend broadly over the trunk and head, even reaching the mouth. Thus, from a positional point of view, there are similarities in the location of secondary sensory cells in tunicates, cephalochordates and vertebrates. Moreover, there is evidence for cell populations with at least some of the characteristics of placodes and neural crest in tunicates and cephalochordates [1,8,12,14], suggesting that the chordate ancestor at least possessed the genes necessary for specifying a primitive anterior pan-placodal region. Secondary sensory cells could then have evolved over time within these domains, so as to become incorporated into group-specific structures. In conclusion, based on several types of data (positional, morphological and developmental), there are good reasons to suggest that secondary sensory cells were present in the last common ancestor of modern chordates and that from these, the differing secondary mechanoreceptor cells in the three subphyla of extant chordates evolved. It is noteworthy that, despite their long independent evolution, vertebrate and ascidian hair cells have a remarkably similar range of morphologies [5,6,13], that probably evolved in response to similar selection pressures.

Acknowledgment

This study was supported by grants from the Italian *Ministero della Università e della Ricerca* to P.B.

References

[1] C.V.H. Baker, G. Schlosser, Editorial: the evolutionary origin of neural crest and placodes, J. Exp. Zool. B (Mol. Dev. Evol.) 304 (2005) 269–273.
[2] S. Bassham, J.H. Postlethwait, The evolutionary history of placodes: a molecular genetic investigation of the larvacean urochordate *Oikopleura dioica*, Development 132 (2005) 4259–4272.
[3] Q. Bone, Nervous system, sense organs, and excitable epithelia, in: Q. Bone (Ed.), The Biology of Pelagic Tunicates, Oxford University Press, Oxford, NY, 1998, pp. 55–80.

[4] P. Burighel, N.J. Lane, F. Gasparini, S. Tiozzo, G. Zaniolo, M.D. Carnevali, L. Manni, Novel, secondary sensory cell organ in ascidians: in search of the ancestor of the vertebrate lateral line, J. Comp. Neurol. 461 (2003) 236–249.
[5] F. Caicci, P. Burighel, L. Manni, Hair cells in an ascidian (Tunicata) and their evolution in chordates, Hear. Res. 231 (2007) 63–72.
[6] A. Coffin, M. Kelley, G.A. Manley, A.N. Popper, Evolution of sensory hair cells, in: G.A. Manley, A.N. Popper, R.R. Fay (Eds.), Evolution of the Vertebrate Auditory System, Springer-Verlag, New York, 2004, pp. 55–94.
[7] F. Delsuc, H. Brinkmann, D. Chourrout, H. Philippe, Tunicates and not cephalochordates are the closest living relatives of vertebrates, Nature 439 (2006) 965–968.
[8] W.R. Jeffery, Ascidian neural crest-like cells: phylogenetic distribution, relationship to larval complexity, and pigment cell fate, J. Exp. Zool. B (Mol. Dev. Evol.) 15 (2006) 470–480.
[9] T.C. Lacalli, Sensory systems in amphioxus: a window on the ancestral chordate condition, Brain Behav. Evol. 64 (2004) 148–162.
[10] G.O. Mackie, P. Burighel, The nervous system in adult tunicates: current research directions, Can. J. Zool. 83 (2005) 151–183.
[11] G.O. Mackie, P. Burighel, F. Caicci, L. Manni, Innervation of ascidian siphons and their resposes to stimulation, Can. J. Zool. 84 (2006) 1146–1162.
[12] L. Manni, N.J. Lane, J.S. Joly, F. Gasparini, S. Tiozzo, et al., Neurogenic and non-neurogenic placodes in ascidians, J. Exp. Zool. B (Mol. Dev. Evol.) 302 (2004) 483–504.
[13] L. Manni, G.O. Mackie, F. Caicci, G. Zaniolo, P. Burighel, Coronal organ of ascidians and the evolutionary significance of secondary sensory cells in chordates, J. Comp. Neurol. 495 (2006) 363–373.
[14] F. Mazet, J.A. Hutt, J. Milloz, J. Millard, A. Graham, et al., Molecular evidence from *Ciona intestinalis* for the evolutionary origin of vertebrate sensory placodes, Dev. Biol. 282 (2005) 494–508.

CONTRIBUTION C

Caicci F., Degasperi V., Gasparini F., Zaniolo G., Del Favero M., Burighel P., Manni L. 2010b

Variabilty of hair cells in the coronal organ of ascidians (Chordata, Tunicata)

Can. J. Zool. Submitted

TITLE: VARIABILITY OF HAIR CELLS IN THE CORONAL ORGAN OF ASCIDIANS (CHORDATA, TUNICATA).

NAMES: CAICCI FEDERICO*, DEGASPERI VALENTINA*, GASPARINI FABIO*, ZANIOLO GIOVANNA*, DEL FAVERO MARCELLO*, BURIGHEL PAOLO*, MANNI LUCIA*.

INSTITUTIONAL AFFILIATIONS: *Department of Biology, University of Padova, via U. Bassi 58/B, 35121 Padova, Italy.

Emails: federico.caicci@unipd.it; valentina.degasperi@unipd; fabio.gasparini@unipd.it; marcello.delfavero@unipd.it; zaniolo@bio.unipd.it; paolo.burighel@unipd.it; lucia.manni@unipd.it

CORRESPONDING AUTHOR: Valentina Degasperi, Department of Biology, University of Padova, via U. Bassi 58/B, 35121 Padova, Italy; tel. +39 049 8276252; fax: +39 049 8276199; e-mail: valentina.degasperi@unipd.it

RUNNING TITLE: Hair cells in Ascidians.

KEY WORDS: ascidians, coronal organ, neural placodes, oral siphon, sensory system, tentacles.

Autors: Caicci F., Degasperi V., Gasparini F., Zaniolo G., Del Favero M., Burighel P., Manni L.

Title: **Variability of hair cells in the coronal organ of ascidians (Chordata, Tunicata).**

Abstract

The tunicate ascidians are non-vertebrate chordates, viewed as an elective group for studying evolution of features, such as the anterior paired sensory organs, considered essential for the radiation of vertebrates. Ascidians possess mechanoreceptor cells in the coronal organ in the oral siphon, monitoring the incoming water flow. Like vertebrate hair cells, they are secondary sensory cells (axonless cells forming afferent and efferent synapses with neurons, the somata of which are located centrally). The coronal cells are accompanied by supporting cells and exhibit morphological diversities of apical specialisations: they are multiciliate, in ascidians of the order Enterogona whereas they in the other order (*i.e.* Pleurogona) they are more complex and possess one or two cilia accompanied by stereovilli, also graded in length. In morphology, embryonic origin, and arrangement, coronal cells closely resemble vertebrate hair cells. Here we present the coronal organs of five ascidians, belonging to Pleurogona, also comprising species of one family (Pyuridae) not yet considered and thus completing our over view of the order. Each species possesses at least two kinds of secondary sensory cells, some of them characterised by stereovilli graded in length. These mechanoreceptor secondary sensory cells appear a plesiomorphic feature of ascidians and, possibly, also of tunicates. We compare the coronal organ in both ascidians and with other chordate sensory organs formed of secondary sensory cells, and discuss their possible homologies.

1. Introduction

Ascidiacea, the main class of Tunicata (or Urochordata), contains sessile, filter-feeding animals, and occupies a privileged position as regards insights into the origins of vertebrates, since study of comparative anatomy and molecular phylogenesis of ascidians place them in a sister group of vertebrates (Dufour et al. 2006). Their anatomy is relatively simple and, together with cephalochordates (e.g. amphioxus), they are non-vertebrate chordates, which have been extensively studied in recent years in order to understand the evolution of the key characters of vertebrates (table 1). The anterior paired sense organs are probably structures which facilitated the evolution of active predation by vertebrates. Developmentally, these sensory organs are derived from tissues the neural crest and cranial placodes classically considered to be unique to vertebrates.. However, recent evidence of placode homologs in tunicates have cast doubt on their status as vertebrate synapomorphies (Manni et al. 2001; Bassham and Postlethwait 2005; Mazet et al. 2005).

An important contribution for elucidating the appearance and evolution of paired sense organs and cranial placodes in vertebrates comes from the study of sensory structures in ascidians. Adult ascidians have a sac-like body, provided with an oral (incurrent) and an atrial (excurrent) siphon. The siphons are the regions most sensitive to tactile stimulation, and primary sensory neurons, each with a single axon that goes to the brain, are located around the rims of the siphons and in complex organs (cupular organs, capsular organs, cupular strand) inside the atrial chamber (Mackie and Burighel 2005; Mackie et al. 2006). A new sensory structure, the coronal organ, has recently been found in the tentacles and velum of the oral siphon of ascidians of all groups so far examined (Burighel et al. 2003, 2008; Caicci et al. 2007; Manni et al. 2006). The organ

is of exceptional interest because its sensory cells are axonless, secondary sensory units, which make both afferent and efferent synapses with neurons whose somata lie centrally in the brain. Neurophysiological studies have shown that these coronal sensory cells are mechanoreceptors, able to detect particles entering with inflowing water (Mackie et al. 2006). Although the picture of the relationships of chordate secondary sensory elements is incomplete, it has been suggested that ascidian and vertebrate hair cells share a common origin in the chordate ancestor, and that the various groups of chordates used pre-existing secondary mechanoreceptors which, over time, became incorporated into group-specific structures (Manni et al. 2004, 2006).

Ascidians are classically distinguished into the two orders of Enterogona and Pleurogona. Previous studies on several species belonging to the order Enterogona have shown that all of them have a coronal organ, formed of ciliated coronal cells lacking typical apical stereovilli and composing synapses with neurites at their bases.. In some species, the sensory cells are accompanied by large cells involved in the synthesis and secretion of proteins (Mackie et al. 2006; Manni et al. 2006). Differently, in the Pleurogona ascidians so far investigated (Burighel et al. 2003, 2008; Caicci et al. 2007; Manni et al. 2004), sensory cells are called hair cells, because they bear many actin-filled microvilli (stereovilli) surrounding or grouped to one side of a single cilium (or a couple of cilia). In particular, in *Styela plicata* (Lesueur, 1823) and *Molgula socialis* Alder, 1848 (Caicci et al 2007; Manni et al. 2004): the stereovilli are graded in length, more than one type of hair cell is present in the same species, and the supporting cells form a groove into which the hair bundles project. The differences between Enterogona and Pleurogona species may be due to different branchial functions in the two orders: it is known that pleurogons have a more complex branchial apparatus and are more

efficient in filtering (Fiala-Medioni 1974): thus, the coronal organ, like the branchial sac, may have evolved more complex organisation. Conversely, as only the atrium of Enterogona contains complex mechanoreceptor organs (Mackie and Burighel 2005), it has been hypothesised that these atrial sensory devices fulfil part of the mechanoreceptor function which, in Pleurogona, depend completely on the coronal organ (Manni et al. 2006). This matches the presence of relatively simple sensory cells in Enterogona, compared with the more sophisticated hair cells in Pleurogona. Therefore, here we extend study to new Pleurogona species, to complete analysis of representatives of all the main taxa of the order, confirming the presence of coronal hair cells in the whole group. We also verify whether a common scheme can be identified in the coronal organ organisation and coronal cell structure of ascidians.

The species described here are both solitary (*Pyura haustor* (Stimpson, 1864) *Pyura stolonifera* (Heller, 1878), *Styela gibbsii* (Stimpson, 1864) and *Styela montereyensis* (Dall, 1872)) and colonial forms (*Polyandrocarpa zorritensis* (Van Name, 1931)), with branched (*P. haustor*, *P. stolonifera*) and unbranched tentacles (*S. gibbsii*, *S. montereyensis* and *P. zorritensis*). Two species (*P. haustor* and *P. stolonifera*), belonging to the Pyuridae family, have not yet been analysed. Previously described Pleurogona species belong to the other two families of the suborder (Styelidae and Molgulidae) (Burighel et al. 2003, 2008; Caicci et al. 2007; Manni et al. 2004). Therefore, this paper furnishes an overview of all the families of Pleurogona and allows a comparative analysis of variability of mechanoreceptor cells in ascidians.

2. Materials and methods

119 *2.1 Animals*

120 Specimens of *P. haustor* (family Pyuridae), *S. gibsii* and *S. montereyensis*
121 (family Styelidae, subfamily Styelinae) were collected at Friday Harbor (WA, USA).
122 Specimens of *P. stolonifera* (family Pyuridae) come from Queenscliff Marine Station
123 (Victoria, Australia) and specimens of *P. zorritensis* (family Styelidae, subfamily
124 Polyzoinae) from the port of Taranto (Southern, Italy).
125
126 *2.2 Transmission electron microscopy*
127 Specimens were anesthetised with 0.02 % MS222 at 4°C. After complete
128 relaxation of the siphon, specimens were fixed in 1.5% glutaraldehyde buffered with
129 0.2M sodium cacodylate, pH 7.4, plus 1.7% NaCl. After washing in buffer, their tunic
130 was removed and specimens were dissected, with surgical forceps, to isolate the area of
131 the oral siphon.
132 After post-fixation in 1% OsO_4 in 0.2M cacodylate buffer, specimens were
133 dehydrated and embedded in Epon Araldite 812. Thick sections (1 μm) were
134 counterstained with toluidine blue; thin sections (70nm) were given contrast by staining
135 with uranyl acetate and lead citrate. Micrographs were taken with a Hitachi H-600
136 electron microscope operating at 75KV. All photos were acquired with an Epson
137 scanner 1200, and collected and typeset in Corel Draw X3.
138
139 *2.3 Scanning electron microscopy*
140 Specimens were fixed in glutaraldehyde solution and dissected as described for
141 transmission electron microscopy. After post-fixation and dehydration, they were
142 critical-point dried, sputter-coated with gold, and observed under a Cambridge

Stereoscan 260 electron microscope. Micrographs were acquired and typeset in Corel Draw X3.

3. Results

3.1 Anatomy and organisation of tentacles and coronal organs

The histological organisation of the inner side of the oral siphon, i.e. the region lying between and comprising the external rim of the siphon and the ring of the velum and tentacles, was analysed in five species of the order Stolidobranchiata: the solitary species *P. haustor, P. stolonifera*, *S. gibsii* and *S. montereyensis* (Figs.1-4) and the colonial species *P. zorritensis* (Fig. 5).

The epithelium lining the internal wall of the siphon is continuous with the external epidermis, and is covered by a layer of tunic which terminates as a thin sheet at the base of the velum and tentacles. All species have tentacles arranged in a ring at the base of the siphon, the number of which generally, varies according to the species, dimension and age of the animal.

In the two Pyuridae species, the tentacles have a branched profile (Fig. 2A and B). Typically, in each tentacle, a number of second-order branches departs from a central axis (first-order branch) and bears smaller, third-order branches, which in turn bear tiny fourth-order branches. In species of the genus *Styela* (Fig. 4A and B) and in *P. zorritensis* (Fig. 5A), the tentacles are not branched but have different lengths. They may be grouped in various orders: the largest ones are designated as first-order tentacles, and the succeeding groups as second-, third-, etc. orders (Millar 1953).

On the surface facing the rim of the siphon, all the examined species have a continuous row of sensory cells running along the outer border of the velum and each

tentacle, representing the coronal organ. This is of the simple type, i.e. consisting only of ciliated cells, accompanied by supporting cells. Coronal organs of the compound type of enterogonids (Manni et al. 2006; Mackie et al. 2006), consisting of sensory cells flanked by secretory cells other than typical supporting cells, were not found. Characteristic, C-shaped, non-ciliated supporting cells always flank the sensory cells; they mainly differ from contiguous epithelial cells in their shape (e.g., Figs. 3B and 4D). Two kinds of sensory cells, in contact with neurites at their base, were identified in the coronal organs: uni-ciliated sensory cells characterised by conventional microvilli, and bi-ciliated sensory cells with typical stereovilli, i.e., actin-filled, rigid rods (thicker and taller than microvilli) paralleling the cilia, with secretory granules in their cytoplasm. The latter cells (present in two types in Pyuridae and Styelidae) are located on the inner side of the tentacle and velum, whereas the former are located on the external border. In addition, all the cells of the velum and tentacles, both sensory and non-sensory, are joined apico-laterally to each other by dense tight junctions (Figs. 3C-D and 4E). As well as to the sensory cells, uni-ciliated cells are often seen scattered on the surface of tentacles, but never touching the neurites at their bases (Figs. 2D and 5C).

As the coronal organ possesses comparable features in species belonging to the same genus, we describe here its organisation in the three genera. We present in detail the coronal organ in the *Pyura* genus as a model, noting the salient features in the other genera.

3.2 P. haustor *and* P. stolonifera

In the coronal organ, supporting cells possess a number of supranuclear, large vacuoles containing a loose matrix and an apical, thin glycocalyx (Fig. 3A and B); these

features also occur on contiguous epithelial cells but not on sensory cells. Unlike the common epithelial cells, the supporting cells are taller, and curved round so as to enclose the sensory cells partially (Figs. 2B and C, 3A, B and E).

The sensory coronal hair cells are arranged to form parallel rows of 2 to 7 contiguous cells (Fig. 2C). The peripheral sensory cells have one cilium central to the group of short microvilli (type 1 sensory cells) (Figs. 2D, 3B and C). The sensory cells with stereovilli, located on the inner side of the tentacle, show two types of apical bundles: the stereovilli may lie on one side (type 2 sensory cells) (Fig. 2E) or as a ring around the two cilia (type 3 sensory cells), in both cases, they are graded in length, the longer stereovilli being close to the cilia (Fig. 2E and F). Type 2 and type 3 sensory cells are randomly distributed in the organ. The stereovilli are stiff, unbranched, and filled with microfilaments continuous with those of the apical cytoplasm. Several coat fibrils extend radially, to establish connections between adjacent stereovilli and between stereovilli and ciliary shafts (Fig. 3D). Each cilium has a conventional 9+2 microtubular arrangement, with a dense, short, basal body, from which poorly developed ciliary rootlets extend; a second centriole is sometimes recognisable, lying perpendicularly to the first one (Fig. 3C).

Type 2 and type 3 sensory cells are cylindrical, with a large basal nucleus and scattered mitochondria. In the supranuclear region, there are numerous, parallel cisternae of rough endoplasmic reticulum; the Golgi complex is apical and composed of a stack of cisternae budding many small granules. Granules also lie close to the apical cell membrane (Fig. 3C and D), and aspects of granular secretion can be observed. The cytoplasmic organelles are less developed in the sensory cells of type 1, which lack secretory granules.

The basal plasmalemma of each sensory cell lies on a basal lamina, extending as a continuous fibrous layer to support both sensory and epithelial cells (Fig. 3E-G). The basal plasmalemma of sensory cells forms a groove, where the typical extracellular matrix is absent. Instead, the groove contains neuritis, and neural synapses are occasionally seen. Most of the latter are clearly identifiable as afferent synapses, due to the presence of synaptic vesicles in the sensory cell cytoplasm adjacent to the synaptic membrane junctions (Fig. 3F-G). Efferent synapses, by contrast, are less clearly defined but still recognisable, due to the presence of synaptic vesicles on the neurite side of the junction, whereas the post-synaptic membrane belongs to the sensory cells.(Fig. 3H).

In one section, a sensory cell with typical features of mitosis was observed (Fig. 3E). It was adjacent to a supporting cell, its nucleus lacked a nuclear membrane, and it had condensed chromatin; apically, it bears some microvilli (i.e. belonged to the type 1 sensory cell) and had a groove at its base containing a thin neurite establishing a synapsis with it (Fig. E, inset). The adjacent sensory cells had a conventional aspect.

3.3 S. gibsii *and* S. montereyensis

These species display similar coronal organs (Fig. 4A-C) which, in transverse section, show 4-5 cylindrical cells forming a button-like thickening (Fig. 4D).

The same types of sensory cells described for Pyuridae are present (Fig 4B-E). The peripheral ones have a single cilium flanked by a bundle of short microvilli of similar length (type 1); most of the central ones have two cilia situated to one side of a crescent-shaped bundle of stereovilli graded in length, with the longest ones in the middle (type 2); a few possess a complete ring of stereovilli around the two cilia (type 3). Type 2 and type 3 cells have a supranuclear region characterised by a Golgi

complex, mitochondria and many secretory granules (Fig. 4E-F).The ciliary membranes are also connected to the surrounding stereovilli by extracellular radial filaments. The sensory cells are flanked by supporting cells whose apical surfaces, covered by a glycocalyx, are raised, so as to form an elongated ridge defining the apices of the hair cells (Fig. 4E).

Groups of neurites lie in the groove formed by the basal plasmalemma, and have small electron-dense granules and microtubules (Fig. 4G). Some of them establish typical afferent synapses with sensory cells at their bases, and make efferent synapses with other neurites.

3.4 P. zorritensis

In *P. zorritensis*, unlike the with other species, the supporting cells of the coronal organ show variations according to their position (Fig. 5B-E): those facing the base of the velum or the middle line of the tentacles (mostly exposed to inflowing water) present a thick, apical cytoplasmic evagination, which defines the hair bundle of adjacent sensory cells. This evagination is reduced in the supporting cells located on the opposite side (on the outer side of the velum and tentacles).

Seen in transverse section, the sensory area is composed of 3-4 cells; the peripheral sensory cells have a single cilium among a bundle of short microvilli of similar length (type 1 sensory cells), whereas the central ones have two cilia lying to one side of a crescent-shaped bundle of stereovilli graded in length (type 2 sensory cells). The latter are characterised by apical secretory granules (Fig. 5E). A basal groove containing nerve fibres is present, and afferent synapses were observed (Fig. 5F).

4. Discussion

4.1 Variability in ascidian hair cells

So far, the coronal organ has been described in twelve species belonging to the two orders of ascidians (Enterogona and Pleurogona) (Burighel et al. 2003, 2008; Caicci et al. 2007; Mackie et al. 2006; Manni et al. 2004, 2006). In the present study, the coronal organ is analysed in detail in five selected species of the order Pleurogona, in such a way as to complete the analysis of the three families forming it (Table 2). Several data indicate that two orders of ascidians diverged very early and that they differ in their relationship with the other taxa of tunicates. In particular, molecular evidence is accumulating supporting the paraphyletic nature of ascidians, Pleurogona together with appendicularians representing a the sister group of Enterogona, together with the thaliaceans (cfr. Table 1) (Delsuc et al. 2006, 2008; Putnam et al. 2008; Tsagkogeorga et al. 2009). This evidence must be taken into account when examining the evolution of coronal hair cells and their variability.

In the five species considered here, the general structure of the ascidian coronal organ and sensory cells is maintained: the organ lies on the borders of the velum and tentacles, always exposed to the incoming water flow; it is formed of ciliated sensory cells, aligned side by side in a linear array, the status of which as secondary sensory cells is indicated by the presence of both afferent and efferent synapses. In addition, like other Pleurogona ascidians, the five species possess coronal cells which clearly qualify for the designation “hair cell”, since they also possess graded stereovilli (Fig. 6). Although the afferent and efferent synapses are not always clearly distinguishable, presumably because of their small size, we are confident that they represent a feature common to all coronal cells. Axons were never seen directly emerging from coronal

cells, nor were neuronal somata observed anywhere in the vicinity of the coronal organ. Although the neurites involved in these junctions have not been traced individually to their origins, it may be assumed that the cell bodies are located in the cerebral ganglion, as nerve tracts running from the ganglion to peripheral locations never contain cell bodies (Mackie and Burighel 2005).

The coronal organ in *P. haustor*, *P. stolonifera*, *S. gibsii* and *S. montereyensis* recalls that of *Molgula socialis* (Pleurogona, Stolidobranchiata) (Caicci et al. 2007), due to the presence of the three types of sensory cells and, with respect to the coronal organ so far described in ascidians, it presents greater complexity. Large variability is found within species belonging to the family Styelidae (Pleurogona, Stolidobranchiata) which comprises the subfamilies Styelinae, Polyzoinae and Botryllinae (Table 2). Other than *S. gibsii* and *Styela montereyensis* (subfamily Styelinae) and *P. zorritensis* (subfamily Polyzoinae) presented here, the previously studied species are *Styela plicata* (Lesueur, 1823) (subfamily Styelinae) (Manni et al., 2004), *Botryllus schlosseri* (Pallas, 1766), *Botrylloides violaceus* (Oka, 1927) and *Botrylloides leachi* (Savigny, 1816) (Botryllinae family) (Burighel et al., 2003, 2008). Therefore, the present study completes information on all three subfamilies of Styelidae. Whereas *S. gibsii* and *S. montereyensis* have three types of coronal cells, the other species have only two types of sensory cells: with microvilli (type 1) and a crescent of stereovilli graded in length (type 2) in *S. plicata* and *P. zorritensis*, with a cilium emerging at the centre or at the side of a tuft of stereovilli of equal length in *B. schlosseri*, *B. leachi* and *B. violaceus*. This variability probably represents adaptations to the ability to respond to different stimuli, such as particles of various sizes and/or variations in water flow. Variability is also common in vertebrate hair cells, where cells with different location, morphology and

311 type of neurons innervating them display different functional ability (Manley and
312 Ladher 2008). Neurophysiological experiments in ascidians have evidenced that the oral
313 tentacles can detect large particles entering with inflowing water, causing either crossed
314 responses (contraction of atrial siphon, while the oral siphon stays open, as a
315 consequence of mechanical stimulation of tentacles) or squirting (all-or-none response,
316 which causes a violent ejection of water and particles from the oral siphon and atrial
317 water from the atrial siphon), and some degree of particle rejection. Conversely, the
318 primary sensory cells in the epidermis of the oral siphon are sensitive to tactile
319 stimulation of oral siphon and vibration (Mackie et al. 2006).
320 Some diversity also regards the supporting cells. These resemble the tentacular
321 epithelial cells, but their lateral plasmalemma adheres to adjacent sensory cells forming,
322 in pleurogonids (Burighel et al. 2003, 2008; Manni et al. 2004; present work) and some
323 enterogonids (Mackie et al. 2006; Manni et al. 2006), an apical lamina, defining a
324 groove occupied by an apical extension of the sensory coronal apparatus. It should be
325 noted that some Enterogona species lack this specialisation. In this study we found that
326 supporting cells in *P. zorritensis* are polarised with respect to organ orientation, since
327 the inner supporting cells (facing the middle of the tentacle) possess an expanded, apical
328 lamina defining sensory bundles, whereas the outer supporting cells have a shorter,
329 apical lamina bordering the sensorial microvilli of type 1 sensory cells. This
330 specialisation has been previously reported only in *Molgula socialis* Alder, 1848 (Caicci
331 et al. 2007). We hypothesise that supporting cells differently oriented with respect to the
332 water flow are a useful device to guide the water flow towards the stereovilli, favouring
333 the formation of laminar flows over them, for better perception of particles entering the
334 branchial basket.

In the species presented here, type 2 and type 3 sensory cells are always characterised by signs of protein synthesis and contain granules scattered through the cytoplasm -- mainly in the middle-apical region, but also very close to the apical plasmalemma. Coronal cells with cytoplasmic granules have been found among Enterogona (Manni et al. 2006) and Pleurogona (Manni et al. 2004; Caicci et al. 2007) and it is hypothesised that they are secreted following stimulation of sensory cells.

In conclusion, this overview on Pleurogona stresses the differences between Enterogona and Pleurogona coronal cells -- mainly the constant presence of hair cells in Pleurogona and their absence in Enterogona. However, the gross anatomy of the organ (cell arrangement, location on the tentacles and velum) and its cellular organisation (presence of cilia; presence of afferent and efferent innervations) remain common features of the coronal organ of all ascidians. Therefore, in view of the long, parallel evolution of the two orders, the ascidians may have evolved different mechanisms for detecting particles and/or water flow, based both on a ciliated coronal organ and on atrial mechanoreceptor organs in Enterogona, and exclusively on a coronal organ with hair cells in Pleurogona.

4.2 Ascidian hair cells can divide mitotically

The finding of a mitotic coronal cell in *P. haustor* requires attention, due to the great interest in the regenerative potential of inner ear hair cells in vertebrates. Whereas mammals have limited hair cell regeneration (with obvious repercussions on hearing loss as a consequence of damage to or death of the sensory cells in the inner ear), in other vertebrates hair cells are able to regenerate, thanks to the proliferation of supporting cells. The latter can re-enter the mitotic cycle forming daughter cells, which

either differentiate into hair cells of supporting cells, or directly transdifferentiate, changing their gene expression and converting into hair cells without dividing (Edge and Chen 2008). In fish, the hair cells of the lateral line organ can regenerate mainly by division of supporting cells and subsequent differentiation into new hair cells (Behra et al., 2009). Moreover, in adult fish, additional neuromasts continuously form and are thought to originate from pre-existing ones, thanks to the migration of supporting cells to their new location (Ghysen and Dambly-Chaudiere 2007). In our opinion, the presence of mitotic hair cells in *P. haustor* indicates the continuous increase in number and length of tentacles during the life-span of the animal, considering how tiny it is when it settles and how short and few its tentacles are in juvenile. In addition, in this species, the coronal cells are located in rows, the number of which increases from the base of the tentacles toward their tips; therefore, during tentacle elongation, hair cells must multiply not only to grow but also to increase the width of the coronal organ. Surprisingly, mitotic cells in *Pyura* are not coronal supporting cells but sensory, as evidenced by the presence of the apical sensorial apparatus and the synaptic junction at its base. This suggests that, in ascidians, hair cells in adults maintain the proliferative ability that is lacking in vertebrates -- a question which should be more deeply investigated.

4.3 Evolution of hair cells in chordates

The number of ascidian species so far investigated, seven Enterogona and ten Pleurogona, belonging to representative taxa, and all possessing a coronal organ, suggests that this sensory organ is a plesiomorphic condition of ascidians. It also offers interesting elements for extending examination to the origin and evolution of

hair cells in chordates, a topic extensively treated in previous papers (Manni et al., 2006). In short, there are resemblances not only in the morphology but also in topology of secondary sensory cells in tunicates, cephalochordates and vertebrates: coronal cells are located around the mouth and find counterparts in both appendicularian tunicates (Bone 1998) and cephalochordates (Lacalli 2004). Among vertebrates, secondary sensory cells occur in the ears, lateral line and derived electroreceptor organs, and extend broadly over the trunk and head, also reaching the mouth.

From a developmental point of view, various data indicate that cell populations showing the characteristics of placodes or neural crests occur not only in vertebrates, but also in tunicates and cephalochordates. Recent papers on amphioxus show the presence of both individually migrating cells in the embryonic ectoderm destined to differentiate sensory neurons, which mimic neural crest cells and placode-derived sensory cells in vertebrates, and homologs of most vertebrate genes involved in the putative neural crest/placodes gene regulatory network (Benito-Gutiérrez et al. 2005; Meulemans and Bronner-Fraser 2007; Rasmussen et al. 2007; Kaltenbach et al. 2009; Yu et al. 2009). In ascidians, the assignment of homology of the ascidian atrial primordium to the vertebrate otic placode rests on aspects of embryonic development and on the similarity of combinatorial gene expression (Mazet et al. 2005; Bassham et al. 2008), and also on the signalling requirement during induction of the placode and its differentiation (Kourakis and Smith 2007).

In conclusion, developmental and morphological data are progressively accumulating in support of the possible homology between secondary sensory cells in chordates, especially in the light of the new concept of homology discussed in

recent years (Manley and Ladher 2008). Although further studies on the morphology and genetic control of ontogeny of these cells and their surrounding structures are necessary to enable firmer conclusions to be reached, all the data so far reported match the idea that the chordate ancestor possessed a gene network for specification of a primitive anterior pan-placodal region (as suggested by Schlosser 2005; see also Schlosser 2008), from which secondary sensory cells also evolved over time, becoming incorporated into group-specific structures.

Acknowledgements

This study was supported by grants from the Italian *Ministero della Università e Ricerca Scientifica e Tecnologica* to P.B. and L.M. For species collection and determination, we thank Prof. G.O. Mackie (*Pyura* and *Styela* genera) and Prof. R. Brunetti (*P. zorritensis*).

421 **References**

422 Bassham, S., Postlethwait, J.H., 2005. The evolutionary history of placodes: a molecular
423 genetic investigation of the larvacean urochordate *Oikopleura dioica*. Development
424 **132**(19), 4259-4272. doi: 10.1242/dev.01973.
425 Bassham, S., Cañesto C., Postlethwait, J.H., 2008. Evolution of developmental roles of
426 *Pax* 2/5/8 paralogs after independent duplication in urochordate and vertebrate
427 lineages. BMC Biology **6**, 35. doi: 10.1186/1741-7007-6-35.
428 Behra, M., Bradsher, J., Sougrat, R., Gallardo, V., Allende M.L., Burgess, M.B., 2009.
429 *Phoenix* is required for mechanosensory hair cell regeneration in the zebrafish
430 lateral line. Plos Genetics **5**(4), 1-14. doi: 10.1371/journal.pgen.1000455.
431 Benito-Gutiérrez, E. Nake, C. Llovera, M. Comella, J. X. Garcia-Fernandez, J., 2005.
432 The single AmphiTrk receptor highlights increased complexity of neurotrophin
433 signalling in vertebrates and suggests an early role in developing sensory
434 neuroepidermal cells. Development **132**(9), 2191-2202. doi: 10.1242/dev.01803.
435 Bone Q., 1998. Nervous system, sense organs, and exitable epithelia. *In* The Biology of
436 Pelagic Tunicates. *Edited by* Q.Bone. Oxford University Press, Oxford. pp:55-80.
437 Burighel, P., Lane, N.J., Gasparini, F., Tiozzo, S., Zaniolo, G., Carnevali, M.D., Manni,
438 L., 2003. Novel, secondary sensory cell organ in ascidians: in search of the ancestor
439 of the vertebrate lateral line. J. Comp. Neurol. **461**, 236–249.
440 doi:10.1002/cne.10666.
441 Burighel, P., Caicci F., Zaniolo G.,Gasparini F., Degasperi V., Manni, L., 2008. Does
442 hair cell differentiation predate the vertebrate appearance? Brain. Res. Bull. **75** 331–
443 334. doi:10.1016/j.brainresbull.2007.10.012.

444 Caicci F., Burighel P., Manni L., 2007. Hair cells in an ascidian (Tunicata) and their
445 evolution in chordates. Hear. Res. **231**, 63–72. doi: 10.1016/j.heares.2007.05.007.
446 Delsuc, F., Brinkmann, H., Chourrout, D., Philippe, H., 2006. Tunicates and not
447 cephalochordates are the closest living relatives of vertebrates. Nature **439**, 965-968.
448 doi:10.1038/nature04336.
449 Delsuc, F., Tsagkogeorga, G., Lartillot, N., Philippe, H., 2008. Additional molecular
450 support for the new chordate phylogeny. Genesis **46**, 592-604.
451 doi:10.1002/dvg.20450.
452 Dufour, H.D., Chettouh, Z., Deyts, C., de Rosa, R., Goridis, C., Joly, J.S., Brunet, J.F.,
453 2006. Precraniate origin of cranial motoneurons. Proc. Natl. Acad. Sci. U.S.A. **103**,
454 8727-8732. doi:10.1073/pnas.0600805103
455 Edge, A.S., Chen, Z.Y., 2008. Hair cell regeneration. Curr. Opin. Neurobiol. 18 (4),
456 377-382.doi:10.1016/j.conb.2008.10.001.
457 Fiala-Medioni, A., 1974. Ethologie alimentaire d'invertébrés benthiques filtreurs
458 (ascidies). II. Variations des taux de filtration et de digestion en fonction de
459 l'espèce. Mar. Biol.**28**, 199-206.
460 Ghysen, A. Dambly-Chaudière, C., 2007. The lateral line microcosmos. Genes Dev. **21**,
461 2118-2130. doi:10.1101/gad.1568407.
462 Kaltenbach, S.L., Yu, J.K., Holland, N.D., 2009. The origin and migration of the
463 earliest-developing sensory neurons in the peripheral nervous system of amphioxus.
464 Evol. Dev. **11**(2), 142-151. doi:10.1111/j.1525-142X.2009.00315.
465 Kourakis, M.J., Smith, W.C., 2007. A conserved role for FGF signalling in chordate
466 otic/atrial placode formation. Dev. Biol. **312**(1), 245-257.
467 doi:10.1016/j.ydbio.2007.09.020.

468 Lacalli, T.C., 2004. Sensory systems in amphioxus: a window on the ancestral chordate
469 condition. Brain Behav. Evol. **64**, 148-162.doi:10.1159/000079744.
470 Mackie, G.O., Burighel, P., 2005. The nervous system in adult tunicates: current
471 research directions Can. J. Zool. **83**, 151-183. doi:10.1139/Z04-177.
472 Mackie, G.O., Burighel, P., Caicci, F., Manni, L., 2006. Innervation of ascidian siphons
473 and their resposes to stimulation. Can. J. Zool. **84**, 1146-1162. doi:10.1139/Z06-
474 106.
475 Manley, G.A., Ladher, R., 2008. Phylogeny and evolution of ciliated mechano-receptor
476 cells. *In* The senses: a comprehensive reference, vol 3, audition. *Edited by* P.
477 Dallos and D. Oertel. Academic press, San Diego. pp. 1-34.
478 Manni, L., Lane, N.J., Burighel, P., Zaniolo, G., 2001. Are neural crest and placodes
479 exclusive to vertebrates? Evolution and Development **3**, 1-2.doi:10.1046/j.1525-
480 142X.2001.01040.
481 Manni, L., Caicci, F., Gasparini, F., Zaniolo, G., Burighel, P., 2004. Hair cells in
482 ascidians and the evolution of lateral line placodes. Evol. Dev. **6**, 379-381.
483 doi:10.1111/j.1525-142X.2004.04046.
484 Manni, L., Mackie, G.O., Caicci, F., Zaniolo, G., Burighel, P., 2006. Coronal organ of
485 ascidians and the evolutionary significance of secondary sensory cells in
486 chordates. J. Comp. Neurol. **495**, 363-373. doi: 10.1002/cne.20867.
487 Mazet, F., Hutt, J.A., Milloz, J., Millard, J., Graham, A., Shimeld, S.M., 2005. Molecular
488 evidence from *Ciona intestinalis* for the evolutionary origin of vertebrate sensory
489 placodes. Dev. Biol. **282**, 494-508. doi:10.1016/j.ydbio.2005.02.021.
490 Meulemans, D., Bronner-Fraser, M., 2007. The amphioxus *SoxB* family: implications
491 for the evolution of vertebrate placodes. Int. J. Biol. Sci. **3**(6), 356-364.

492 Millar, R.H., 1953. *Ciona*. *In* L.M.B.C. Memoirs, Vol. 35, *Edited by* J.S. Colmann. The
493 University Press of Liverpool, Liverpool.
494 Putnam, N.H., Butts, T., Ferrier, D.E., Furlong, R.F., Hellsten, U., Kawashima, T.,
495 Robinson-Rechavi, M., Shoguchi, E., Terry, A., Yu, J.K., Benito-Gutiérrez, E.L.,
496 Dubchak, I., Garcia-Fernandez, J., Gibson-Brown, J.J., Grigoriev, I.V., Horton,
497 A.C., de Jong, P.J., Jurka, J., Kapitonov, V.V., Kohara, Y., Kuroki, Y., Lindquist,
498 E., Lucas, S., Osoegawa, K., Pennacchio, L.A., Salamov, A.A., Satou, Y., Sauka-
499 Spengler, T., Schmutz, J., Shin, I.T., Toyoda, A., Bronner-Fraser, M., Fujiyama,
500 A., Holland, L.Z., Holland, P.W., Satoh, N., Rokhsar, D.S., 2008. The amphioxus
501 genome and the evolution of the chordate karyotype. Nature **453**, 1064-71.
502 doi:10.1038/nature06967.
503 Rasmussen, S. L., Holland, L. Z., Schubert, M., Beaster-Jones, L., Holland, N. D., 2007.
504 Amphioxus AmphiDelta: evolution of Delta protein structure, segmentation, and
505 neurogenesis. Genesis **45**, 113-122. doi:10.1002/dvg.20278.
506 Schlosser, G., 2005. Evolutionary origins of vertebrate placodes: insights from
507 developmental studies and from comparisons with other deuterostomes J. Exp.
508 Zoolog. B. Mol. Dev. Evol. **304** (4), 347-99.doi:10.1002/jez.b.21055.
509 Schlosser, G., 2008. Do vertebrate neural crest and cranial placodes have a common
510 evolutionary origin? Bioessays **30**, 659-672. doi: 10.1002/bies.20775.
511 Tsagkogeorga, G., Turon, X., Hopcroft, R. R., Tilak, M-K., Feldstein, T., Shenkar, N.,
512 Loya, Y., Huchon, D., Douzery, E.J.P., Delsuc, F., 2009 An updated 18S rRNA
513 phylogeny of tunicates based on mixture and secondary structure models.. BMC Evol.
514 Biol., **9**, 187 doi:10.1186/1471-2148-9-187.

515 Yu, J.K., Meulemans, D., McKeown, S.J., Bronner-Fraser, M., 2009. Insights from the
516 amphioxus genome on the origin of vertebrate neural crest. Gen. Res. **18**, 1127-
517 1132. doi:10.1101/gr.076208.108.
518

519 **TABLES**

520 Table 1. Classic classification of ascidians.

521

522 Table 2. List of Pleurogona species. For Enterogona species, see Manni et al. (2006).

523 Asterisks: species described in present work.

524

525

526 **LEGENDS**

527 Fig. 1. Sketches of *Styela montereyensis*. A) A solitary ascidian with an elongated body,

528 supported on a thinner stalk. Siphons close together at distal end; oral siphon is

529 characteristically curved whereas atrial siphon points upward. Arrows: directions of

530 water flow. (B) Oral siphon, showing velum and tentacles. Tunic omitted for simplicity.

531

532 Fig. 2. A-D *Pyura* genus. Scanning electron microscopy. A, B: *Pyura haustor*; C-F:

533 *Pyura stolonifera*. (A, B) Lateral second-order (II) and third-order (III) branches

534 (central axis of tentacle is not visible). Arrows: coronal organ; SP, supporting cell. Scale

535 bar =25µm in A, 10µm in B. (C) Coronal organ is composed of parallel rows composed

536 of 2-7 ciliated sensory cells. SP: supporting cells; c: cilia. Scale bar =5µm. (D) Coronal

537 organ viewed from outer side of tentacle, showing sensory cells with cilia (black

538 arrows) surrounded by corolla of microvilli (mv); arrowheads: apical membrane

539 extroflession of supporting cells. White arrow: cilium in epithelial cell. Scale bar =

540 1µm. (E) Coronal organ viewed from inner side of tentacle. Note sensory cells with two

541 cilia (white arrows) and a corolla of graded stereovilli (sv) in form of crescent (type 2

542 sensory cell) (2) and ring (type 3 sensory cell) (3). Scale bar =1µm. (F) Detail of type 3
543 sensory cell. C, cilia, sv: stereovilli. Scale bar = 0.5µm
544
545 Fig. 3. *Pyura haustor* . Transmission electron microscopy. (A, B) Transverse section of
546 coronal organ (squared area in A is enlarged in B) in a small tentacle branch: sensory
547 cells (SN) have basal nucleus (n), many rough endoplasmic reticulum cisternae (rer) and
548 granules (white arrowheads). Supporting cells (SP) are lengthened and curved to receive
549 sensory cells. Asterisk: blood sinus in tentacle; c: cilia; mv: microvilli; sv: stereovilli;
550 arrow: vacuoles with loose matrix in supporting cells. Scale bar = 5µm in A; 2µm in B.
551 (C-D) Detail of sensory cell apexes showing granules (white arrowhead) in cytoplasm
552 and hair bundle. Note, in D, transversal section of sensory bundle showing arrangement
553 of cilia (c) and stereovilli (sv), and fibrils (arrowheads) extending radially between
554 adjacent stereovilli. Black arrows: tight junctions; cc: couple of centrioles; mv,
555 microvilli. Scale bar = 1µm in C; 1µm in D. (E) A mitotic coronal cell (white asterisk),
556 with condensed chromatin, close to a supporting cell (SP) and a sensory cell (SN).
557 Squared area is enlarged in inset to show a neurite in basal groove forming a synapsis
558 (arrows) with mitotic cell. bl: basal lamina; c: cilia; mv: microvilli; sv: stereovilli. Scale
559 bar = 1µm in E, 55nm in inset. (F-H) Nerve fibres (nf) located in groove formed by
560 sensory cell basal plasmalemma. Afferent (F, G) and efferent synapses, marked by
561 many vesicles in neurites, (H) Synaptic area (arrows) at base of sensory cell.
562 Arrowheads: vesicles in neurites; bl: basal lamina; mt: mitochondria; SN: sensory cells;
563 ve: vesicles in nerve fibres. Scale bar = 0.5µm in F, 0.5µm in G, 1µm in H.
564

Figure 4. *Styela gibsii* (A-B) and *Styela montereyensis* (C-G). A-C. Scanning electron microscopy; D-G Transmission electron microscopy. (A) Tentacles of first (I), second (II) and third (III) orders. Scale bar = 250µm. (B) Coronal organ recognisable by rows of sensory cilia (arrowheads) at borders of tentacle. Scale bar = 25µm. (C) Detail of type 2 sensory cells (2; with two cilia and a crescent of stereovilli) and type 3 (3;with two cilia and a ring of stereovilli). c: cilia; s, stereovilli. Scale bar = 1µm. (D-E) Sensory cells (SN) in transverse section, showing basal nucleus (n) and many granules (white arrowheads) scattered in cytoplasm. Apically, they bear some cilia (c) and stereovilli (sv). Sensory cells (SN) are flanked by supporting cells (SP) which border sensory cilia (c) and microvilli (mv) with their laminar protrusions (arrowheads in E).. White arrow: neurites in blood lacuna; mt: mitochondria; black arrows: tight junctions. Scale bar = 4µm in D, 2µm in E. (F) Detail of sensory cells, showing cytoplasm rich in granules (arrowheads). G: Golgi field; rer: cisternae of rough endoplasmic reticulum. Scale bar = 0.4µm. (G) Neurites (nr) insinuate in basal lamina (bl) to contact the basal plasmalemma of sensory cell (SN). Arrows: afferent synapses. Scale bar= 0.25µm.

Fig. 5. *Polyandrocarpa zorritensis*. (A) Interior view of dissected oral siphon, showing ring of tentacles of different orders. V: velum; arrowheads: tentacles. Scale bar = 200µm. (B-C) Scanning electron microscope. Coronal organ in C is seen from outer side. Note microvilli (mv) of type 1 peripheral sensory cells (1) and stereovilli (sv), graded in length, of type 2 (2) sensory cells. c: cilium; black arrows, cytoplasmic evagination of peripheral supporting cells (i.e., facing opening of siphon); white arrow: isolated cilia. Scale bar = 10µm in B, 1 µm in C. (D-F) Transmission electron microscopy. (D-E) Transverse section of coronal organ, showing sensory (SN) and

589 supporting (SP) cells. Square area in D is enlarged in E. Type 2 sensory cells have
590 granules (arrowheads) in apical cytoplasm. Cytoplasmic evaginations (white arrows) of
591 supporting cells differ in length those facing middle line of tentacle are longer than
592 peripheral ones. bc: blood cell; c: cilium; mv: microvilli, st: stereovilli; black arrows:
593 tight junction. Scale bar = 2.8µm in D, 1.5µm in E. (F) Nerve fibre (nf) in basal groove
594 of sensory cell (SN). bl: basal lamina; ve: vesicles in nerve fibres. Scale bar = 0.5µm.
595
596 Fig. 6. Sketch of transverse view of coronal organs, showing various kinds of sensory
597 cells (light grey) and supporting cells (dark grey) in Pleurogona species analysed so far,
598 Sensory cells with graded stereovilli are randomly distributed in two or more rows on
599 inner side of tentacle; a single row of sensory cells with microvilli is always peripheral.
600 Only one supporting cell is drawn, except for *Molgula socialis* and *Polyandrocarpa*
601 *zorritensis*, where inner and peripheral supporting cells are differently specialised.
602 Asterisk: species analysed in present work; grey neurites: afferent fibre; black neurites:
603 efferent fibre. See Table 2 for references.

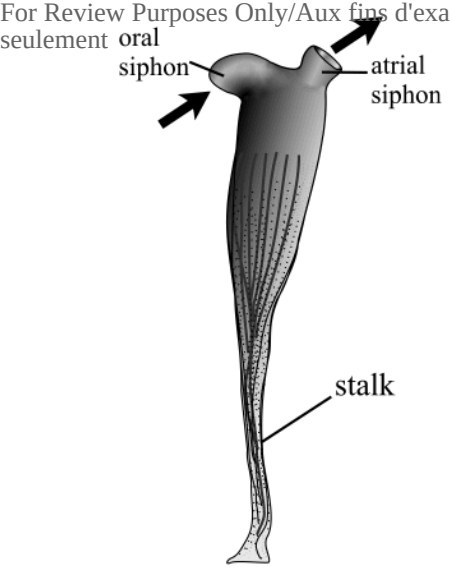

A

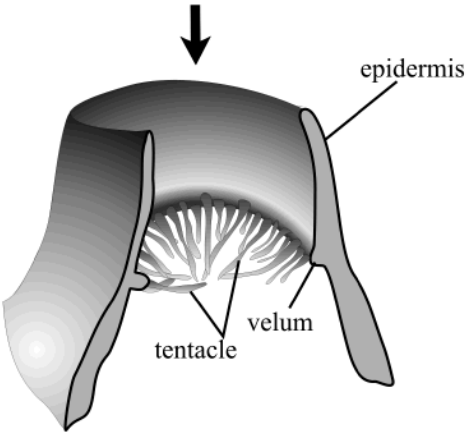

B

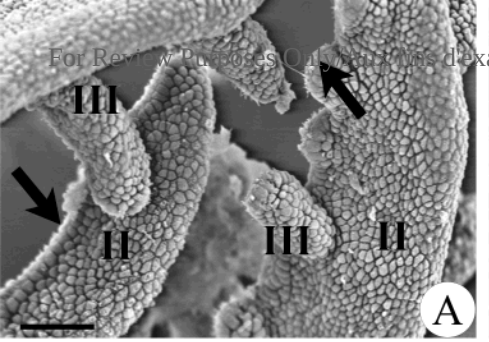

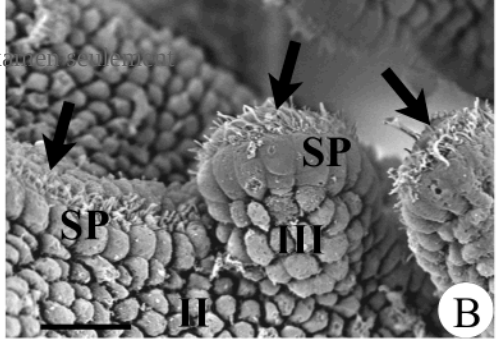

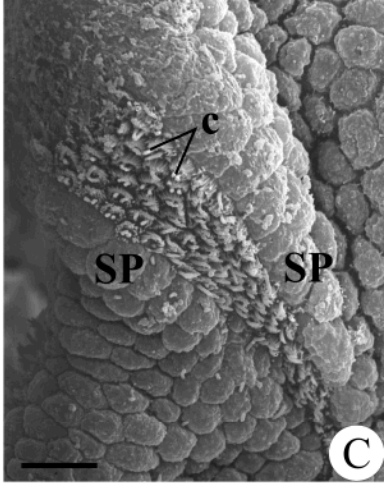

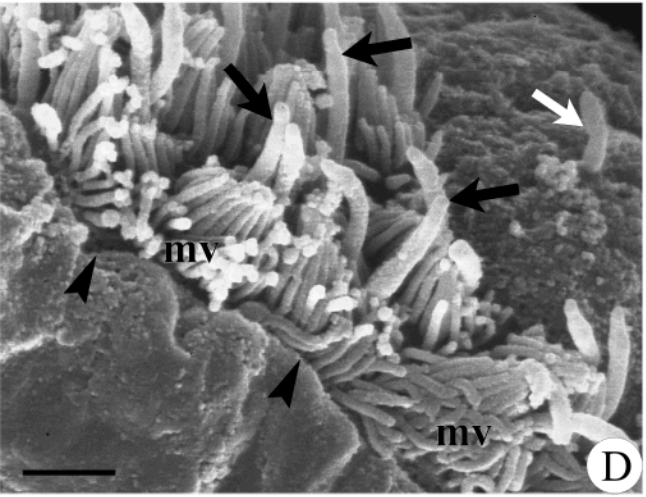

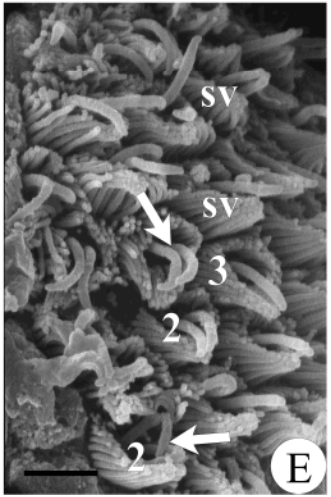

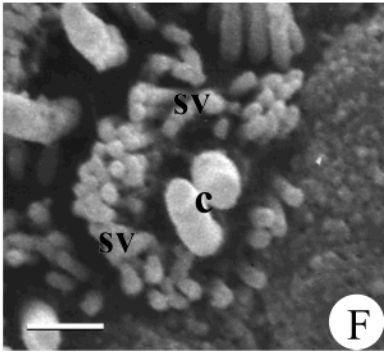

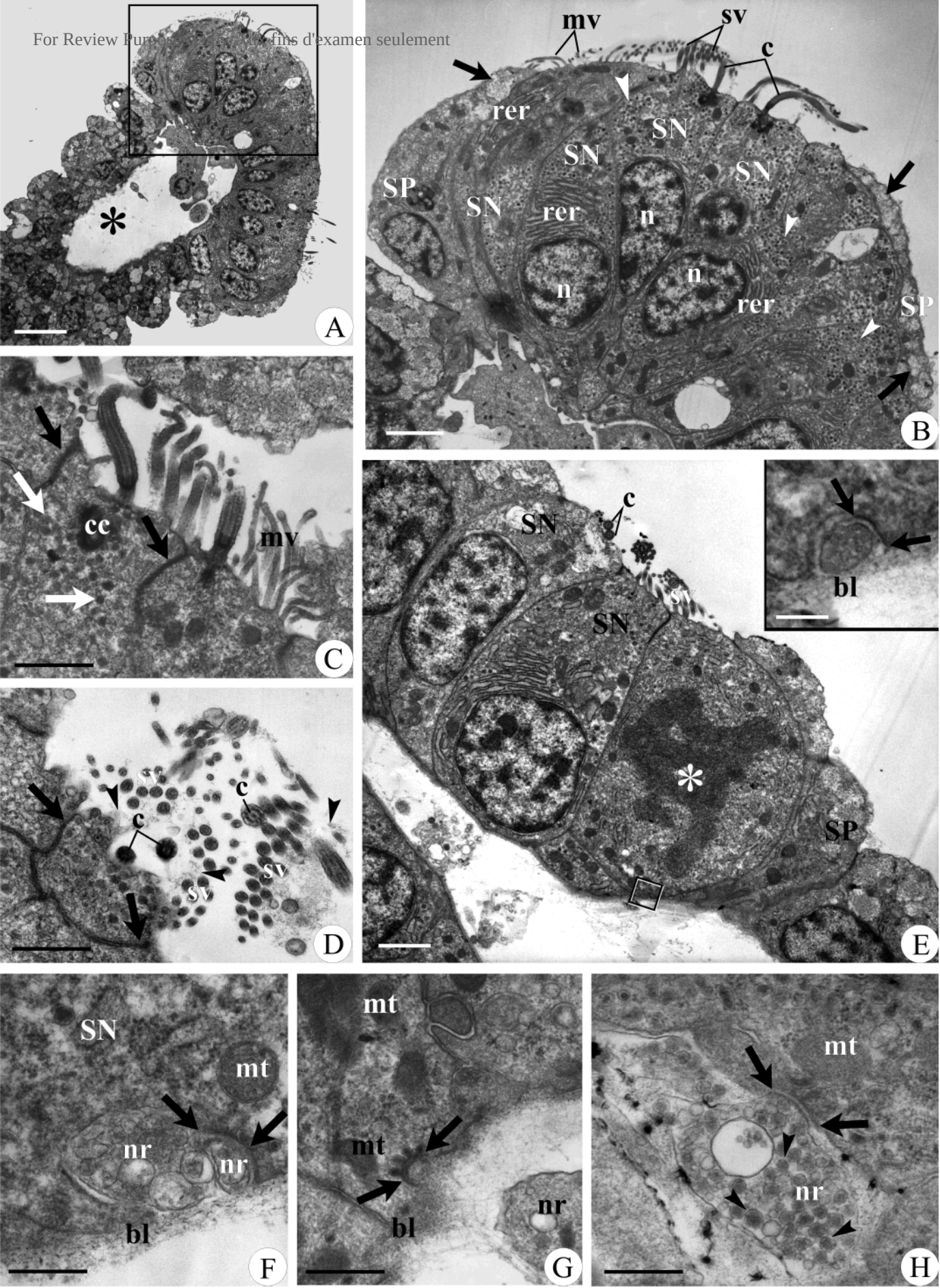

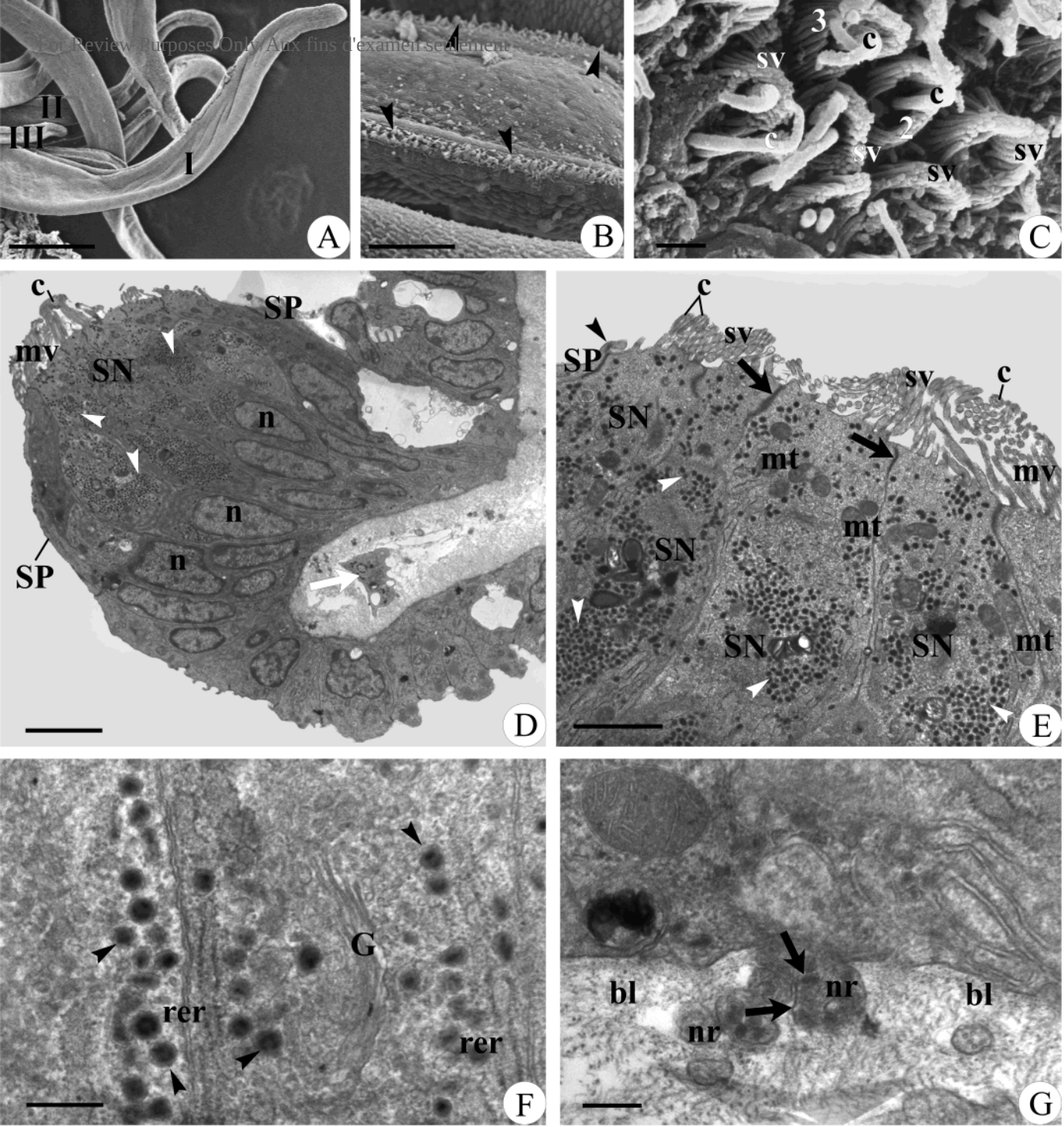

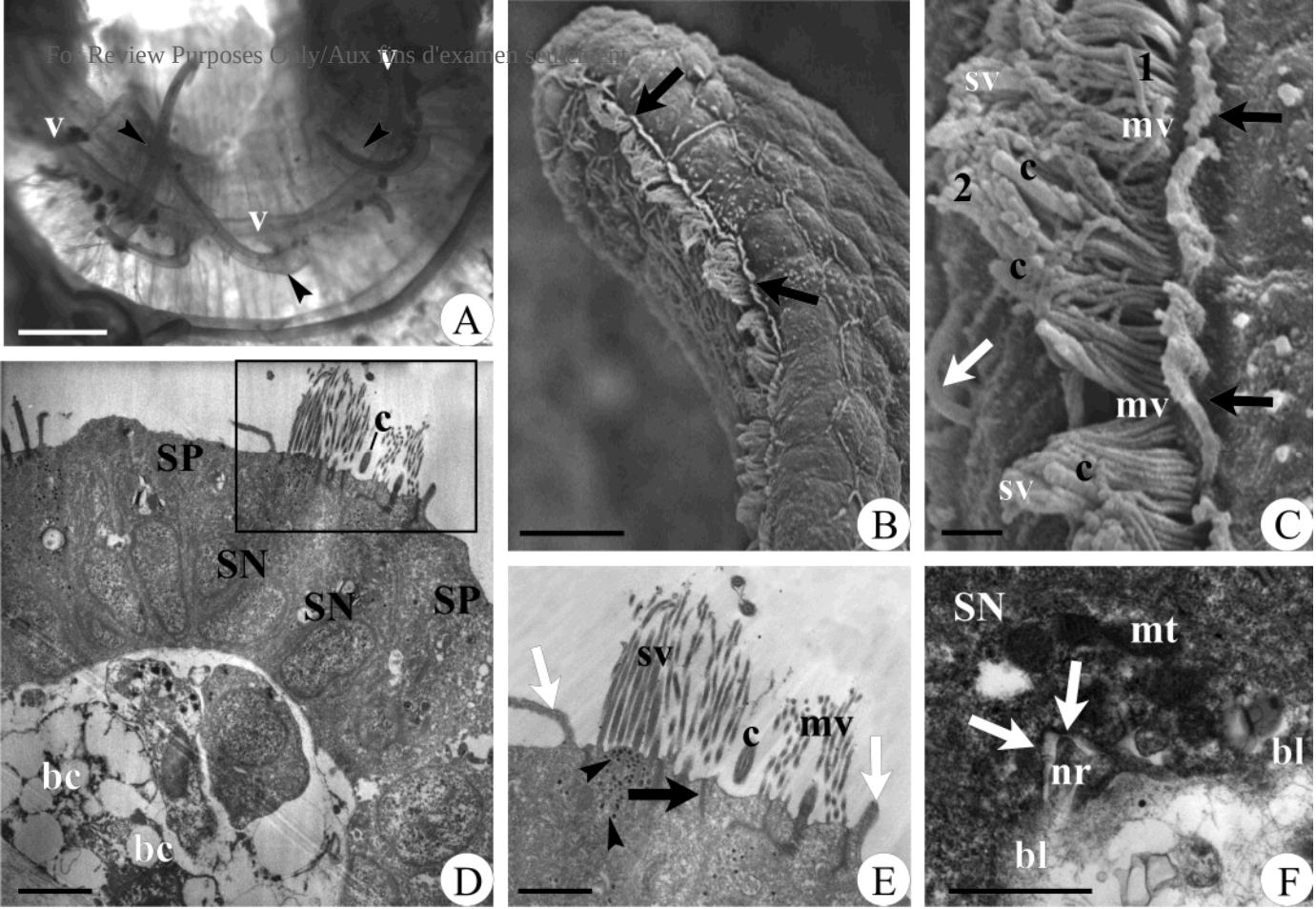

PLEUROGONA

Pyuridae

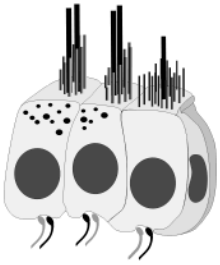

Pyura stolonifera
Pyura haustor

Molgulidae

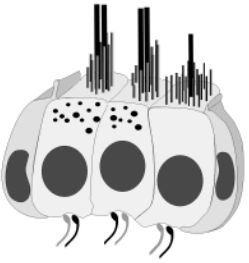

Molgula socialis

Styelidae

Styelinae

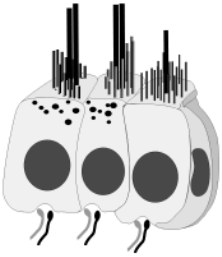

Styela montereyensis
Styela gibbsii

Styela plicata

Polyzoinae

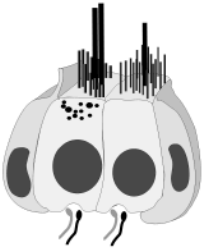

Polyandrocarpa zorritensis

Botryllinae

Botryllus schlosseri
Botrylloides violaceus
Botrylloides leachi

Phylum	Subphylum	Class	Order
Chordata	Cephalochordata		
	Tunicata	Appendicularia	
		Thaliacea	
		Ascidiacea	Enterogona
			Pleurogona
	Vertebrata		

Table 1. Classic classification of ascidians.

Order	Suborder	Family	Subfamily	Species	References
Enterogona	Aplousobranchiata				
	Phlebobranchiata				
Pleurogona	Stolidobranchiata	Pyuridae		*Pyura haustor*	*
				Pyura stolonifera	*
		Molgulidae		*Molgula socialis*	Caicci *et al.*, 2007
			Styelinae	*Styela plicata*	Manni *et al.*, 2004
				Styela gibsii	*
				Styela montereyensis	*
		Styelidae	Polyzoinae	*Polyandrocarpa zorritensis*	*
				Botryllus schlosseri	Burighel *et al.*, 2003
				Botrylloides violaceus	
			Botryllinae	*Botrylloides leachi*	Burighel *et al.*, 2008

Table 2. List of Pleurogona species. For Enterogona species, see Manni et al. (2006). Asterisks: species described in present work.

CONTRIBUTION D

Degasperi V., Shimeld S.M., Gasparini F., Burighel P., Manni L. 2010

Expression analysis of placodal genes during the blastogenetic cycle of the colonial ascidian *Botryllus schlosseri*

In preparation

Expression analysis of placodal genes during the blastogenetic cycle of the colonial ascidian *Botryllus schlosseri*

Valentina Degasperi[a], Sebastian M Shimeld[b], Fabio Gasparini[a,]*, Paolo Burighel[a], Lucia Manni[a]

[a] Dipartimento di Biologia, Università degli Studi di Padova, Via Ugo Bassi 58/B, 35131, Padova, Italy.

[b] Department of Zoology, University of Oxford, South Parks Road, Oxford OX1 3PS, UK.

* Corresponding author

Email addresses:

VD: valentina.degasperi@unipd.it

SMS: sebastian.shimeld@zoo.ox.ac.uk

FG: fabio.gasparini@unipd.it

PB: paolo.burighel@unipd.it

LM: lucia.manni@unipd.it

Introduction

Historically, it was supposed that placodes and neural crest are typical features of vertebrates and that their common ancestor possessed precursors of similar structures involved in the sensory tissue development. Particularly, on the basis that lower deuterostomes, such as hemichordates and echinoderms, have an ectodermal nerve plexus that do not share the vertebrate placode features, some authors hypothesised that placodes rapidly arose and evolved within the early vertebrates (Gans and Northcutt, 1983).

Cranial placodes are specialised ectodermal areas that characterise the vertebrate head, able to undergo cell shape changes forming a thickened columnar epithelium located at the neural plate border (Baker and Bronner-Fraser, 2001; Schlosser, 2005; 2006; Bailey and Streit, 2006). These modifications allow cell migration and/or the participation in morphogenetic movements of evagination/invagination to generate multiple non-epidermal cells (*e.g.* neurons of the sensory ganglia, glia and secretory cells).

The cranial placodes are subdivided on the basis of the development type and fate: those characterised by invagination movements (adenohypophyseal, olfactory, lens and otic placodes) and those that form a primordium, which moves along the basal lamina of the ectoderm. The placodal structures prevalently originate cell types able to delaminate (except for the lens placode), to give rise to glia cells (olfactory placode), neurosecretory cells (adenohypophyseal and olfactory placodes) and sensory neurons (profundal/trigeminal, otic, lateral line and epibranchial placodes). Moreover, they also differentiate primary sensory cells, supporting and secretory cells, contributing to the formation of the cranial sensory ganglia, lateral line system and inner ear (Schlosser, 2005).

The placodal differentiating cells are induced by specific nets of signals and express a subset of genes that specifies the later fate and their migration follows the neural crest to the sites of destination (Begbie and Graham, 2001a; 2001b). Recent studies show that delamination of placodal cells follows a basically divergent mechanism in respect to the neural crest. There are good evidences that they do not undergo to an epithelial-to-mesenchymal transition (EMT): an exam of the delaminating cells morphology revealed a rounded shape with a large nucleus, in agreement with their migration as neuroblast. Indeed, *RhoB* GTPase and *Snail/Snail2*, genes normally expressed during delamination and shape changes of neural crest cells, seem to be not implicated in the placodal movements (Savagner, 2001; Thiery, 2002; Tucker, 2004; Graham *et al.*, 2007).

The mechanisms involved in the placodal induction and specification are less explored in respect to neural crest. The first step in the induction of the placodal fate is the establishment, during the gastrula stage, of a horseshoe-shaped pre-placodal domain located around the neural plate, at the border of the non-

neural ectoderm. This domain is defined by the expression of transcription factors such as Six, Eya and Dach (Streit, 2002; McLarren *et al.*, 2003; Bhattacharyya *et al.*, 2004; Kozlowski *et al.*, 2005; Litsiou *et al.*, 2005). The manipulation of the Wnt, FGF and TGFβ pathways resulted in a different location of the neural plate border, in association with an abnormal formation of the pre-placodal domain, suggesting a role for these genes in its induction (Ahrens and Schlosser, 2005; Litsiou *et al.,* 2005; Bailey *et al.*, 2006). There are many transcription factors involved in the placodal specification, some of which possess an expression that comprises the adjacent ectoderm, but others are localised only in sub-regions of the pre-placodal domain. Moreover, it is not yet identified a single factor that could be recognised as mediator for the common neural plate border. This suggests that probably the placodal identity is conferred by the combinatorial action of different genes (Schlosser, 2008). At this regard, two hypotheses arise on the origin of neural crest and placodes. The "neural plate border state" model assumes that both derive from a common region bordering the neural plate and successive signals define respectively the neural crest and pre-placodal ectoderm (Baker and Bronner-Fraser, 2001; McLarren *et al.*, 2003; Brugmann *et al.*, 2004; Glavic *et al.*, 2004; Litsiou *et al.*, 2005). On other hand, the "binary competence" model proposes that transcription factors expressed both in neural crest and placodes possess independent regulatory functions in the two tissues, in accord with the evidence that neural crest differentiate from neural ectoderm, whereas pre-placodal domain from non-neural ectoderm (Ahrens and Schlosser, 2005; Schlosser, 2006; Schlosser, 2007).

Following these models, it is possible to suggest two different developmental origins. In the first case, neural crest and placodes displayed a common origin: at the beginning, a region localised around the neural plate became recognisable and could differentiate sensory neurons and migratory cells. Only after this stage the placodal and neural crest ectoderm are defined, recruiting other factors in response to inductive signals from the bordering territories. In the "binary competence" model, the development of neural crest and placodes followed an independent origin, with independent acquisition of signalling molecules, even if some overlap of the genetic mechanism could be explain with a convergence, due to the presence of similar signalling molecules and transcription factors coming from the neighbouring tissues (Schlosser, 2008).

These hypotheses open the interest to investigate the origin and presence of similar structures out of vertebrates. The recent molecular and morphological findings on the neural development in the most representative species of chordate groups can provide new insights on the evolution of these structures. Homologues of transcription factors, that are known to play a pivotal role in the neural crest and placodes development, were found in ascidians and amphioxus, with an expression pattern extended along the neural plate border and the non-neural

ectoderm. Despite this, the entire molecular signalling is evolved only in the vertebrate lineage (Holland and Holland, 2001; Meulemans and Bronner-Fraser, 2004; 2005; Holland, 2005; Schlosser, 2005; Schlosser, 2007).

Studies on ascidian embryogenesis revealed expression of genes normally involved in placodes formation, such as *Pax*, *Six*, *Eya* and *FoxI*, together with the presence of thickened ectodermal primordial in the larva (Wada *et al.*, 1998; Manni *et al.*, 2004; Mazet *et al.*, 2005). Recent researches demonstrated that during the embryogenesis of *Ciona*, it is possible to recognise two different regions, one anterior and one posterior, where the placodal genes are expressed. On this basis, it was proposed that ascidian embryos could possess transitory territories comparable to olfactory, adenohypophyseal, otic and lateral line placodes (Manni *et al.*, 2004; Tiozzo *et al.*, 2005; Bassham and Postlethwait, 2005; Mazet *et al.*, 2005).

Our aim is to investigate the presence of genes associated with the placodal formation in a colonial ascidian. These types of organisms provide us the advantage to analyse and compare events occurring during sexual and asexual reproduction. The colonial species *Botryllus schlosseri* includes the required features: each colony is formed by blastozooids organised into star-shaped systems and is interconnected by a vascular network running throughout the common tunic. In general, three blastogenic generations coexist in the colony because each adult blastozooid bears two primary buds evaginating from the peribranchial chamber wall, one on each side, which in turn produce two secondary buds. The developmental stages of the buds are closely correlated with those of the parent and are synchronous in the same blastogenic generation.

The nervous system of the larva directly derives from a region of the anterior neural plate, while in blastozooid it derives from a territory of the inner bud vesicle, but both reach the same final structure and organisation (Brien, 1968; Nishida, 1987; Manni *et al.*, 1999). Noteworthy, the neural components show a morphological placodal-like derivation that was ultrastructurally reconstructed, thus we can assume that a molecular analyses can provide a more comprehensive interpretation on the controversial question of the presence of neurogenic placodes in tunicates (Burighel *et al.*, 1998; Manni *et al.*, 1999). A first study has evidenced expression of the homologous of *Pitx* gene (Pituitary homeobox), which is normally involved in the craniate adenohypophysis development, in the stomodeum/neural complex of *B. schlosseri* during both embryogenesis and blastogenesis (Tiozzo *et al.*, 2005). Thus, we extended the study on four orthologues of vertebrate placodal genes, *Six1/2*, *Six3/6*, *Eya* and *FoxI*, following their expression pattern with *in situ* hybridisation on serial sections. To describe the tissues involved, we accompanied the molecular data with an ultrastructural analysis that can provide additional information on the cellular organisation.

Our results show that the genes considered are expressed during the

blastogenetic cycle of *B. schlosseri* only in regions in active differentiation. Moreover, each gene considered presents a specific pattern, which can be compared with data obtained in *Ciona* larva and juvenile (Mazet *et al.*, 2005). Antisense probes against *Six1/2* and *Eya* transcripts showed an overlapped expression, marking both siphons and branchial sac in the primary buds. *FoxI* domain appears confined to the peribranchial chamber of the secondary bud, but the signal is also maintained in the early primary bud, limited to the ectodermal component of the branchial chamber. Finally, *Six3/6* expression is very similar to *Pitx*, as previous described in *Ciona* and *Botryllus* (Mazet *et al.*, 2005; Tiozzo *et al.*, 2005), and specifically regards few cells between the anterior motor fibres of the cerebral ganglion and the ciliated duct of the primary bud.

We discuss our data taking together the recent findings on nervous system development and evolution during the invertebrate/vertebrate transition.

Materials and Methods

Animals

Colonies of *B. schlosseri* (Styelidae, Stolidobranchia) were collected in the Lagoon of Venice, cultured according to Sabbadin's technique (Sabbadin, 1955) and fed with Liquifry Marine (Liquifry Co., Dorking, England). The transparency of the colonies allowed us to follow the daily development *in vivo* of buds under the stereomicroscope, thereby permitting the selection of appropriate stages. Before utilisation, colonies were staged following Sabbadin's method (see Manni *et al*., 2007) and anesthetised with MS222 (Sigma) before fixation for subsequent *in situ* hybridisation.

Light microscopy

Colonies were anesthetised with MS222 and fixed in 1.5% glutaraldehyde buffered with 0.2 M sodium cacodylate, pH 7.4, and 1.6% NaCl. After washing in buffer and postfixation in 1% OsO_4 in 0.2 M cacodylate buffer, specimens were dehydrated and embedded in Epon 812 resin. Thanks to the transparency of the resin, the specimens were oriented before ultramicrotome cutting. Series of thick sections (1 μm) were stained with toluidine blue and observe with a Leica 5000B light microscope accessorised with a Leica DFC 480 digital photo camera; images were then organised with Corel Draw 11.

Identification of transcripts

Pools of cDNA were obtained from poly A^+ RNA extracted from mixed developmental stages of fresh *B. schlosseri* colonies (Qiagen RNeasy Mini Kit). Using the SMART™ RACE cDNA Amplification Kit (Clontech), pools of

cDNAs were tested with specific primers for transcripts coding for *Six1/2*, *Six3/6*, *Eya* and *FoxI* in according to the manufacturer's instructions (see Table 1 for primer sequences). Touchdown PCRs (Polymerase Chain Reaction) were done following the subsequent cycling conditions: (94°C for 30'', 72°C for 3') for 5 cycles, (94°C for 30'', 70°C for 30'', 72°C for 3') for 5 cycles and (94°C for 30'', 68°C for 30'', 72°C for 3') for 30 cycles. Overlapping 5'- and 3'-RACE fragments were gel purified (QIAquick Gel Extraction Kit, Qiagen), cloned into pCRII vector (Invitrogen) and cloned on both strands (BMR Genomics).

Table 1. Primers used in the 5'- and 3'-RACE protocol (SMART^{TM} RACE cDNA Amplification Kit, Clontech).

BsSix1/2	5'-RACE	5'- TTCTCGGCAATGGGAACTTCCTCC -3'	GSP1
	3'-RACE	5'- AACAAGGCGGTAACATCGAAAGGC -3'	GSP2
BsSix3/6	5'-RACE	5'- CAGAGTATGATGCCAGGAAGTGTCTCG -3'	GSP1
	3'-RACE	5'- TGCTACGAGCTAGAGCCATTGTCGC -3'	GSP2
BsEya	5'-RACE	5'- TGTCCGTCACCGTCTCCAAATCC -3'	GSP1
	3'-RACE	5'- GACAACGGTCAGGACCTCACGAAC -3'	GSP2
BsFoxI	5'-RACE	5'- GGTCCAGCGTCCAGTAATTTCCCTTG -3'	GSP1
	3'-RACE	5'- CGAAGGAGAAGAAACTGACTCTGGCG -3'	GSP2

Molecular phylogeny

Alignments were constructed with ClustalX 2.0 (Myers and Miller, 1988; Larkin *et al*., 2007) using default parameters on datasets respectively formed by 34 sequences for the Six analysis, 16 for Eya, 121 for Fox and 11 for FoxI, also comprehending the *B. schlosseri* predicted amino acid sequences and trimmed to the conserved domains. Sequences from other species were downloaded from GenBank or JGI (accession numbers and alignments are organised in separated files). Bayesian phylogenetic analyses were conducted in MrBayes3.1 using default settings (Huelsenbeck and Ronquist, 2001; Ronquist and Huelsenbeck, 2003). The analyses were continued for 1 million generations, examined for convergence and the first 25% discarded when compiling summary statistics and consensus trees. Phylogenetic trees were viewed in Treeview (Page, 1996) and then imported into Corel Draw 11 for labelling.

In situ *hybridisation (ISH)*

RNA probes for *BsSix1/2, BsSix3/6, BsEya-N, BsEya-C* and *BsFoxI* were obtained from 5'- or 3'-RACE fragments in pCRII vector (Invitrogen). The probes are coding respectively for a 1004 bp, 1106 bp, 905bp and 514 bp specific region referred to the annotated transcripts. According to the protocol supplied with the DIG RNA Labelling kit (Roche Molecular Biochemicals) and the vector,

an appropriate restriction enzyme (*Not*I or *Hin*dIII, Promega) and T7 or SP6 RNA polymerase (Promega) were used to linearise the vector and obtain antisense probe.

B. schlosseri colonies for ISH were fixed overnight in freshly prepared MOPS buffered (0.1 M MOPS (Sigma), 1 mM $MgSO_4$ (Sigma), 2 mM EGTA (Fluka), 0.5 M NaCl) 4% paraformaldehyde (Taab). ISH experiments were performed as previously described (Degasperi *et al*., 2009). Sections were photographed with a Leica 5000B light microscope accessorised with a Leica DFC 480 digital photo camera; images were then organised with Corel Draw 11.

Results

Cloning and identification of transcripts

In our work, we wanted to determine if *B. schlosseri* possesses genes that normally mark placodal territories in vertebrates. After 5'- and 3'-RACE protocols (see materials and methods), we obtained cDNA clones coding for two members of *Six*, one of *Eya* and *FoxI* genes. The sequences were characterised after alignment and identified the specific protein domains. Moreover, the predicted amino acid sequence of each transcript was trimmed and used for phylogenetic analyses that comprise orthologous genes from vertebrates and invertebrates (Figs. 1-3). The described cDNA clones were then used to construct antisense RNA probes for *in situ* hybridisation experiments on section of *B. schlosseri* systems.

Expression of Six1/2 *and* Six3/6

The *Six* (*Sine oculis* homeobox) gene family comprises transcription factors involved in embryonic cell fate determination (Kawakami *et al.*, 2000). These genes have been identified in many metazoan species where bind the DNA with a function of transcriptional activators or repressor, depending on which cofactors they interact (Relaix and Buckingham, 1999; Kawakami *et al.*, 2000; Hanson, 2001; Epstein and Neel, 2003). There are three *Six* subfamilies, classified on the relationships occurring between the nine vertebrate members with those present in *Drosophila melanogaster* (*Six1/2/so*, *Six3/6/7/9/optix* and *Six4/5/8/D-Six4*). Only *Six1/2* and *Six4/5* exhibit a pan-placodal domain, whereas *Six3/6* expression is restricted to the anterior placodal territories (Oliver *et al.*, 1995; Loosli *et al.*, 1998; Jean *et al.*, 1999; Lopez-Rios *et al.*, 1999; Zuber *et al.*, 1999; Bernier *et al.*, 2000; Zhou *et al.*, 2000).

The phylogenetic analysis shows that in the Six proteins Bayesian tree (Fig. 1), the sequences identified as belonging to the Six family fall into the Six1/2 and Six3/6 clade and, in accord with this, we chose to denominate them *BsSix1/2* (*B.*

schlosseri Sine oculis homeobox 1/2) and *BsSix3/6* (*B. schlosseri Sine oculis* homeobox 3/6) respectively. As previously evidenced in Kozmik *et al.* (2007), there is a well-supported division between the three subfamilies (Six1/2, Six3/6 and Six4/5) that probably were present in the urbilaterian ancestor and then split in the vertebrate lineage.

We have investigated *BsSix1/2* expression during the blastogenetic cycle of *B. schlosseri*. In the initial stages, when the bud appears as an elongated double vesicle, the probe marked two defined areas recognisable as the presumptive regions of the peribranchial epithelium (Fig. 4A). These regions are subjected to invagination movements and subsequently they elongate as folds to divide the inner vesicle into the branchial and peribranchial chambers. In the successive phases, *BsSix1/2* expression is maintained during the development and differentiation of this domain and the signal becomes diffused through the entire atrial primordium (Fig. 4B). At this stage, the transcript is also recognisable around the siphons border and at the oral opening level the signal is not uniformly distributed but localised in groups of cells facing the lumen on opposite sides, where the tentacles will differ (Fig. 4C).

In the primary bud, *BsSix1/2* expression is maintained around the siphons and is uniformly distributed around the oral siphon circumference only in dorsal sections (Fig. 4D) and ventrally appears restricted to the anterior opening side (Fig. 4E). In the branchial chamber, there is no expression in endostyle and dorsal lamina, whereas the stigmata primordia show an intense signal (Figs. 4F, G). Here, *BsSix1/2* follows a dorso-ventral and antero-posterior progression that recalls the spatio-temporal pattern of stigmata development. The expression is confined to the columnar cells of the peribranchial epithelium and is maintained when it invaginates, becoming in contact with the thickened branchial sheet. The signal also persists during the stigmata perforation and then it decreases and stops when the openings extend antero-posteriorly to assume an elliptical shape. There is no expression in the adult blastozooid even if, located in the ampullae or circulating in the radial and marginal vessels, it is possible to recognise some blood cells that display signal for the transcript (Fig. 4H). Some of these cells are grouped in the blood lacunae of the branchial chamber.

As in the previous experiments, we analysed *BsSix3/6* expression during the blastogenesis stages (Figs. 5A-C). The secondary bud is not marked; however, in the primary bud the transcript becomes recognisable in the oral siphon rudiment, in the ciliated duct, in the neural gland and cerebral ganglion (Figs. 5D, E), where is confined to few neurons enclosed between the two horns of the anterior fibres (Figs. 5A, B). Expression during the oral siphon development regards only the branchial epithelial evagination in the primary bud and it extends until the velum (Fig. 5C). Differently from the other analysed genes, this transcript is found only in the branchial epithelium, between the velum and the region that will be

involved in the contact with the overlying epidermis. *BsSix3/6* is maintained during the development of these structures, but decreasing slowly with the approach of the complete differentiation.

***Expression of* Eya**

The *Eya* gene family codifies for proteins with dual function, as tyrosine phosphatase and transcriptional cofactors, homologous to the *eyes absent* of *D. melanogaster*, essential regulator for the composed eye development (Relaix and Buckingham, 1999; Wawersik and Maas, 2000). Invertebrates possess only one *Eya* gene, whereas they are four in vertebrates and, depending on the species, one or a combination of these, displays a pan-placodal expression (Duncan *et al.*, 1997; Xu *et al.*, 1997; Zimmerman *et al.*, 1997; Borsani *et al*., 1999; Mazet *et al*., 2005; Schlosser, 2005).

A Bayesian tree is produced from an alignment composed by our isolated clone against a set of Eya amino acid sequences of both vertebrates and invertebrates. The analysis confirms that our transcript, named as *BsEya* (*B. schlosseri Eyes absent*), is grouped together with sequences identified in other tunicates, as *C. intestinalis* and *Oikopleura dioica*. Tunicate sequences are clustered with those of vertebrate ones, whereas the cephalochordate Eya protein is grouped with the echinoderms, separately from the other chordates (Fig. 2).

In *C. intestinalis*, it has been identified one *Eya* gene that can produce, through alternative splicing of the 5' exons, three different transcripts with different expression patterns, named respectively *Eyaα*, *Eyaβ* and *Eyaγ* (Mazet *et al*., 2005). For our ISH experiments on *B. schlosseri* colonies, we chose to construct two different RNA antisense probes. The first is designed in the 5' segment of the transcript, a region highly variable that confers isoform specificity and identified as *BsEya-N*. The second probe, *BsEya-C*, contains the EYA domain at the 3' that is conserved in the three isoforms and involved in the interaction with Six and Dachsound.

BsEya-N shows an expression limited to some blood cells circulating in the tunic vessel, but also in the lacunae of adult zooids and primary buds. Group of cells are localised around the differentiating siphons, where they are in close proximity to the oral siphon epithelium, especially in the primordium of the tentacules (Fig. 6A).

In parallel experiments using *BsEya-C*, containing the conserved "core" domain, we expected and obtained a signal that summarises the pattern of each isoform. Moreover, the expression corresponds to what obtained for *BsSix1/2*, in line with the evidence that Eya protein regulates as cofactor the Six function (Li *et al*., 2003; Rayapureddi *et al*., 2003; Tootle *et al*., 2003). *BsEya-C* first appears in the secondary bud, when vesicle begins to elongate according the antero-posterior axis: at this stage, expression is confined to the ventral region, where cells that

will form the peribranchial chambers are differentiating (Fig. 6B). The expression regards the developing siphons and the peribranchial epidermis, but in this case the signal is only to refer to the epithelium forming the external sheet of the branchial basket (Figs. 6C, D). Analysing it at cellular level, it should be noted that *BsEya-C* does not mark the flattened parietal cells, but only those cells, which subsequently will participate in the stigmata formation (Fig. 6E). In an initial phase, the signal is observable in the thickened columnar cells of the stigma primordium and, decreasing in intensity, persists at this level during the successive invagination, until shortly after the perforation and before the final differentiation of the ciliated cells (Fig. 6F). Expression is no more recognisable in adult stigmata, even if some blood cells are marked, as evidenced with the first probe, *BsEya-N*.

***Expression of* FoxI**

FoxI genes belong to a subclass of transcription factors discovered only in deuterostomes and included in the wider *Fox* family, found in many organisms, comprising animals and fungi, but not in plants (Mazet *et al.*, 2003). The Fox protein family is subdivided into 17 subclasses (A-Q) and characterised by a conserved forkhead domain of 100 amino acids involved in the DNA binding. In vertebrates, three *FoxI* genes have been identified and recently also in *C. intestinalis*, the presence of which derives from duplication events independent from those of vertebrates (Solomon *et al*., 2003; Ohyama and Groves, 2004; Mazet *et al*., 2005). In the latter, *FoxI* expression constantly interests the otic placode, as well the epibranchial placodes, the pharyngeal pouches and the kidneys.

As is resulted from the Fox Bayesan tree (Fig. 3), our deduced amino acid sequence is grouped with the FoxI proteins, in a separate cluster in respect of the other Fox subclasses. Focusing the attention only on the FoxIs, we constructed another Bayesian tree showing that our sequence is more related to the *C. intestinalis* FoxIb (CiFoxIb) hence, together with the alignment analysis results, we designated our clone as *BsFoxI* (*B. schlosseri* Forkhead box I) (Fig. 3, grey box).

In order to extend the previous studies on *FoxI* during the *Ciona* embryogenesis, we followed the expression of this gene throughout the different blastogenetic stages of *B. schlosseri* colonies. As for the other analysed genes, also *FoxI* signal is found only in active developing structures, such as primary and secondary buds, except for some interspersed blood cells (Fig. 7A). *BsFoxI* becomes recognisable very early and its expression is diffused into the entire primordium of the secondary bud, when it appears such as thickened disc on parental atrial wall (Fig. 7B). Proceeding with the differentiation, the signal loses its ubiquitous pattern. When the atrial folds begin to be visible and they extend to

separate the branchial and peribranchial chambers, *BsFoxI* marks the peribranchial component, deriving from an invagination of the inner vesicle epithelium, such as described following serial section of the bud (Fig. 7C). The expression is also maintained in this region in the primary bud, even if the domain is limited to the peribranchial epithelium in direct contact with the branchial sheet (Fig. 7D). At this level, we observe that the marked area, during the steps of stigmata differentiation becomes more restricted until define only the thickened peribranchial disc, directly juxtaposed to the thinner branchial component of the future stigma. These results evidence that *BsFoxI* domain follows the antero-posterior and dorso-ventral gradient of stigmata differentiation.

Discussion

Expression in the primordium of siphons

The basic mechanisms of siphons formation in the blastozooid of *B. schlosseri* recall in several features their development during the embryogenesis and the sequence of events involves morphogenetic movements such as those occurring during the placodal differentiation. In the bud, the rudiments of siphons are early recognisable as localised dorsal thickened areas of branchial and peribranchial epithelia covered by a disc of columnar epidermis. Subsequently, the epidermis fuses with the underlying epithelium and the tentacles become visible as short evaginations around the velum rim.

BsSix1/2 and *BsEya* transcripts are expressed in the primary bud, where they mark both the epidermis and the branchial and atrial epithelium, when come in contact each other to form respectively the oral and atrial siphon. This situation recalls the stigmata differentiation that is first defined by the formation of a thickened epithelium and then by its evagination and fusion with the branchial component. Nonetheless, in the case of siphon development, the expression appears later, when the columnar cells of the epidermis are yet defined and the two layers begin the evagination and become in contact.

The expression of *BsSix3/6* during the oral siphon development display different domains in respect to the previous analysed genes. The ISH experiments showed that the transcript is limited to the branchial epithelium and is maintained until it evaginates to contact the overlying epidermis. It is important to note that in this region the expression profile is not overlapped to the *Bs-pitx* domain, which marks two short segments of the adjacent non-columnar epithelium (Tiozzo *et al*., 2005). This suggests that during the oral siphon development in the bud, the two genes play different roles. In particular, *Six3/6* is expressed in a branchial epithelium region involved in typical morphological modifications, such as thickening, evagination, epithelial fusion and perforation and this indicate that it is

implicated in events that recall the formation of the placodal-derived structures.

Neural complex differentiation and gene expression in the bud

The neural complex in the bud originates from a thickened region of the inner vesicle epithelium that evaginates dorso-posteriorly. This evagination, the dorsal tube, represents the neural gland rudiment that grows anteriorly to fuse with the oral siphon primordium, while the posterior aperture closes. The region of the branchial sheet contacting the dorsal tube forms the ciliated duct; however, the real contribute of the branchial versus neural gland region during blastogenesis remains unclear. During the differentiation of the *B. schlosseri* bud, no evident evaginations of the branchial epithelium are recognisable, even if in the embryo the neural gland clearly derives from a stomodeal evagination. In *B. schlosseri*, the cerebral ganglion becomes located ventrally in respect to the neural gland and is formed by the aggregation of migrating neuroblasts deriving from the wall of the gland body. In previous works, morphological similarities between the early steps of embryonic differentiation of these structures and vertebrate placodes have been proposed, mainly based on the cytological organisation and modifications involved (Manni *et al*., 2004; Manni and Burighel, 2006). Despite some differences, other processes are shared between the two developmental pathways, such as the derivation of the neural complex from a tube evaginated by a thickened epithelial area, the fusion of this tubular structure with the oral siphon primordium and the formation of the cerebral ganglion by aggregation of migrating cells (Manni and Burighel, 2006).

Our experiments showed that *BsSix3/6* is expressed not only during the oral siphon formation, but also in the neural complex of the primary bud. This profile partially overlaps the *Bs-pitx* expression, in particular in the ciliated duct where the probe marks the entire lumen and in the cerebral ganglion. At this level, both genes evidence a group of neurons located between the two anterior fibres, formed by axons bundles directed towards the oral siphon and endostyle (Zaniolo *et al*., 2002). The ganglion body is subdivided into an inner medulla, composed by neuronal processes, wrapped by a cortex of body cells. *Six3/6* expression interests an area that appears as a thicker layer of neuron body cells (Figs. 5D, E). The mechanisms underlying the cerebral ganglion development are not still understood. An open question is if the delaminating neuroblasts migrate and aggregate reaching the final number after few divisions, or if they are able to subdivide *in situ*, in region of the ganglion or after the ganglion formation.

On these bases, we could identify the anterior cortex marked by *Six3/6* and *Pitx* such as a proliferation/differentiation region. In support of this hypothesis, functional studies on vertebrates revealed that *Six3/6* genes promote and regulate the development of many structures, including the forebrain, the retina and the rostral placodes, after induction of cell proliferation and delaying neuronal

differentiation (Kobayashi *et al*., 1998; Zuber *et al*., 1999; Li *et al*., 2002; Del Bene *et al*., 2004; Gestri *et al*., 2005).

In the primary bud, in contrast to *Pitx*, both the neural gland and the ciliated duct display an intense signal of *BsSix3/6*, that is not in continuity with the expression domain of the oral siphon primordium. As described above, during the blastogenesis there is no obvious presence of a branchial epithelium evagination contacting the dorsal tube. The different expression pattern in the neural gland and ciliated duct suggest that during the formation, the opening region could be induced and specified by a different set of genes (including *Pitx*) in respect to the posterior dorsal tube domain that differentiates into the neural gland.

The co-expression of *Pitx* and *Six3/6* also in the ciliated duct of the larva together with the indication that in bud the neural gland derives from the dorsal tube, which in turn originates from the inner vesicle (functionally similar to the stomodeum), could suggest that the differentiation steps of these structures remain comparable with the embryogenesis (Manni and Burighel, 2006). In addition, the comparison of neural complex formation between the two developmental pathways revealed that there are strong similarities based on multiple levels, both cellular and molecular. This could raise the hypothesis for a co-option of the molecular machinery between embryogenesis/blastogenesis, since embryo and bud share the same genome. Moreover, because it has been suggested that in tunicates both neural complex and oral siphon could be considered, on molecular and morphological bases, as homologues to the adenohypophyseal placode of vertebrates, so we can also extend this comparison to the neural complex/oral siphon differentiation of the bud (Manni *et al*., 2004; Mazet *et al*., 2005; Bassham and Postlethwait, 2005).

Placodal genes during stigmata differentiation

To elucidate the meaning of the presence of *Six1/2*, *Eya* and *Foxl* during the branchial fissures (stigmata) formation, it is necessary to take into consideration the stages of differentiation and the origin of the tissues involved. The stigma is composed by seven rows of cells inserted in the branchial wall, which is composed of two epithelial sheets facing the branchial and peribranchial chambers and delimiting a space where the blood flows (Fig. 8A) (Casagrande *et al.*, 1993). These sheets are formed by flattened parietal cells deriving respectively from the branchial and peribranchial component. During the asexual reproduction, the bud originates from an evagination of the thickened peribranchial epithelium covered by an epidermis layer. The inner component forms two invaginations that grow to divide the vesicle into the branchial and the peribranchial chambers. Each invagination is formed by the branchial (inner) and the peribranchial (outer) epithelium. Regularly arranged thickened discs are formed in the two facing epithelia, representing the stigmata primordia. Subsequently, the thicker

peribranchial discs invaginate and contact the branchial component, while the cells change their polarity and junctional disposition. Later, the stigmatal fissures appear and the cells extend the cilia. The differentiation of stigmata follows an antero-posterior and dorso-ventral gradient on the walls of the branchial basket (Fig. 8B) (Manni *et al.*, 2002).

BsSix1/2 and *BsEya* share the same expression pattern, in line with the evidence that the Eya protein interacts as cofactor with Six. The presence of the signal seems to correlate with the differentiation of the future atrial epithelium and is uniformly maintained during the stigmata development. At this stage, the expression is confined to the thickened disc of the peribranchial epithelium and does not involve the parietal cells. The signal persists during the invagination and the contact with the branchial sheet, but now it decreases in intensity until ending shortly after the stigma perforation. A slightly different spatio-temporal pattern of *BsFoxI* expression is recognisable in respect to the previous described genes. *FoxI* begins to be expressed earlier, already when the thickened evagination of the secondary bud becomes visible, indicating its probable role in the first phases of tissues and/or cells commitment. As described for *BsSix1/2* and *BsEya*, initially the transcript marks the entire peribranchial epithelium and then becomes restricted to the thickened disc implicated in the stigmata differentiation. With serial section of buds, it is possible to follow in detail the timing of expression and it seems that the signal ends when the columnar cells begin to invaginate. Taken together, these data evidence that *BsSix1/2*, *BsEya* and *BsFoxI* are generally expressed in ectodermal thickening that undergo throughout different morphologic modifications. In specific, *FoxI* is expressed before the tissue movements, whereas *Six1/2* and *Eya* are maintained through the invagination, the epithelial fusion and subsequent stigmata perforation. A probable role of *FoxI* in the initial stages of tissues differentiation is also supported by the presence of the transcript in the first phases of bud formation, as previously described. Focusing on this event, the epidermis forms the outer sheet, whereas the inner sheet derives from the peribranchial wall (Manni and Burighel, 2006). In these first stages, *BsFoxI* expression regards both vesicles (inner and outer), but then it is restricted to the inner component, which will differentiate the gut, the branchial and peribranchial chambers.

The phylogenetic analyses show that *B. schlosseri* sequence is related to *CiFoxIb* gene, which is expressed in lateral epidermal cells of the early tailbud embryo where the atrial primordial will differ (Mazet *et al.*, 2005). It is important to note that the expression is concluded before the beginning of the atria invagination, similarly to our observation for *BsFoxI*, whereas *CiFoxIc* expression is maintained during this morphogenetic process. This suggests that our *FoxI* gene plays a precocious role in the differentiation of these structures and that *B. schlosseri* possesses other *FoxI* genes, such as evidenced in *C. intestinalis* and in

the otic placode of *Danio rerio* (Solomon *et al*., 2003; Mazet *et al*., 2005).

Co-optation of vertebrate placodal genes during the blastogenesis

The asexual reproduction in ascidians leads to the formation of a completely formed organism through a variety of mechanisms. *B. schlosseri* offers the possibility to follow weekly the buds formation and their subsequent differentiation into an adult zooid. The investigation of this process can give intriguing suggestions on the tissues pluripotentiality. Making a comparison on multiple levels between embryogenesis and blastogenesis, it is remarkable that the starting point is completely different. During the sexual reproduction, we can follow the typical steps of the chordate embryogenesis, with the formation of a gastrula, in which respectively the ectoderm differentiate into the larval central nervous system and the peribranchial chambers, the mesoderm into the notochord, mesenchyme, muscle, heart and blood, the endoderm into branchial basket and gut. Conversely, the bud arises from a double vesicle deriving from an evagination of the atrial wall and therefore is of ectodermal origin (in other ascidian species the bud can derive from the endoderm or mesoderm). Thus, we can observe that many developmental and molecular mechanisms are comparable between embryogenesis and blastogenesis and two completely different starting points converge towards overlapping processes. As the colonial blastozooids share the same genome with the embryo, it is possible to make some comparisons between the organogenesis in the two ways.

In the last ten years, the genome sequencing project extension and the application of new molecular methods on a broad variety of organisms, renovated the interest to extend the studies to tunicates and cephalochordates to better understand the switches that led to placodes development and evolution. In amphioxus, now considered at the base of the chordate lineage, the members of the *Pax-Six-Eya-Dach* placodal network are expressed in many tissues during the embryogenesis, including non-neural ectoderm that differentiates putative sensory cells, and in the putative homolog of the vertebrate pituitary, the Hatschek's left diverticulum (Kozmik *et al*., 2007; Delsuc *et al*., 2008; Swalla and Smith, 2008). Between tunicates, expression of *Six* and *Eya* genes has been found in the larvacean *Oikopleura dioica*, where identify, accompanied by morphological evidences, domains that resemble the vertebrate olfactory and adenohypophyseal placodes (Bassham and Postlethwait, 2005). In *C. intestinalis* embryo, *Six1/2* gene initially marks the ectoderm bordering the anterior neural plate and then extends its domain to the future oral and atrial siphons, areas for which an homology with the vertebrate adenohypophyseal and otic/lateral line placodes were proposed (Manni *et al*., 2004; Mazet and Shimeld, 2005). *Six3/6* is expressed around the oral opening and in a small cells population anterior to the larval oral vesicle, strictly resembling the *Pitx* domain, as previously reported in *Botryllus* (Mazet *et*

al., 2005; Tiozzo *et al*., 2005). *Eya* shows a complex spatio-temporal pattern depending on the isoforms that detect the head mesenchyme, palps and oral and atrial siphons primordia. The three *FoxI* genes recognised mesenchyme cells and atrial invagination primordia (Mazet *et al*., 2005). Our results on *B. schlosseri* colonies showed that buds express orthologs of the vertebrate placodal genes *Six1/2*, *Six3/6*, *Eya* and *FoxI* in differentiating tissues with a pattern very similar to that found during the *Ciona* embryogenesis. We observed that each transcript, both in *Botryllus* and *Ciona*, recognises structures and cells that are not only in active differentiation, but also subjected to morphological changes as evagination/invagination and delamination. Moreover, these regions develop migratory cells (neuroblasts of the neural complex), primary and secondary sensory cells (respectively in the atrial and oral siphon) and cells immunopositive to GnRH, prolactin and adrenocorticotropin (neural complex plus stomodeum) in both larva and bud. *BsSix1/2* and *BsEya-C* are expressed in oral and atrial siphons primordia, where the epidermis proceeds through steps of thickening and movement that terminate in epithelial fusion. After this final event, these genes are no longer expressed and also do not appear to be involved in the subsequent differentiation of velum and tentacles. Along the tentacles margin runs a row of secondary sensory cells forming the coronal organ resembling the neuromasts of the lateral line and the hair cells, that faces the siphon lumen in contact with the entering water flow (Burighel *et al*., 2003). In the ISH experiments, we did not find expression of orthologs of placodal genes at this level. In agreement with this, we can observe that also *BsFoxI* terminates its expression before the later tissue differentiation, in this case when the thickened peribranchial epithelium begins to invaginate during the stigmata formation (*BsSix1/2* and *BsEya-C* are present until the fusion with the branchial epithelium).

In *B. schlosseri*, *FoxI* messenger appears when the bud primordium begins to evaginate from the parental atrial wall and is maintained during the atrial chambers development. This data recalls what observed in *C. intestinalis* embryo, where the posterior epidermis thicken and then invaginate following a process similar to the vertebrate otic placode invagination, characterised by *FoxI* expression. An additional important consideration about the relation between the atrial invaginations and otic placode, is that they can differentiate primary sensory cells acting as mechanoceptors, that is a typical features of placodes (Fedele, 1923; Millar, 1953; Goodbody, 1974; Bone and Ryan, 1978; Mackie and Singla, 2003).

The different results obtained using *BsEya-N* and *BsEya-C* probes suggest that *B. schlosseri* could possess other isoforms deriving from alternative splicing phenomena of the 5'exons, such as happens in *C. intestinalis*, where the expression regulation varies spatio-temporally in the ectoderm and mesoderm.

Despite the completely different starting point of blastogenesis versus

embryogenesis, we can conclude that co-option of the molecular networks plays a pivotal role during the bud organogenesis. An explanation could be the repetition, between the two ways, of developmental mechanisms for which these genes cascade are normally recruited. Convergent evolution of the *Six-Pax-Dach* pathways seems to be less probable, as explained in Mazet *et al.* (2005), because the interaction between these genes appeared early during animal evolution and it is unlikely that this network could be evolved a second time. *FoxI* genes instead, evolved only in deuterostomes, but their expression domain is characterised by typical epidermal movements that can differentiate sensory cells, strictly in agreement with the homology hypothesis of this region with placodes.

Our results extend the study on placodes development and evolution in chordates. Four ectodermal territories are found in the ascidian embryo possessing common proprieties with the neurogenic placodes and that were denominated as rostral, stomodeal, neurohypophyseal and atrial placodes (Manni *et al*., 2004).

In conclusion, vertebrate placodal genes and morphological modifications involved in placodal movements and fates are also present during the asexual reproduction of the colonial ascidian *B. schlosseri*. The capacity of this organism to recruit genic networks for different processes, such as the blastogenesis, where the organogenesis steps are comparable with the embryogenesis, confirms its remarkable molecular and morphologic plasticity.

Now, the presence in tunicates of homologues to the olfactory, adenohypohyseal, otic and lateral placodes of vertebrates is strongly supported (Manni *et al*., 2004; Mazet *et al*., 2005; Bassham and Postlethwait, 2005). The proposed scenario is focused on the presence in an ancestral chordate of the molecular machinery that permitted the subsequent placodal evolution, in agreement with the wider distribution of these genes through the animal kingdom, where are involved in the specification of neuronal/neurosecretory cells (Schlosser, 2008). In non-chordate species, these genes are broadly expressed in the anterior ectoderm, such as described in hemichordates for *Six3/6* and *Pax6*. However, in tunicate embryo these genes begin to assume a more specialised profile, allowing the recognition of two regions of anterior non-neural ectoderm that expressed placodal gene sets, respectively typical of the anterior (*Six3/6*, *Pitx*) and posterior vertebrate placodes (*Six4/5*, *FoxI*), or with a pan-placodal domain (*Six1/2*, *Eya*) (Lowe *et al*., 2003). We can reconduct these evidences to our experiments, where *Six1/2* and *Eya* showed an expression domain that include regions considered as belonging to both anterior and posterior placodal areas (both siphons and peribranchial epithelium). Thus, the vertebrate placodal evolution probably began from this situation, developing then a more complex network of interaction with the recruitment of new transcription factors in vertebrates. The developmental studies suggest that different placodes could have an independent evolutionary origin, where each lineage developed specific

structures and cell types from these pluripotential ectodermal pan-placodal regions.

References

Ahrens K., Schlosser G. 2005. Tissues and signals involved in the induction of placodal *Six1* expression in *Xenopus laevis*. *Dev. Biol.* 288: 40-59

Bailey A.P., Streit A. 2006. Sensory organs: making and breaking the pre-placodal region. *Curr. Top. Dev. Biol*. 72: 167-204.

Bailey A.P., Bhattacharyya S., Bronner-Fraser M., Streit A. 2006. Lens specification is the ground state of all sensory placodes, from which FGF promotes olfactory identity. *Dev. Cell.* 11: 505-517.

Baker C.V., Bronner-Fraser M. 2001. Vertebrate cranial placodes I. Embryonic induction. *Dev. Biol.* 232: 1-61.

Bassham S., Postlethwait J.H. 2005. The evolutionary history of placodes: a molecular genetic investigation of the larvacean urochordate *Oikopleura dioica*. *Development* 132: 4259-4272.

Bernier G., Panitz F., Zhou X., Hollemann T., Gruss P., Pieler T. 2000. Expanded retina territory by midbrain transformation upon overexpression of *Six6* (*Optx2*) in *Xenopus* embryos. *Mech. Dev.* 93: 59-69.

Bhattacharyya S., Bailey A.P., Bronner-Fraser M., Streit A. 2004. Segregation of lens and olfactory precursors from a common territory: cell sorting and reciprocity of *Dlx5* and *Pax6* expression. *Dev. Biol.* 271: 403-414.

Begbie J., Graham A. 2001a. The ectodermal placodes: a dysfunctional family. *Philos. Trans. R. Soc. Lond. B Biol. Sci*. 356: 1655-1660.

Begbie J., Graham A. 2001b. Integration between the epibranchial placodes and the hindbrain. *Science* 294: 595-598.

Bernier G., Panitz F., Zhou X., Hollemann T., Gruss P., Pieler T. 2000. Expanded retina territory by midbrain transformation upon overexpression of *Six6* (*Optx2*) in *Xenopus* embryos. *Mech. Dev.* 93: 59-69.

Bone Q., Ryan K.P. 1978. Cupular sense organs in *Ciona* (Tunicata: Ascidiacea). *J. Zool. Lond.* 186: 417–429.

Borsani G., DeGrandi A., Ballabio A., Bulfone A., Bernard L., Banfi S., Gattuso C., Mariani M., Dixon M., Donnai D., Metcalfe K., Winter R., Robertson M., Axton R., Brown A., van Heyningen V., Hanson I. 1999. EYA4, a novel vertebrate gene related to *Drosophila eyes absent*. *Hum. Mol. Genet.* 8: 11-23.

Brien P. 1968. Blastogenesis and morphogenesis. *Adv. Morphog.* 7: 151-203.

Brugmann S.A., Pandur P.D., Kenyon K.L., Pignoni F., Moody S.A. 2004. Six1 promotes a placodal fate within the lateral neurogenic ectoderm by

functioning as both a transcriptional activator and repressor. *Development* 131: 5871-5881.

Burighel P., Lane N.J., Zaniolo G., Manni L. 1998. Neurogenic role of the neural gland in the development of the ascidian, *Botryllus schlosseri* (Tunicata, Urochordata). *J. Comp. Neurol.* 394: 230-241.

Burighel P., Lane N.J., Gasparini F., Tiozzo S., Zaniolo G., Carnevali M.D., Manni L. 2003. Novel, secondary sensory cell organ in ascidians: in search of the ancestor of the vertebrate lateral line. *J. Comp. Neurol.* 461: 236-249. Erratum in: 2003, *J. Comp. Neurol.* 464: 114.

Casagrande L., Martinucci G.B., Burighel P. 1993. Origin and differentiation of branchial stigmata in the compound ascidian *Botryllus schlosseri* (Tunicata). *Anim. Biol.* 2: 111-121.

Del Bene F., Tessmar-Raible K., Wittbrodt J. 2004. Direct interaction of geminin and Six3 in eye development. *Nature* 427: 745-749.

Degasperi V., Gasparini F., Shimeld S.M., Sinigaglia C., Burighel P., Manni L. 2009. Muscle differentiation in a colonial ascidian: organisation, gene expression and evolutionary considerations. *BMC Dev. Biol.* 9: 48.

Delsuc F., Tsagkogeorga G., Lartillot N., Philippe H. 2008. Additional molecular support for the new chordate phylogeny. *Genesis* 46: 592-604.

Duncan M.K., Kos L., Jenkins N.A., Gilbert D.J., Copeland N.G., Tomarev S.I. 1997. *Eyes absent*: a gene family found in several metazoan phyla. *Mamm. Genome* 8: 479-485. Erratum in: 1997, *Mamm. Genome* 8: 877.

Epstein J.A., Neel B.G. 2003. Signal transduction: an eye on organ development. *Nature* 426: 238-239.

Fedele M. 1923. Sulla organizzazione e le caratteristiche funzionali dell'attività nervosa dei Tunicati. I. Ricerche sul sistema nervoso periferico degli Ascidiacea. Rend. *Accad. Naz. Lincei* 32: 98–102.

Gans C., Northcutt R.G. 1983. Neural Crest and the Origin of Vertebrates: A New Head. *Science* 220: 268-273.

Gestri G., Carl M., Appolloni I., Wilson S.W., Barsacchi G., Andreazzoli M. 2005. *Six3* functions in anterior neural plate specification by promoting cell proliferation and inhibiting *Bmp4* expression. *Development* 132: 2401-2413.

Glavic A., Maris Honoré S., Gloria Feijóo C., Bastidas F., Allende M.L., Mayor R. 2004. Role of BMP signaling and the homeoprotein Iroquois in the specification of the cranial placodal field. *Dev. Biol.* 272: 89-103.

Goodbody I. 1974. The physiology of ascidians. *Adv. Mar. Biol.* 12: 1–149.

Graham A., Blentic A., Duque S., Begbie J. 2007. Delamination of cells from neurogenic placodes does not involve an epithelial-to-mesenchymal transition. *Development* 134: 4141-4145.

Hanson I.M. 2001. Mammalian homologues of the *Drosophila* eye specification

genes. *Semin. Cell. Dev. Biol.* 12: 475-484.

Holland L.Z. 2005. Non-neural ectoderm is really neural: evolution of developmental patterning mechanisms in the non-neural ectoderm of chordates and the problem of sensory cell homologies. *J. Exp. Zool. B Mol. Dev. Evol.* 304: 304-323.

Holland L.Z., Holland N.D. 2001. Evolution of neural crest and placodes: amphioxus as a model for the ancestral vertebrate? *J. Anat.* 199: 85-98.

Huelsenbeck J.P., Ronquist F. 2001. MRBAYES: Bayesian inference of phylogenetic trees. *Bioinformatics* 17: 754-755.

Jean D., Bernier G., Gruss P. 1999. *Six6* (*Optx2*) is a novel murine *Six3*-related homeobox gene that demarcates the presumptive pituitary/hypothalamic axis and the ventral optic stalk. *Mech. Dev.* 84: 31-40.

Kawakami K., Sato S., Ozaki H., Ikeda K. 2000. *Six* family genes--structure and function as transcription factors and their roles in development. *Bioessays* 22: 616-626.

Kobayashi M., Toyama R., Takeda H., Dawid I.B., Kawakami K. 1998. Overexpression of the forebrain-specific homeobox gene *six3* induces rostral forebrain enlargement in zebrafish. *Development* 125: 2973-2982.

Kozlowski D.J., Whitfield T.T., Hukriede N.A., Lam W.K., Weinberg E.S. 2005. The zebrafish dog-eared mutation disrupts *eya1*, a gene required for cell survival and differentiation in the inner ear and lateral line. *Dev. Biol.* 277: 27-41.

Kozmik Z., Holland N.D., Kreslova J., Oliveri D., Schubert M., Jonasova K., Holland L.Z., Pestarino M., Benes V., Candiani S. 2007. *Pax-Six-Eya-Dach* network during amphioxus development: conservation *in vitro* but context specificity *in vivo*. *Dev. Biol.* 306: 143-159.

Larkin M.A., Blackshields G., Brown N.P., Chenna R., McGettigan P.A., McWilliam H., Valentin F., Wallace I.M., Wilm A., Lopez R., Thompson J.D., Gibson T.J., Higgins D.G. 2007. Clustal W and Clustal X version 2.0. *Bioinformatics* 23: 2947-2948.

Li X., Perissi V., Liu F., Rose D.W., Rosenfeld M.G. 2002. Tissue-specific regulation of retinal and pituitary precursor cell proliferation. *Science* 297: 1180-1183.

Li X., Oghi K.A., Zhang J., Krones A., Bush K.T., Glass C.K., Nigam S.K., Aggarwal A.K., Maas R., Rose D.W., Rosenfeld M.G. 2003. Eya protein phosphatase activity regulates Six1-Dach-Eya transcriptional effects in mammalian organogenesis. *Nature* 426: 247-254. Erratum in: 2004, *Nature* 427: 265.

Litsiou A., Hanson S., Streit A. 2005. A balance of FGF, BMP and WNT signalling positions the future placode territory in the head. *Development* 132: 4051-4062. Erratum in: 2005, *Development* 132: 4895.

Loosli F., Köster R.W., Carl M., Krone A., Wittbrodt J. 1998. *Six3*, a medaka homologue of the *Drosophila* homeobox gene *sine oculis* is expressed in the anterior embryonic shield and the developing eye. *Mech. Dev.* 74: 159-164.

López-Ríos J., Gallardo M.E., Rodriguez de Córdoba S., Bovolenta P. 1999. *Six9* (*Optx2*), a new member of the *six* gene family of transcription factors, is expressed at early stages of vertebrate ocular and pituitary development. *Mech. Dev.* 83: 155-159.

Lowe C.J., Wu M., Salic A., Evans L., Lander E., Stange-Thomann N., Gruber C.E., Gerhart J., Kirschner M. 2003. Anteroposterior patterning in hemichordates and the origins of the chordate nervous system. *Cell* 113: 853-865.

Mackie G.O., Singla C.L. 2003. The capsular organ of *Chelyosoma productum* (Ascidiacea: Corellidae): a new tunicate hydrodynamic sense organ. *Brain Behav. Evol.* 61: 45-58.

Manni L., Burighel P. 2006. Common and divergent pathways in alternative developmental processes of ascidians. *Bioessays* 28: 902-912.

Manni L., Lane N.J., Sorrentino M., Zaniolo G., Burighel P. 1999. Mechanism of neurogenesis during the embryonic development of a tunicate. *J. Comp. Neurol.* 412: 527-541.

Manni L., Lane N.J., Zaniolo G., Burighel P. 2002. Cell reorganisation during epithelial fusion and perforation: the case of ascidian branchial fissures. *Dev. Dyn.* 224: 303-313.

Manni L., Lane N.J., Joly J.S., Gasparini F., Tiozzo S., Caicci F., Zaniolo G., Burighel P. 2004. Neurogenic and non-neurogenic placodes in ascidians. *J. Exp. Zool. B Mol. Dev. Evol.* 302: 483-504.

Manni L., Zaniolo G., Cima F., Burighel P., Ballarin L. 2007. *Botryllus schlosseri*: a model ascidian for the study of asexual reproduction. *Dev. Dyn.* 236: 335-352.

Mazet F., Shimeld S.M. 2005. Molecular evidence from ascidians for the evolutionary origin of vertebrate cranial sensory placodes. *J. Exp. Zoolog. B Mol. Dev. Evol.* 304: 340-346.

Mazet F., Yu J.K., Liberles D.A., Holland L.Z., Shimeld S.M. 2003. Phylogenetic relationships of the *Fox* (Forkhead) gene family in the Bilateria. *Gene* 316: 79-89.

Mazet F., Hutt J.A., Milloz J., Millard J., Graham A., Shimeld S.M. 2005. Molecular evidence from *Ciona intestinalis* for the evolutionary origin of vertebrate sensory placodes. *Dev. Biol.* 282: 494-508.

McLarren K.W., Litsiou A., Streit A. 2003. DLX5 positions the neural crest and preplacode region at the border of the neural plate. *Dev. Biol.* 259: 34-47.

Meulemans D., Bronner-Fraser M. 2004. Gene-regulatory interactions in neural

crest evolution and development. *Dev. Cell.* 7: 291-299.
Meulemans D., Bronner-Fraser M. 2005. Central role of gene cooption in neural crest evolution. *J. Exp. Zool. B Mol. Dev. Evol.* 304: 298-303.
Millar R.H. 1953. *Ciona*. LMBC Memoirs. Colman J.S., editor. Liverpool: University press.
Myers E.W., Miller W. 1988. Optimal alignments in linear space. *Comput. Appl. Biosci.* 4:11-17.
Nishida H. 1987. Cell lineage analysis in ascidian embryos by intracellular injection of a tracer enzyme. III. Up to the tissue restricted stage. *Dev. Biol.* 121: 526-541.
Ohyama T., Groves A.K. 2004. Expression of mouse *Foxi* class genes in early craniofacial development. *Dev. Dyn.* 231: 640-646.
Oliver G., Mailhos A., Wehr R., Copeland N.G., Jenkins N.A., Gruss P. 1995. *Six3*, a murine homologue of the *sine oculis* gene, demarcates the most anterior border of the developing neural plate and is expressed during eye development. *Development* 121: 4045-4055.
Page R.D. 1996. TreeView: an application to display phylogenetic trees on personal computers. *Comput. Appl. Biosci.* 12: 357-358.
Rayapureddi J.P., Kattamuri C., Steinmetz B.D., Frankfort B.J., Ostrin E.J., Mardon G., Hegde R.S. 2003. Eyes absent represents a class of protein tyrosine phosphatases. *Nature* 426: 295-298.
Relaix F., Buckingham M. 1999. From insect eye to vertebrate muscle: redeployment of a regulatory network. *Genes Dev.* 13: 3171-3178.
Ronquist F., Huelsenbeck J.P. 2003. MrBayes 3: Bayesian phylogenetic inference under mixed models. *Bioinformatics* 19: 1572-1574.
Sabbadin A. 1955. Osservazioni sullo sviluppo, l'accrescimento e la riproduzione di *Botryllus schlosseri* (Pallas), in condizioni di laboratorio. *Boll. Zool.* 22: 243-265.
Savagner P. 2001. Leaving the neighborhood: molecular mechanisms involved during epithelial-mesenchymal transition. *Bioessays* 23: 912-923.
Schlosser G. 2005. Evolutionary origins of vertebrate placodes: insights from developmental studies and from comparisons with other deuterostomes. *J. Exp. Zoolog. B Mol. Dev. Evol*. 304: 347-399.
Schlosser G. 2006. Induction and specification of cranial placodes. *Dev. Biol.* 294: 303-351.
Schlosser G. 2007. How old genes make a new head: redeployment of *Six* and *Eya* genes during the evolution of vertebrate cranial placodes. *Integr. Comp. Biol.* 47: 343-359.
Schlosser G. 2008. Do vertebrate neural crest and cranial placodes have a common evolutionary origin? *Bioessays* 30: 659-672.
Solomon K.S., Logsdon J.M. Jr., Fritz A. 2003. Expression and phylogenetic

analyses of three zebrafish *FoxI* class genes. *Dev. Dyn.* 228: 301-307.

Streit A. 2002. Extensive cell movements accompany formation of the otic placode. *Dev. Biol.* 249: 237-254.

Swalla B.J., Smith A.B. 2008. Deciphering deuterostome phylogeny: molecular, morphological and palaeontological perspectives. *Philos. Trans. R. Soc. Lond. B Biol. Sci.* 363: 1557-1568.

Thiery J.P. 2002. Epithelial-mesenchymal transitions in tumour progression. *Nat. Rev. Cancer.* 2: 442-454.

Tiozzo S., Christiaen L., Deyts C., Manni L., Joly J.S., Burighel P. 2005. Embryonic versus blastogenetic development in the compound ascidian *Botryllus schlosseri*: insights from *Pitx* expression patterns. *Dev. Dyn.* 232: 468-478.

Tootle T.L., Silver S.J., Davies E.L., Newman V., Latek R.R., Mills I.A., Selengut J.D., Parlikar B.E., Rebay I. 2003. The transcription factor Eyes absent is a protein tyrosine phosphatase. *Nature* 426: 299-302.

Tucker R.P. 2004. Neural crest cells: a model for invasive behavior. *Int. J. Biochem. Cell Biol.* 36: 173-177.

Wada H., Saiga H., Satoh N., Holland P.W. 1998. Tripartite organization of the ancestral chordate brain and the antiquity of placodes: insights from ascidian *Pax-2/5/8*, *Hox* and *Otx* genes. *Development* 125: 1113-1122.

Wawersik S., Maas R.L. 2000. Vertebrate eye development as modeled in *Drosophila*. *Hum. Mol. Genet.* 9: 917-925.

Xu P.X., Woo I., Her H., Beier D.R., Maas R.L. 1997. Mouse *Eya* homologues of the *Drosophila eyes absent* gene require *Pax6* for expression in lens and nasal placode. *Development* 124: 219-231.

Zaniolo G., Lane N.J., Burighel P., Manni L. 2002. Development of the motor nervous system in ascidians. *J. Comp. Neurol.* 443: 124-135.

Zhou X., Hollemann T., Pieler T., Gruss P. 2000. Cloning and expression of *xSix3*, the *Xenopus* homologue of murine *Six3*. *Mech. Dev.* 91: 327-330.

Zimmerman J.E., Bui Q.T., Steingrímsson E., Nagle D.L., Fu W., Genin A., Spinner N.B., Copeland N.G., Jenkins N.A., Bucan M., Bonini N.M. 1997. Cloning and characterization of two vertebrate homologs of the *Drosophila eyes absent* gene. *Genome Res.* 7: 128-141.

Zuber M.E., Perron M., Philpott A., Bang A., Harris W.A. 1999. Giant eyes in *Xenopus laevis* by overexpression of *XOptx2*. *Cell* 98: 341-352.

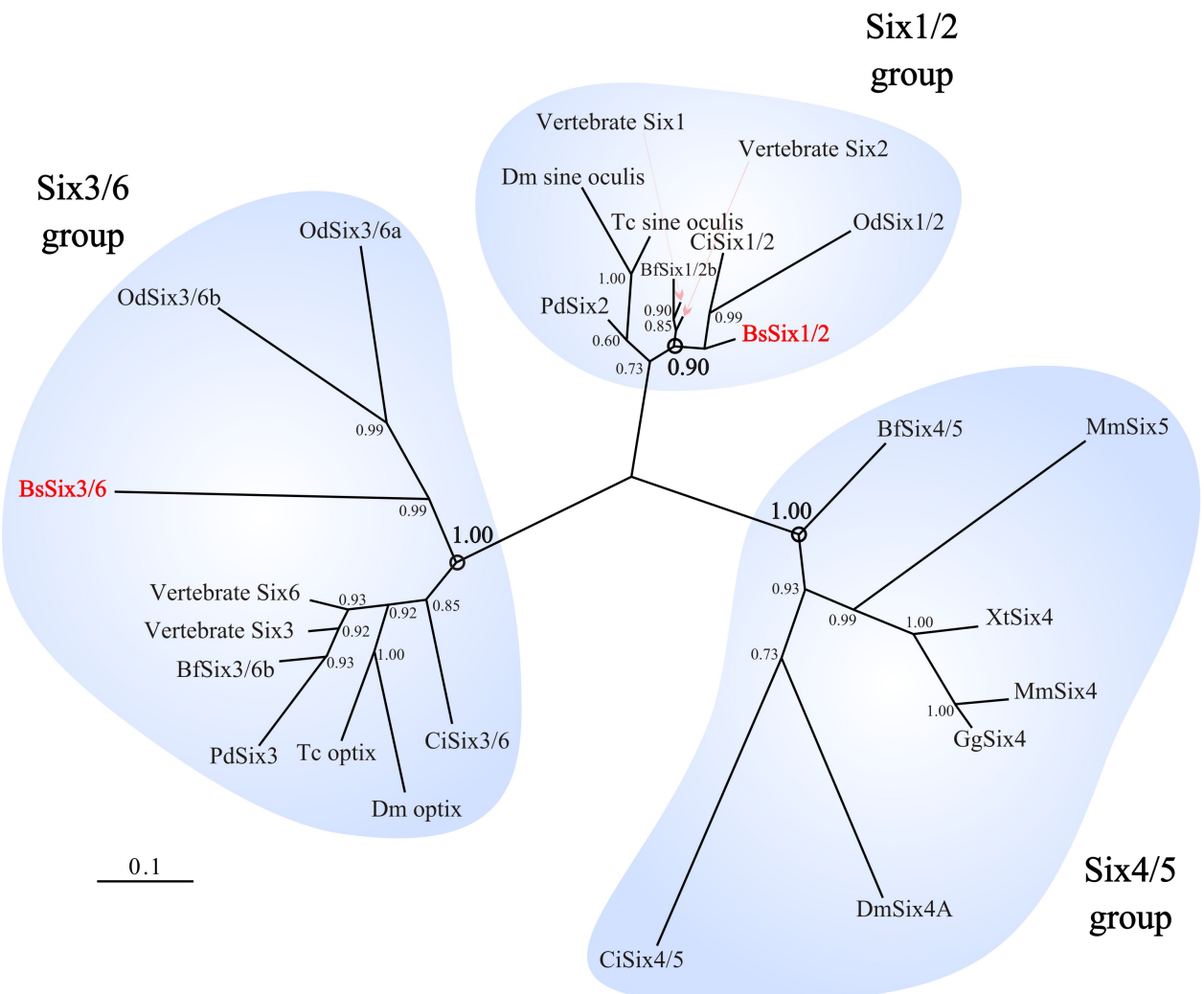

Figure 1

Molecular phylogenetic analysis of *B. schlosseri* Six protein family.

Unrooted phylogram constructed with the Bayesian methodology and based upon the Six and Six-type domains. *B. schlosseri* sequences are indicated in red and fall into groups formed by their respective orthologs. Six1/2, Six3/6 and Six4/5 clades are encircled in blue; in the Six1/2 and Six3/6 clades, the vertebrate sequences are grouped together. Numbers adjacent to nodes indicate posterior probabilities; other abbreviations: Dm, *Drosophila melanogaster*; Tc, *Tribolium castaneum*; Pd, *Platynereis dumerilii*; Bf, *Branchiostoma floridae*;Od, *Oikopleura dioica*; Ci, *Ciona intestinalis*; Xt, *Xenopus tropicalis*; Gg, *Gallus gallus* and Mm, *Mus musculus*. The scale bar refers to the phylogenetic distance of 0.1 amino acid substitutions per site.

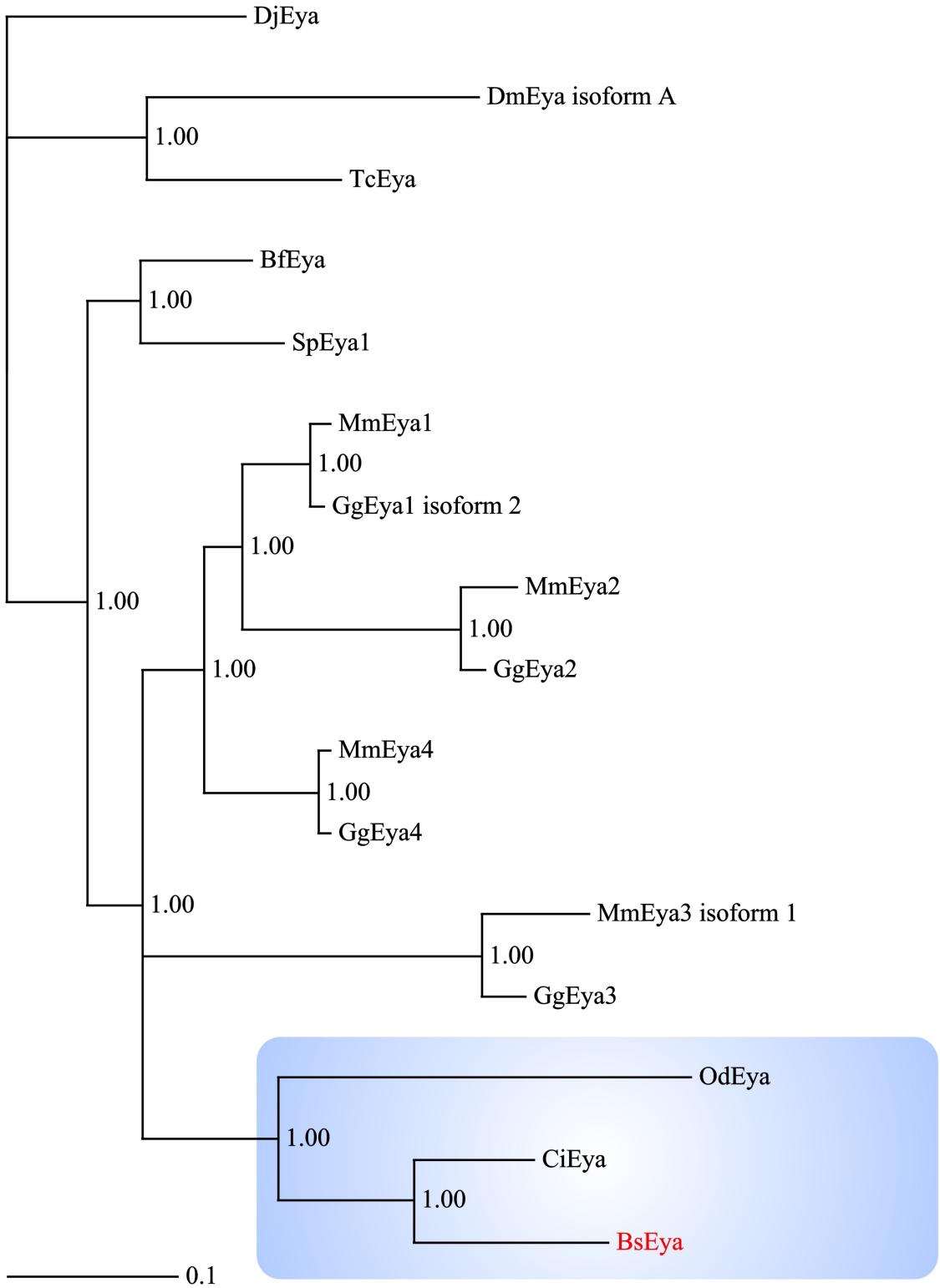

Figure 2

Molecular phylogenetic analysis of *B. schlosseri* Eya protein family.

Bayesian tree constructed using the predicted amino acid sequence coding for Eya. The analysis is based upon a trimmed alignment that includes the EYA domain. *B. schlosseri* sequence is indicated in red and fall into a clade that includes the tunicate sequences (blue box); note that *B. floridae* Eya is grouped with the echinoderms. Numbers adjacent to nodes indicate posterior probabilities; other abbreviations: Dj, *Dugesia japonica* and Sp, *Strongylocentrotus purpuratus*. The scale bar refers to the phylogenetic distance of 0.1 amino acid substitutions per site.

Figure 3

Bayesian analysis of *B. schlosseri* Fox protein family.

Simplified unrooted phylogenetic tree based upon a trimmed alignment that includes the fork head domain of Fox protein of different organisms. *B. schlosseri* sequence is indicated in red and fall into the FoxI clade (blue box). Light grey box: unrooted Bayesian analysis using only FoxI trimmed sequences, in which the *Botryllus* FoxI is clustered with CiFoxIb. Numbers adjacent to nodes indicate posterior probabilities; the scale bar refers to the phylogenetic distance of 0.1 amino acid substitutions per site in both trees.

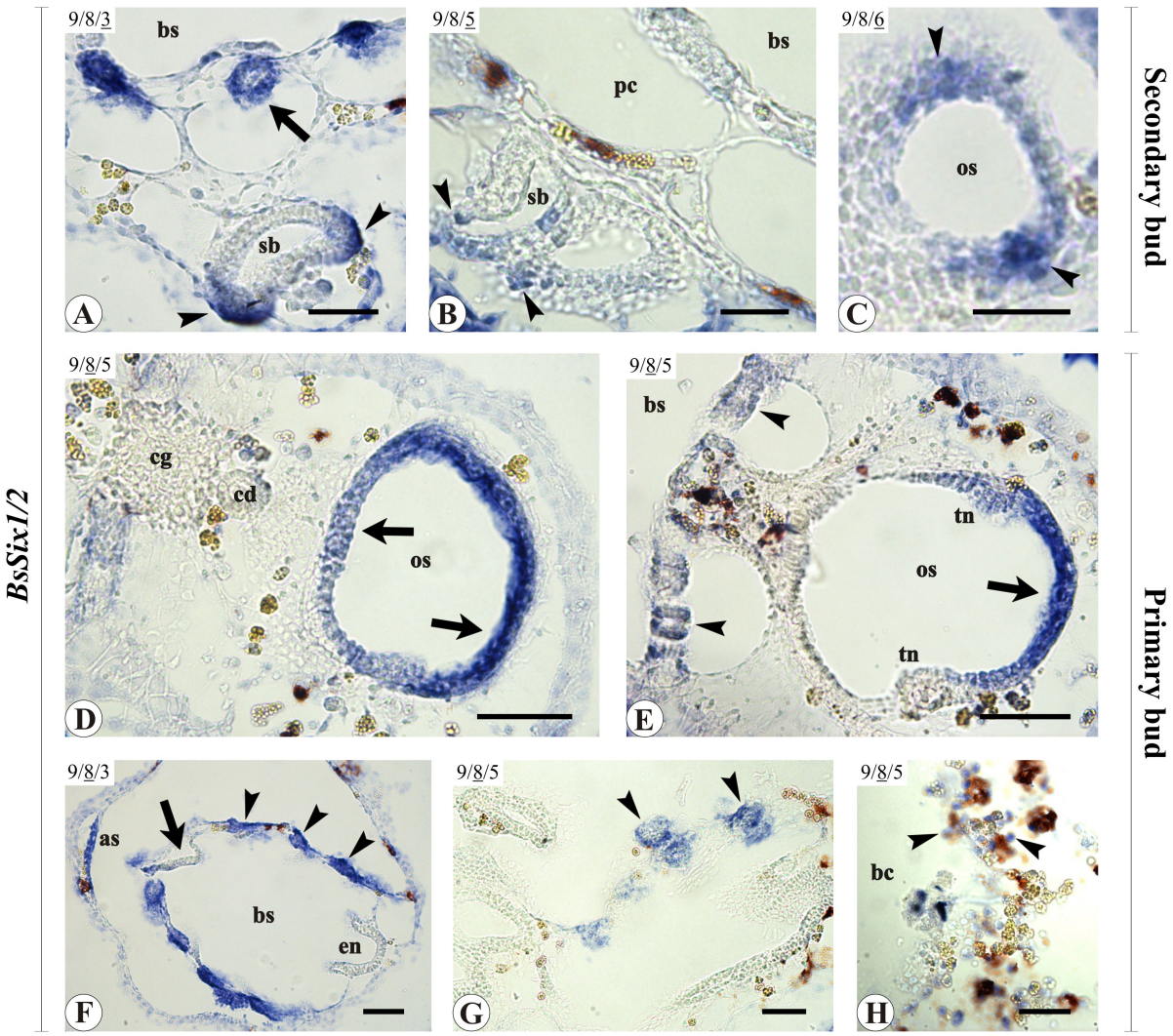

Figure 4

***In situ* hybridisation of *BsSix1/2* during the bud differentiation.**

Secondary (A-C) and primary bud (D-H). **A)** Stage 3; when the secondary bud (sb) appears as an elongated vesicle the probe marks the presumptive peribranchial epithelium (arrowheads). Arrow: stigmata of the primary bud expressing *BsSix1/2*; (bs) branchial sac. **B)** In the subsequent stages the signal becomes diffused through the entire atrial primordium (arrowheads); (sb) secondary bud; (pc) peribranchial chamber; (bs) branchial sac. **C)** Stage 6; the transcript is localised in groups of cells facing the oral siphon lumen (arrowheads); (os) oral siphon. **D)** In the primary bud (stage 8), the expression (arrows) is uniformely distribuited around the oral siphon (os) in dorsal sections, but ventrally it is located only in the anterior opening side and in the differentiating stigmata (arrowheads, **E**). (tn) tentacles; (cd) ciliated duct; (cg) cerebral ganglion; (bs) branchial sac. **F, G)** In the branchial sac (bs) of the primary bud only the stigmata are marked (arrowheads); no signal in the dorsal lamina (arrow) and endostyle (en) is recognisable. The atrial siphon is marked (as). **H)** Blood cells (bc) expressing *BsSix1/2*, arrowheads. Scale bar = 20 μm (A-G); scale bar = 10μm (H).

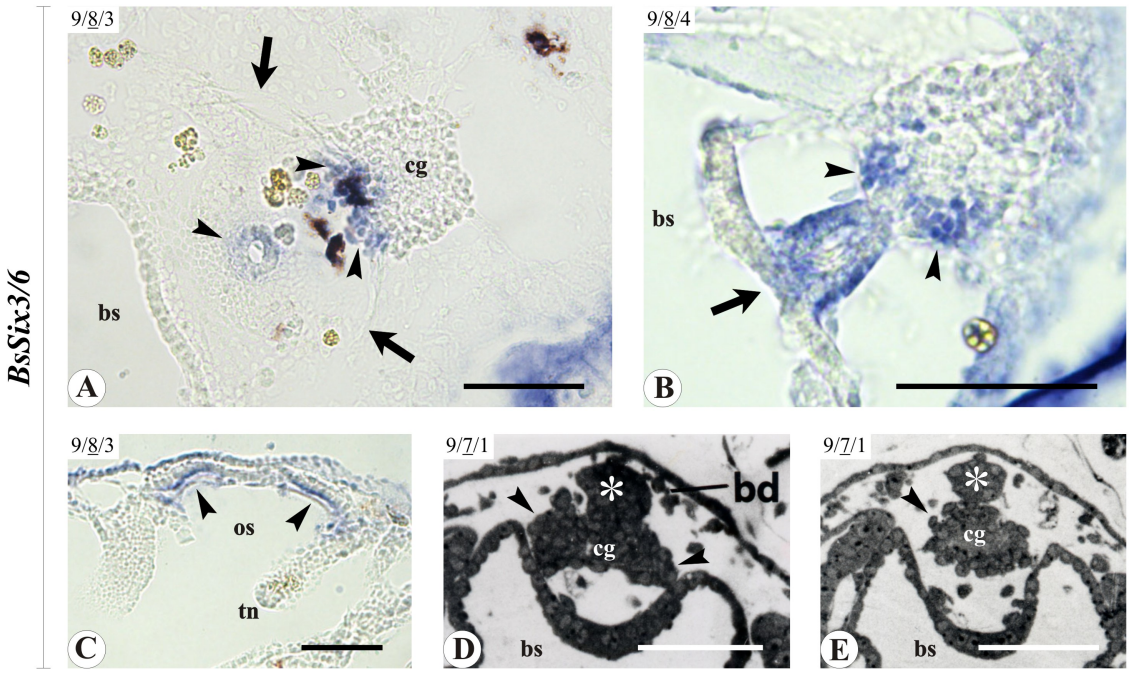

Figure 5

Expression of *BsSix3/6* in the neural complex and oral siphon of the bud.

A) In the neural complex of the primary bud, ISH experiments evidenced expression in the ciliated duct and cerebral ganglion (arrowheads); arrows: anterior nervous fibres. (bs) branchial sac. **B)** *BsSix3/6* transcript limited to the anterior region of the cerebral ganglion (arrowheads); the ciliated duct and the neural gland are marked (arrow). (bs) branchial sac. **C)** Oral siphon (primary bud, stage 8): the signal is limited to a region of the branchial epithelium (arrowheads); (os) oral siphon; (tn) tentacle. **D, E)** Cerebral ganglion (cg) formation in bud: arrowheads indicate the neuroblasts migrated from the neural gland (asterisk); (bs) branchial sac. Scale bar = 20 μm.

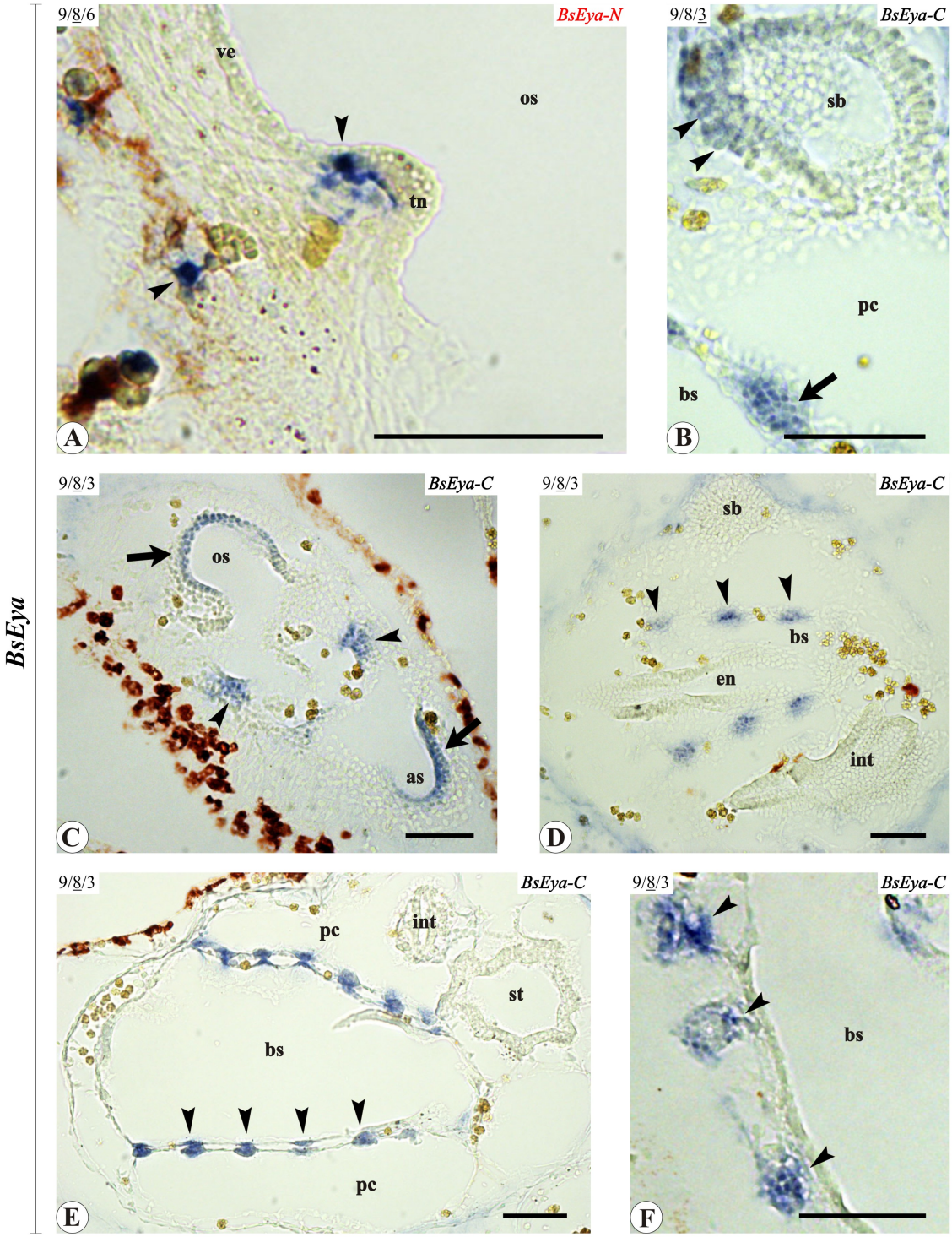

Figure 6

***In situ* hybridisation of *BsEya-N* and *BsEya-C* during the bud differentiation.**

A) *BsEya-N* expression in groups of cells (arrowheads) localised in close proximity to the oral siphon (os) epithelium; (ve) velum; (tn) tentacle. **B)** *BsEya-C* transcript (arrowheads) first appears in the ventral region of the secondary bud (sb). Arrow: stigma in differentiation; (pc) peribranchial chamber; (bs) branchial sac. **C)** Primary bud (stage 8); expression regards the developing siphons (arrows) and the stigmata (arrowheads). (os) oral siphon; (as) atrial siphon. **D, E)** *BsEya-C* marks only the cells that participate in the stigmata differentiation (arrowheads); (sb) secondary bud; (bs) branchial sac; (en) endostyle; (st) stomach; (int) intestine; (pc) peribranchial chamber. **F)** The signal is maintained until the stigmata perforation (arrowheads); (bs) branchial sac. Scale bar = 20 μm.

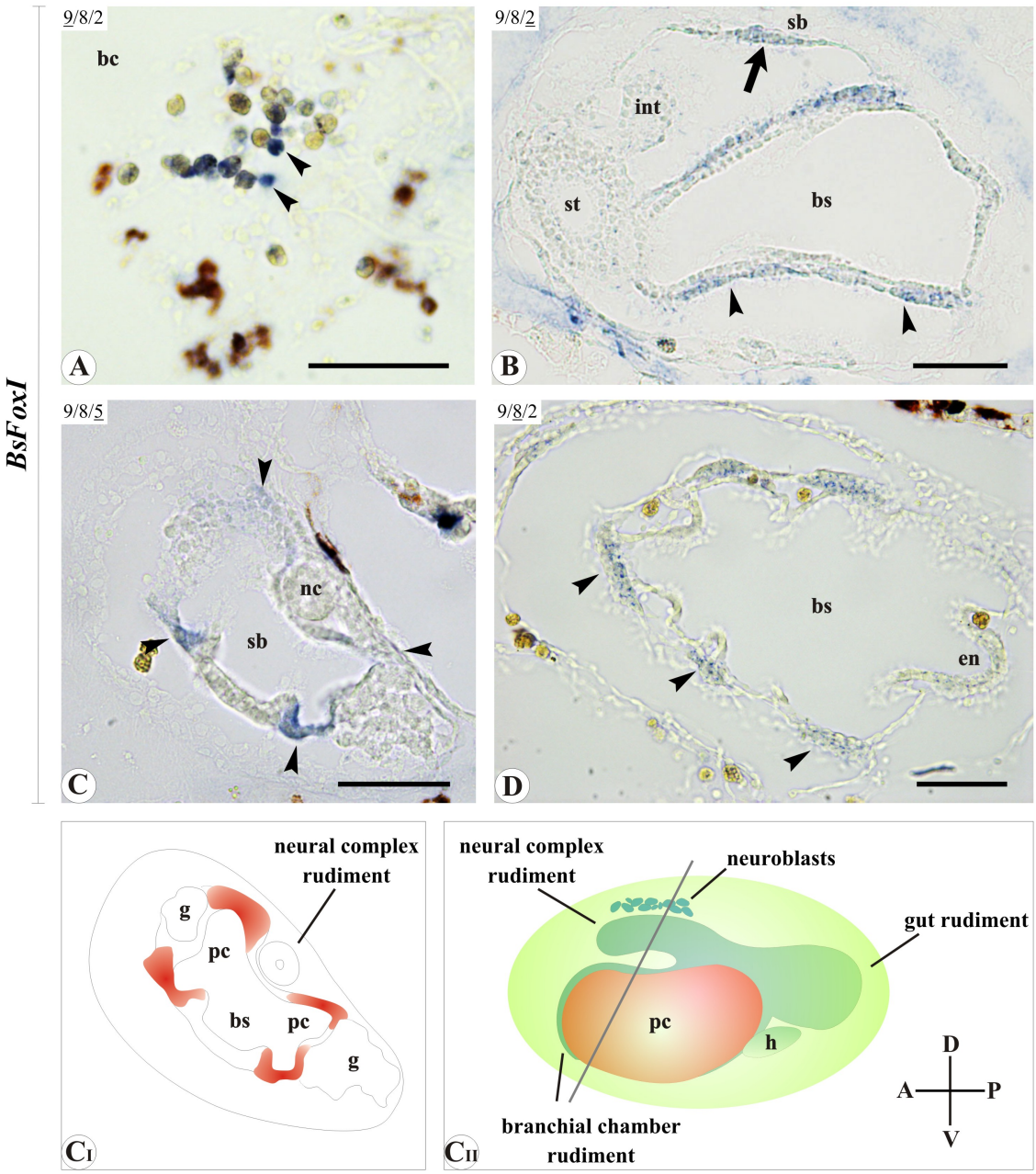

Figure 7

***In situ* hybridisation of *BsFoxI* during the bud differentiation.**

A) In the adult blastozooid the transcript is limited to interspersed blood cells (bc, arrowheads). **B)** *BsFoxI* expression (arrow) is diffused into the secondary bud primordium (sb); arrowheads: peribranchial epithelium marked by the probe. (bs) branchial sac; (st) stomach, (int) intestine. **C)** Secondary bud (stage 5); *BsFoxI* is confined to the peribranchial chamber in differentiation (arrowheads); (nc) neural complex; (sb) secondary bud. The schematic drawing in **C**I displays the marked regions (red) and shows the internal organisation of the bud at this stage; (g) gonad; (bs) branchial sac; (pc) peribranchial chamber. **C**II**)** Bud stage 5 with the cutting plane of the section showed in **C** (grey bar) and the inner organisation. The regions displaying *BsFoxI* expression are indicated in red; (pc) peribranchial chamber; (h) heart. Scale bar = 20 μm.

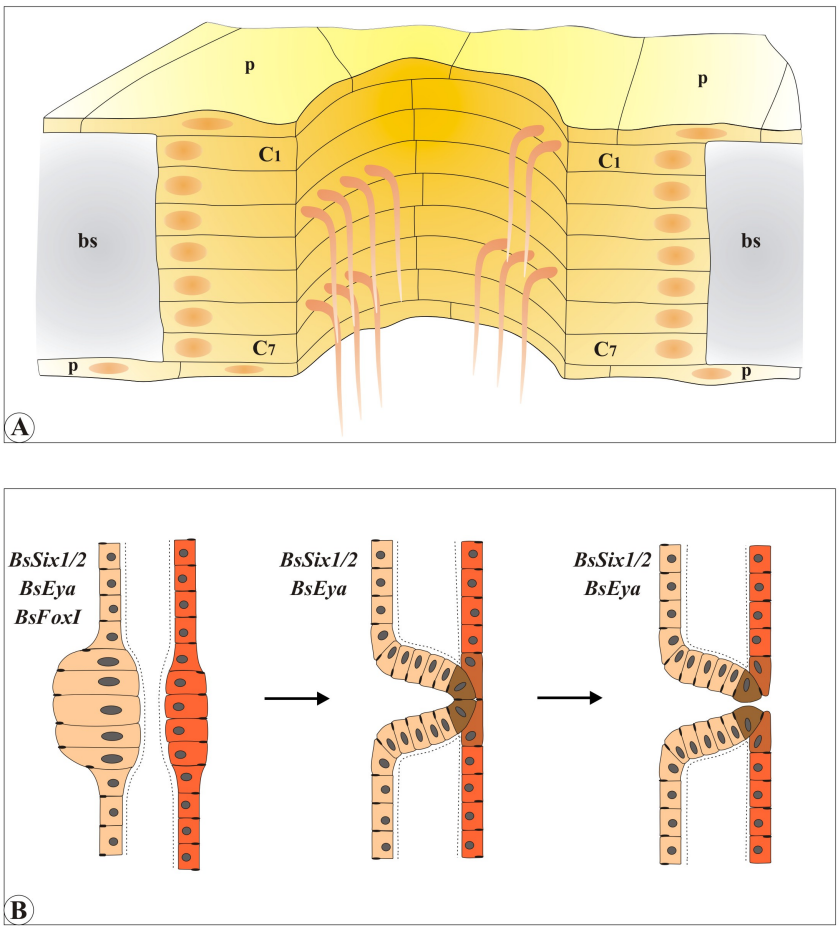

Figure 8

Schematic drawing of branchial stigmata organisation and development.

A) Organisation of the stigma; each stigma is bordered by seven ciliated cells (C_1-C_7) through which the water flows. The parietal cells (p) form the inner and outer branchial epithelium, also delimiting blood spaces (bs). **B)** Stigma primordium appears as a thickened disc of the peribranchial (light brown) and branchial (orange) epithelium; in the subsequent steps the peribranchial cells invaginate, become in contact and fuse with the branchial counterpart. The presence of expression for *BsSix1/2*, *BsEya* and *BsFoxI* is indicated for each stage.

CONTRIBUTION E

Degasperi V., Gasparini F., Shimeld S.M., Sinigaglia C., Burighel P., Manni L. 2009

Muscle differentiation in a colonial ascidian: organisation, gene expression and evolutionary considerations

BMC Dev. Biol. 9: 48

BMC Developmental Biology

Research article

Muscle differentiation in a colonial ascidian: organisation, gene expression and evolutionary considerations

Valentina Degasperi[1], Fabio Gasparini*[1], Sebastian M Shimeld[2], Chiara Sinigaglia[1], Paolo Burighel[1] and Lucia Manni[1]

Address: [1]Dipartimento di Biologia, Università degli Studi di Padova, Via Ugo Bassi 58/B, 35131, Padova, Italy and [2]Department of Zoology, University of Oxford, South Parks Road, Oxford OX1 3PS, UK

Email: Valentina Degasperi - valentina.degasperi@unipd.it; Fabio Gasparini* - fabio.gasparini@unipd.it; Sebastian M Shimeld - sebastian.shimeld@zoo.ox.ac.uk; Chiara Sinigaglia - chiara.sinigaglia@sars.uib.no; Paolo Burighel - paolo.burighel@unipd.it; Lucia Manni - lucia.manni@unipd.it

* Corresponding author

Published: 8 September 2009

BMC Developmental Biology 2009, **9**:48 doi:10.1186/1471-213X-9-48

Received: 18 March 2009
Accepted: 8 September 2009

This article is available from: http://www.biomedcentral.com/1471-213X/9/48

Abstract

Background: Ascidians are tunicates, the taxon recently proposed as sister group to the vertebrates. They possess a chordate-like swimming larva, which metamorphoses into a sessile adult. Several ascidian species form colonies of clonal individuals by asexual reproduction. During their life cycle, ascidians present three muscle types: striated in larval tail, striated in the heart, and unstriated in the adult body-wall.

Results: In the colonial ascidian *Botryllus schlosseri*, we investigated organisation, differentiation and gene expression of muscle beginning from early buds to adults and during zooid regression. We characterised transcripts for troponin T (*BsTnT-c*), adult muscle-type (*BsMA2*) and cytoplasmic-type (*BsCA1*) actins, followed by *in situ* hybridisation (ISH) on sections to establish the spatio-temporal expression of *BsTnT-c* and *BsMA2* during asexual reproduction and in the larva. Moreover, we characterised actin genomic sequences, which by comparison with other metazoans revealed conserved intron patterns.

Conclusion: Integration of data from ISH, phalloidin staining and TEM allowed us to follow the phases of differentiation of the three muscle kinds, which differ in expression pattern of the two transcripts. Moreover, phylogenetic analyses provided evidence for the close relationship between tunicate and vertebrate muscle genes. The characteristics and plasticity of muscles in tunicates are discussed.

Background

Ascidians (Tunicata) are marine filter-feeding invertebrates that possess a chordate-like swimming larva, which undergoes metamorphosis to form a sessile adult. Typically, they develop three types of muscles during their life cycle: striated in the larval tail, striated in the heart and unstriated in the adult body-wall [1]. The later is commonly called 'smooth muscle', though evidence for homology to vertebrate smooth muscle is weak.

In the larval tail, two bands of mononucleated muscle cells are localised in paraxial position, flanking the notochord and the neural tube. The organisation of their myofibrils resembles that of vertebrate muscle, especially

in the arrangement of thin and thick filaments [2-4]. In solitary ascidian embryos, a predetermined number of cells define the muscle lineage (B4.1, A4.1 and b.4.2 blastomeres of the 8-cell stage) [5-8]. Recently, it has been observed that homologues of the transcription factors *MyoD*, *Snail* and *Tbx6*, important regulators of vertebrate myogenesis, are expressed during mesoderm differentiation of ascidian embryos [9,10].

During ascidian embryogenesis, the B7.5 blastomeres give rise to the heart precursors which, after the neurulation, are localised bilaterally and named trunk ventral cells (TVCs) [11]. During metamorphosis, these cells migrate ventrally and contribute to heart tube formation [12]. The myocardium is formed of mononucleated muscle cells with a degree of homology with the heart of vertebrates, in their general structure and the sarcomeric organisation of the myofilaments [13]. At metamorphosis, the larva adheres to a substrate and its tail regresses completely, while the unstriated muscle of the sessile juvenile begins to be recognisable.

The unstriated muscle forms a series of circular and longitudinal bands, which run in the mantle around the oral and atrial siphons and the remaining body-wall. The caudal larval musculature does not contribute to adult body-wall muscle formation. It was proposed that the atrial siphon and circular muscles, together with heart muscle, derive from TVCs, localised laterally to the ventral endoderm [14] and that oral siphon and longitudinal muscles differentiate from trunk lateral cells (TLCs), flanking the visceral ganglion [11]. These muscles have multinucleated cells and do not show any clearly regular sarcomeric arrangement; however, contraction occurs through the troponin/tropomyosin (Tn/Tm) system and is regulated by calcium ions like in striated muscle of vertebrates [15-19]. Moreover, the ascidian body-wall muscle is activated through both muscarinic and nicotinic-type acetylcholine receptors [20-23], as occurs respectively in vertebrate smooth and skeletal muscle [24].

The study of genes coding for proteins associated with the contractile regulatory system can help us to understand the evolution of chordate muscle and the developmental mechanisms in which these genes are involved, and amongst these genes the actins are notable for their highly conserved sequences. Actins are encoded by a multigene family and the expression of each isoform characterises a specific developmental stage or tissue. In several species of solitary ascidians, multiple genes have been characterised that code for both muscle actins (MAs) and non-muscle cytoplasmic actins (CAs) [25-34]. In particular, sequence analyses of cDNA clones have shown at least two different MA isoforms, one in larval muscle and another in body-wall muscle, and while it is not clear which actin is expressed in the heart, it seems to also be different from the larval form [35]. The Tn/Tm regulatory system is common to both vertebrate and invertebrate striated muscle [36], but Tn does not play a role in vertebrate smooth muscle. The troponin complex constitutes TnT, TnI and TnC, which with Tm act as a regulatory switch for striated muscle contraction [37]. Ascidian unstriated muscle has the peculiarity to possess Tns whose presence has been demonstrated both in *Halocynthia roretzi* and *Ciona intestinalis* [15,16,34].

Previous molecular studies of ascidian actins and Tns have all addressed solitary species with studies focused on expression at embryonic stages.

Botryllus schlosseri is a colonial ascidian emerging as a model for the study of the developmental mechanisms involved in formation of similar zooids by alternative developmental way, that is the oozooid derived from metamorphosed larva and blastozooid derived from palleal budding [38]. It forms colonies of numerous clonal individuals organised in star-shaped systems embedded in a thin common tunic. Three blastogenetic generations develop synchronously in each colony: the filtering adults, their buds and the budlets of the last generation. Weekly, all the adults regress and are resorbed, while their buds become the new filtering adults and a new generation of budlets is produced. Different to embryonic and larval tissues, which all derive from germ cells, all the blastozooid tissues arise from somatic cells.

In this study, we described the musculature in *B. schlosseri* analysing its organisation, differentiation and gene expression in larvae and in developing blastozooids, beginning from the early bud to the adult and regression stages. We isolated and characterised *B. schlosseri* cDNA clones encoding homologues of a MA (*BsMA2*), a TnT (*BsTnT-c*) and a CA (*BsCA1*); we also obtained the genomic sequences coding for both *BsMA2* and *BsCA1*, comparing exon-intron organisation to other metazoan actin genes. Phylogenetic analyses with both *BsMA2* and *BsTnT-c* showed a close relationship between urochordate and vertebrate muscle genes. *In situ* hybridisation (ISH), in parallel with phalloidin staining experiments allowed us to follow the differentiation of the three muscle kinds, which differed in the expression pattern of the two transcripts. The ultrastructure of striated cardiac and unstriated muscle cells was also investigated during the entire blastogenetic cycle from early bud to zooid regression.

Methods

Animals and embryos

Colonies of *Botryllus schlosseri* (Styelidae, Stolidobranchia) were collected in the Lagoon of Venice, cultured according to Sabbadin's technique [39] and fed with Liquifry Marine

(Liquifry Co., Dorking, England). The transparency of the colonies allowed us to follow the daily development *in vivo* of buds under the stereomicroscope, thereby permitting the selection of appropriate stages. Before utilisation, colonies were staged following Sabbadin's method (see [40]) and anesthetised with MS222 (Sigma) to prevent muscle contractions. Embryos are brooded and mature colonies release swimming tadpole larvae, utilised for the below described *in situ* hybridisation procedure.

Phalloidin staining

Fragments of colonies were fixed in 4% paraformaldehyde (Sigma) in seawater at 4°C overnight. After washes in phosphate buffered saline (PBS), the fragments were transferred in a buffer solution of PBS containing 1% Triton X-100 (Sigma) at 4°C for 2 h to increase tissue permeability. Subsequently, for F-actin labelling, samples were incubated in a 1:100 phalloidin -FITC or -TRITC conjugated (Sigma) PBS solution, for 2 h in the dark at RT (room temperature). To remove unbound phalloidin conjugate, specimens were washed in PBS and then mounted with Vectashield (Vector Laboratories) and observed. Samples were photographed with a Leica 5000B light microscope accessorised with a Leica DFC 480 digital photo camera and images organised with Adobe Photoshop CS3.

Transmission electron microscopy (TEM)

Colonies were anesthetised with MS222 and fixed in 1.5% glutaraldehyde buffered with 0.2 M sodium cacodylate, pH 7.4, and 1.6% NaCl. After washing in buffer and post-fixation in 1% OsO_4 in 0.2 M cacodylate buffer, specimens were dehydrated and embedded in Epon 812 resin. Thanks to the transparency of the resin, the specimens were oriented before ultramicrotome cutting. Series of thick sections (1 μm) were stained with toluidine blue and observed to check appropriate levels for preparing ultrathin sections (60 nm), which were given contrast by staining with uranyl acetate and lead citrate. Photomicrographs were taken with a Hitachi H-600 electron microscope (Hitachi High-Technologies Europe GmbH, Krefeld, Germany) operating at 80 V; images were then organised with Adobe Photoshop CS3.

Identification of transcripts

Partial sequences of cDNAs coding for *BsMA2*, *BsCA1* and *BsTnT-c* were obtained by screening EST clusters derived from *B. schlosseri* colonies enriched full-length cDNA library (for details see [41]). Resequencing of the *BsMA2* clones (BMR Genomics) revealed the complete coding sequence, plus part of 5' and 3' UTRs (untranslated region) [EMBL: FN178503]. *BsCA1* and *BsTnT-c* cDNA clones were incomplete in 5' and 3' regions respectively. The complete transcripts of *BsCA1* and *BsTnT-c* [EMBL: FN178501 and FN178505] were hence obtained by PCR using, as template, an amplified plasmid library purified pool. The amplification of the library was made following the manufacturer instructions (Creator™ SMART™ cDNA Library Construction Kit, Clontech); the plasmid purification of the pool was obtained using QIAprep Midiprep Kit (Qiagen). The primers were designed (see additional file 1) and used as follows: i) the forward primer pDNR-Lib-FW1 (in the vector sequence) with the reverse primer BsCA-RW1 (in the known partial sequence of the *BsCA1*), ii) one of the forward primers BsTnT-FW1 and BsTnT-FW2 (in the known partial sequence of *BsTnT-c*) with the reverse primer pDNR-Lib-RW1 (in the vector sequence). PCR cycling was performed in a Mastercycler epGradient S (Eppendorf) thermocycler as follow: 94°C for 2', (94°C for 30", 68°C for 30", 72°C for 2') for 35 cycles, 72°C for 8', using Biotaq (Bioline) DNA Polymerase. Ethidium Bromide (Fluka) stained bands from 0.8% agarose gel electrophoresis of the PCRs were subsequently extracted (QIAquick Gel Extraction Kit, Qiagen), cloned into pCRII-TOPO vector (Invitrogen) and sequenced on both strands (BMR Genomics).

Identification of actin genomic sequences

Genomic DNA from *B. schlosseri* was obtained by incubating a small colony overnight in an extraction buffer (Tris-HCl 50 mM pH 8, EDTA 0.1 mM pH 8, SDS 1%, Proteinase K 0.5 μg/μl). This was followed by: i) centrifugation at 13,000 rpm in a benchtop microcentrifuge, ii) a phenol/chloroform purification and iii) ethanol precipitation and re-suspension in 100 μl H_2O. PCRs were done using this genomic DNA as template and primers (see additional file 1) designed to the *BsMA2* and *BsCA1* sequences obtained: MAgen_R and MAgen_F primers for *BsMA2*, 5'BsCA-gen and 3'BsCA-gen primers for *BsCA1*. Ethidium Bromide stained bands from agarose gel (0.8%) electrophoresis of the PCRs were treated as described previously. After cloning and sequencing, the sequences were identified as the annotated genomic *BsMA2* and genomic *BsCA1* [EMBL: FN178504 and FN178502]. All the above mentioned primers were purchased from Sigma-Aldrich.

Molecular phylogeny and in silico *prediction*

Alignments and pairwise identity scores were constructed with CLUSTALW2 on the EMBL-EBI site http://www.ebi.ac.uk/Tools/clustalw2/index.html[42-44]. using default parameters on datasets comprising the *B. schlosseri* predicted amino acid sequences deposited in EMBL. Sequences from other species were downloaded from GenBank, JGI or HGSC (see additional files 2, 3 and Figure 1 for accession numbers). Bayesian phylogenetic analysis was conducted in MrBayes3.1 (default settings [45,46]) using the aligned complete amino acidic sequences of 65 actins and the trimmed alignment of 54 complete amino acidic sequences of TnTs (see supplementary material for alignments). The analysis was con-

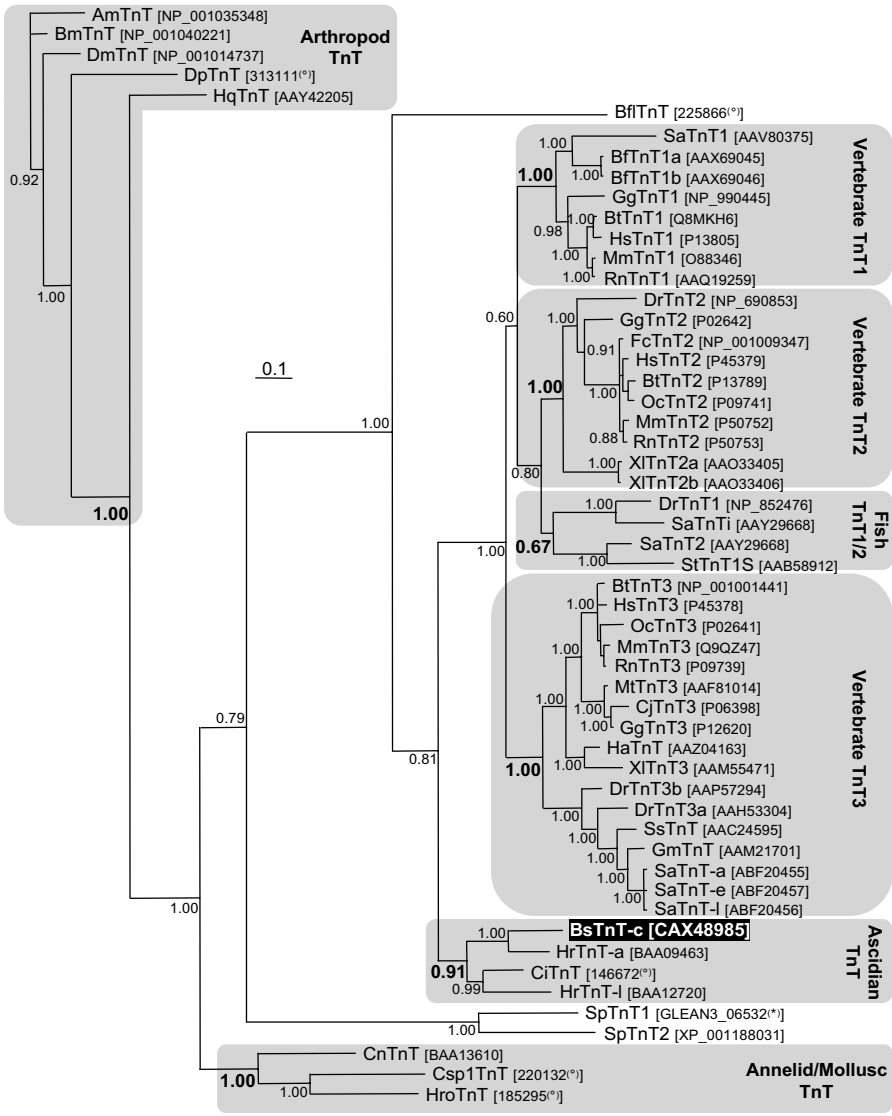

Figure 1

Molecular phylogenetic analysis of the troponin T protein family. Bayesian methodology based upon the alignment trimmed (this included removal of both ends, plus some sites in the middle with large insertions in one or a small subset of sequences) as shown in additional file 5. Values adjacent to nodes indicate posterior probabilities. Some inferred groupings are boxed in grey, labelled to the right of the figure and with supporting value in bold. The vertebrate sequences fall into three groups reflecting the well-characterised TnT1, TnT2 and TnT3 genes, with a fourth group (labelled Fish TnT1/2) containing only bony fish sequences, the relationship of which to other TnT groups cannot be determined. The *B. schlosseri* (BsTnT-c, black highlighted) sequence falls into a group of ascidian sequences. Note that another ascidian, *H. roretzi* (Hr), has two TnT protein, and the *B. schlosseri* sequence is most closely related to the adult (HrTnT-a) one. Protostome sequences have been used to root the tree, as TnT genes have not been identified outside the bilateria. The positioning of echinoderm (*S. purpuratus*; Sp) and amphioxus (*B. floridae*; Bfl) sequences reflects the likely phylogenetic relationships of these taxa. Accession numbers of sequences are shown in brackets adjacent to the protein name ((*) and (°) are downloaded from HGSC and JGI database respectively, all the others are from GenBank). Other abbreviations: -a, adult; -e, embryonic; -l, larval; Am, *Apis mellifera*; Bf, *Bufo marinus*; Bm, *Bombyx mori*; Bt, *Bos taurus*; Ci, *Ciona intestinalis*; Cj, *Coturnix japonica*; Cn, *Chlamys nipponensis*; CspI, *Capitella* sp. I; Dm, *D. melanogaster*; Dp, *Daphnia pulex*; Dr, *Danio rerio*; Fc, *Felis catus*; Gg, *Gallus gallus*; Gm, *Gadus morhua*; Hc, *Hyla chrysoscelis*; Hq, *Haemaphysalis qinghaiensis*; Hro, *Helobdella robusta*; Mm, *Mus musculus*; Mt, *Mitu tomentosa*; Oc, *Oryctolagus cuniculus*; Rn, *Rattus norvegicus*; Sa, *Sparus aurata*; Ss, *Salmo salar*; St, *Salmo trutta*; Xl, *Xenopus laevis*.

tinued for 1 million generations, examined for convergence and the first 25% discarded when compiling summary statistics and consensus trees. Phylogenetic trees were viewed in Treeview [47] and then imported into PowerPoint for labelling. NetPhosK and NetAcet [48,49] were used to improve prediction of kinase specific protein phosphorylation sites and substrates of N-acetyltransferase A respectively. Determination of exon-intron arrangements of *BsCA1* and *BsMA2* genes was performed by aligning mRNA to genomic sequences with Spidey tool [50].

In situ *hybridisation (ISH)*

An RNA probe for *BsMA2* was obtained by cloning the original insert of the cDNA library clone in pGEM-3Z vector (Promega); the probe, coding for a 1375 bp specific region, comprises the complete annotated transcript. RNA antisense probe for *BsTnT-c* was obtained from a clone in pCRII-TOPO vector, resulting from the PCR described above on the amplified cDNA pool; the probe comprises a 1004 bp specific 3' region, and includes the entire coding sequence of the annotated transcript. According to the protocol supplied with the DIG RNA Labelling kit (Roche Molecular Biochemicals) and the vectors, an appropriate restriction enzyme (*Not*I or *Hin*dIII, Promega) and T7 or SP6 RNA polymerase (Promega) were used to linearise the vector and obtain antisense probe.

Specimens for ISH (*B. schlosseri* colonies or mature larvae) were fixed overnight in freshly prepared MOPS buffered (0.1 M MOPS (Sigma), 1 mM $MgSO_4$ (Sigma), 2 mM EGTA (Fluka), 0.5 M NaCl) 4% paraformaldehyde (Taab). Fixative was removed by washing twice in PBS pH 7.4 (Oxoid) and then samples were dehydrated through graded PBS/Ethanol to 100% then washed in xylene and embedded in Paraplast Plus (Sherwood Medical). Samples were serially sectioned (12 μm) and left to adhere to microscope slides, cleaned from the Paraplast with xylene (15 min), rehydrated in a graded series of ethanol to PBS, then used immediately. Sections were incubated (6 min) in 10 μg/ml proteinase K (Promega) in PBS; the enzyme action was then stopped with a solution of 0.2% glycine in PBS, washed in PBS, postfixed in a 4% paraformaldehyde plus 0.2% glutaraldehyde solution in PBS and rewashed in PBS. Samples were then incubated in the hybridisation mix (50% formamide (Fluka), 1% Blocking Reagent (Roche), 5 mM EDTA (Fluka), 0.1% Tween-20 (Sigma), 0.1% CHAPS (Roche), 1 mg/ml heparin (Sigma) and 1 mg/ml tRNA (Roche), SSC 5×) 1 h at 65°C and after overnight with 1-2 μg/ml DIG-labelled riboprobes. Specimens were washed twice in 2× SSC pH 4.5, three times in formamide 50% in 2× SSC pH 4.5 30 min at 65°C, and twice in PBS-T (0.1% Tween-20 in PBS). Subsequently slides were: i) incubated in a blocking solution (2% Blocking Reagent, 10% goat serum (Sigma) in PBS-T) 1 h at RT and then overnight with an alkaline phosphatase conjugate anti-DIG-antibody (Roche) for riboprobe detection, ii) treated with a NBT/BCIP solution (Roche) as alkaline phosphatase substrate, until the dye was detectable, iii) dehydrated in ethanol to a final step of xylene (15 min) and mounted in Eukitt (Electronic Microscopy Sciences). Sections were photographed with a Leica 5000B light microscope accessorised with a Leica DFC 480 digital photo camera; images were then organised with Adobe Photoshop CS3.

Results

Isolation and characterisation of BsMA2, BsCA1 *and* BsTnT-c

From a full-length cDNA library derived from *B. schlosseri* colonies we isolated three clones that a BLAST search identified as encoding probable muscle-type actin, cytoplasmic-type actin and troponin T respectively. The three cDNA clones each include the complete predicted open reading frame (ORF), plus part of the 5' and 3' untranslated regions (UTRs). Moreover, genomic sequences encompassing the exons encoding the complete ORF of both actin genes were isolated from genomic DNA obtained from *B. schlosseri* colonies.

Actins

The two actin cDNA clones are 1375 and 1700 bp long, with ORFs of 1140 and 1131 bp from which we deduce respective sequences of 379 and 376 amino acids. The predicted amino acid sequences are aligned with actins of other metazoans and specific amino acid residues distinctive for vertebrate muscle and cytoplasmic actin forms are compared [51,52] (see additional file 4 for a schematic view; see additional file 5 for the complete alignment). As shown in additional file 4, the sequence that shares 13 of 20 diagnostic residues in common with the mammalian α-skeletal actin is named *BsMA2* (***B**. **s**chlosseri* **M**uscle **A**ctin **2**) and is coding for a muscular actin form. The other sequence is more related to the vertebrate cytoplasmic actins, so we named it *BsCA1* (***B**. **s**chlosseri* **C**ytoplasmic **A**ctin **1**). We note that a region of the transcript here characterised was identified in a previous work [53].

The alignment analysis reveals that *BsMA2* is characterised by the same amino acid residues as the ascidian adult muscle actins at diagnostic positions (103, 176 and 272). The amino-terminal region is highly variable between *BsMA2* and *BsCA1*, as was found in other species (additional file 6). The adult muscle actin of *B. schlosseri* (*BsMA2*) lacks the Cys residue after the first Met and possesses a series of six acidic amino acids (D and E). This is consistent with the situation of the other chordates, where the muscle actins are characterised by at least four acidic residues in the first positions.

The amino-terminal of *BsCA1* has a Cys next to the first Met like the non-chordate cytoplasmic actins and lacks

both the typical acidic amino acids and additional residues that characterise the muscle isoforms (Thr[6], Cys[10], Leu[16] and Val[17]; additional file 4).

Troponin T

The third cDNA clone isolated from the cDNA library is 1103 bp long and encodes for a predicted protein of 261 amino acids, deduced from an open reading frame of 786 nucleotides. An alignment with other isoforms of troponin T isoforms showed the presence of specific amino acids in conserved positions (see additional file 7). We hence named the clone *BsTnT-c* (***B**. **s**chlosseri* **T**roponin **T-c**). The TnTs of both vertebrates and ascidians are normally composed of a single polypeptide chain of about 250 to 300 residues, whereas the invertebrate forms exhibit an additional polar C-terminal extension of about 100 amino acids [54]. The N-terminal displays a series of acidic residues, rich in glutamic acid. BsTnT-c also has this glutamic acid rich N-terminal region, though it is shorter than that in most vertebrates. Ser[2], the first residue after methionine, is normally acetylated and phosphorylated by casein kinase II (CKII) in the rabbit skeletal muscle TnT isoform ($OcTnT_{2f}$) [55,56]. BsTnT-cpossesses both the Ser[2] and a sequence that is compatible with the consensus site of casein kinase II (**S**[2]*XX***E**, additional file 7) [57]. This also conforms to NetPhosK and NetAcet software predictions (see methods) of BsTnT-c Ser[2] residue as phosphorylated and acetylated site with a score of 0.71 and 0.52 respectively. The alignment with other ascidian and vertebrate TnTs reveals that the central region of the protein is more conserved than the N- and C-terminals and probably contains the interaction site for Tm (see additional file 7) [58-60]. Taking into consideration what it is known in vertebrates, we found that regions displaying a certain degree of similarity with other components of the troponin complex, such as Tm, TnC and TnI (see additional file 8) are recognisable by comparison and demonstrated to be more conserved [[54,58,59,61] and [62]].

The analysis extended to the entire length of the sequence shows that the two ascidian species possess a TnT that is more similar to $OcTnT_{2f}$, a vertebrate isoform, with respect to the cephalochordate and echinoderm TnTs. This pattern is also maintained when we consider only the regions subject to the interaction with other proteins.

Exon-intron organisation of BsMA2 *and* BsCA1

Fragments of genomic DNA corresponding to both *BsMA2* and *BsCA1* were amplified by polymerase chain reaction (PCR) and subsequently sequenced. We obtained clones of 1975 and 1752 nucleotides, corresponding respectively to the entire coding region for the *BsMA2* and to the coding region together with part of the 3' UTR for *BsCA1*. The exon-intron organisation, analysed between the start and stop codons, revealed the presence of four introns in *BsMA2*, which interrupt the sequence at the amino acid positions 45-3, 153-1, 208-2 and 271-1 (additional file 2; numbers after the amino acid residue indicate codon phase number of intron). Six intron positions are present in *BsCA1* (42-3, 114-3, 150-3, 204-1, 247-3 and 308-1; additional file 2), as previously reported in the ascidian *HrCA1* [35].

Phylogenetic analysis of actin and troponin T sequences

The deduced amino acid sequences of *BsCA1*, *BsMA2* and *BsTnT-c* were used for the molecular phylogenetic analyses. The Bayesan phylogenetic tree for actins (see additional file 3) results in many nodes poorly supported or collapsed. The cytoplasmic actins together with the non-chordate invertebrate forms are separated from the chordate muscle isoforms. BsCA1 and BsMA2 fall to the first and the second groups respectively. Further, BsMA2 is placed in a robustly supported group of ascidian adult MAs. Interestingly, ascidian larval MAs form a robustly supported separate group.

A Bayesian phylogenetic tree was also constructed for TnT (Figure 1). In this tree BsTnT-c groups with the other ascidian TnTs, and in particular is most related to the adult TnT of *H. roretzi*. Ascidian TnTs group with vertebrate TnTs, when the tree is rooted with protostome TnTs. Vertebrate TnTs reflect the well-characterised skeletal-slow (TnT1), cardiac (TnT2) and skeletal-fast (TnT3) groups, with a fourth poorly supported group (posterior probability 0.67) containing only bony fish sequences.

General organisation of musculature in the adult blastozooid

Body-wall

We describe the musculature in the colonial ascidian *B. schlosseri*, analysing muscle organisation in the adult blastozooid (Figure 2A-N) using phalloidin-staining, ISH on sections and TEM. In blastozooids stained with phalloidin-FITC, superficial muscles are organised in a tightly packed network of circular and longitudinal fibres, which run throughout the whole body-wall (Figures 2A-C). Circular fibres are mainly concentrated around the siphons, whereas the longitudinal ones constitute muscles that depart from the external wall of the oral siphon to the lateral region of the zooid. The combination of phalloidin staining and ISH against the *BsMA2* and *BsTnT-c* mRNAs (Figures 2D-H) permitted a detailed reconstruction of the arrangement of muscle fibres (Figure 3). An inner and an outer fibre system are evident at the oral siphon level. The outer system is formed by a series of about twenty bundles that surround the opening, with a concentric disposition from the apical portion of the siphon to the base of velum. From this point about ten fibres extend in the direction of the pericoronal bands, until the conjunction between the branchial sac and mantle: radial bundles

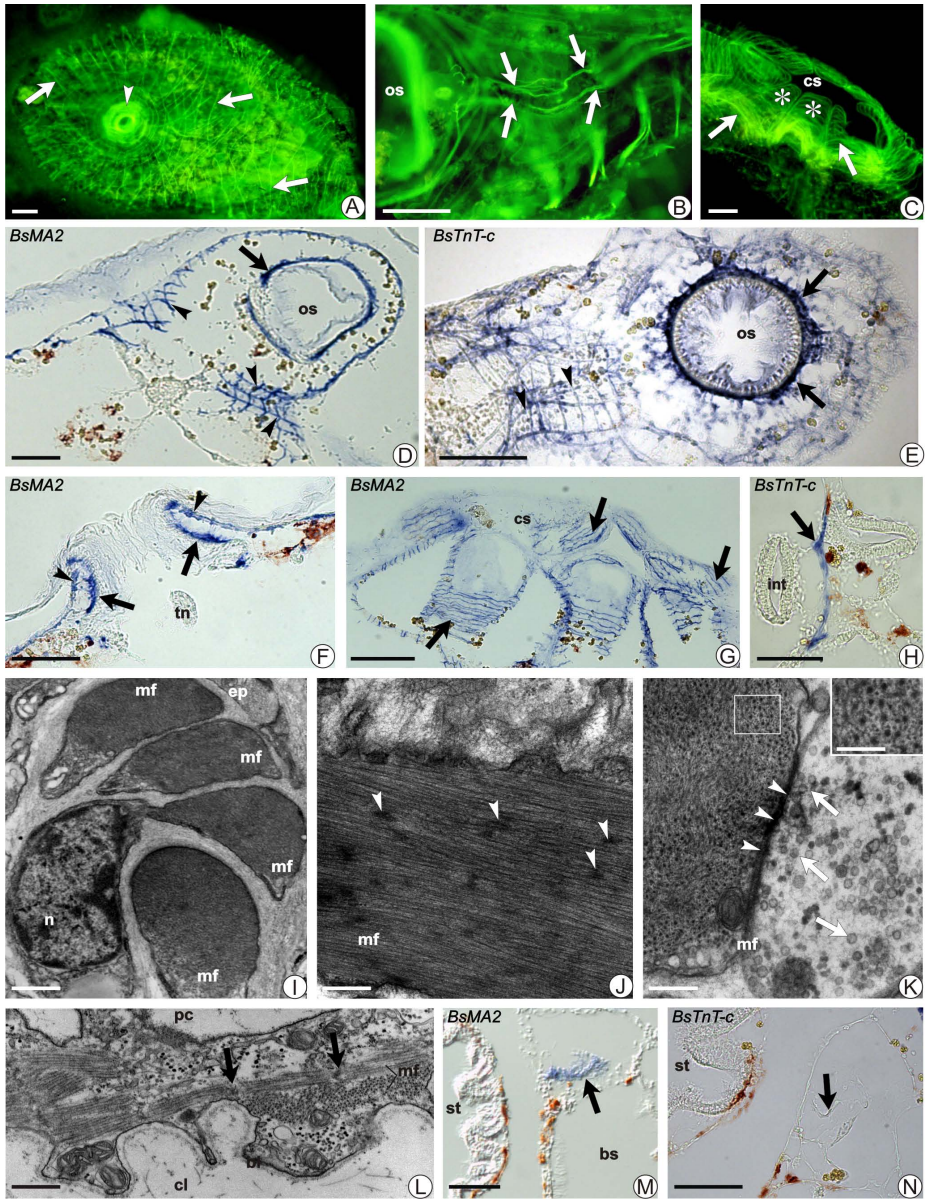

Figure 2

Aspects of the adult blastozooid musculature of *B. schlosseri*. Phalloidin -FITC staining (A-C), ISH onsection (D-H; M, N) and TEM (I-L). **A)** Dorsal view; general organisation of musculature (arrows). Arrowhead: oral siphon. Scale bar = 0.1 mm. **B)** Two longitudinal fibres (arrows) accompany the dorsal lamina. (os), oral siphon. Scale bar = 50 μm. **C)** Cloacal siphon (cs)formed by the confluence of dorsal languets (*). Arrows: musclefibres. Scale bar = 0.1 mm. **D, E)** Tangential sections. Muscle fibres (arrows) around the oral siphon (os). ISH of *BsMA2* (D) and *BsTnT-c* (E). Arrowheads: transverse fibres. Scale bar = 50 μm. **F)** Oral siphon: inner (arrows) and outer (arrowheads) systems of fibres (*BsMA2*). (tn) tentacle not stained. Scale bar = 50 μm. **G)** Tangential section of cloacal siphon (cs) of a system (*BsMA2*). Arrows: dorsal languets with muscle fibres (arrows). Scale bar = 0.15 mm. **H)** Fibre (arrow) in therecto-oesophageal trabecula (*BsTnT-c*). (int), intestine. Scale bar = 50 μm. **I)** Transverse section of unstriated muscle fibres (TEM). Muscle cellsare polarised. (mf), contractile elements; (ep), epidermis; (n), nucleus. Scale bar = 0.75 μm. **J)** Longitudinal section of an unstriated muscle fibre (mf). Arrowheads: dense bodies. Scale bar = 0.2 μm. **K)** Neuromuscular junction. Small vesicles (arrows) fill the nerve termination; arrowheads: dense material in the junctional space. In transverse section of an unstriated fibre (mf), no regular disposition of filaments is recognisable (inset; scale bar = 0.09 μm). Scale bar = 0.18 μm. **L)** Longitudinal section of myocardium. Sarcomeres are defined by arrows. Thin basal lamina (bl) faces the cardiac lumen (cl). (mf), myofibrils; (pc), pericardial cavity. Scale bar = 1 μm. **M, N)** Cardiac area (arrow). ISH of *BsMA2* labels myocardium (M); no signal for *BsTnT-c* expression (N). (bs), branchial sac; (st), stomach. Scale bar = 50 μm.

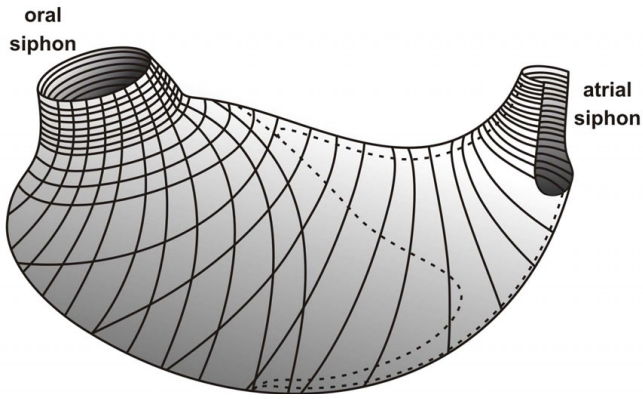

Figure 3
Representation of the musculature of a blastozooid of *B. schlosseri*. On the left is shown the oral siphon, while at the opposite site is atrial siphon. Filaments of body-wall musculature are shown, starting from the siphons.

originate from the oral siphon reaching a perpendicular disposition with the circular fibres, both forming a regular network of filaments in the anterior and lateral region of the zooid (Figures 2A, D-E).

A complex of numerous transverse bundles forms the inner muscular system, placed around the siphon opening. At the base of the siphon, muscle fibres concentrate around the velum but do not penetrate into the tentacles (Figure 2F) [63]. The common cloacal siphon forms after the confluence of the atrial siphons of each zooid, and possesses a dense musculature (Figures 2C, G). At this level, the transverse fibres appear more packed and surround the atrial siphon, extending subsequently along the dorsal languets, which are connected to each other to constitute the common cloacal chamber (Figures 2C, G). The internal organs do not show signs of musculature, except for two longitudinal fibres that depart from the neural complex area, move down along the dorsal lamina and run in the mantle through the gastric trabecula (Figures 2B, H). Anteriorly, fibres elongate around the oral siphon, following the pericoronal sinuses border (Figure 2B).

The ultrastructural organisation of musculature shows that all the unstriated muscle fibres share similar features in each part of the zooid. The cytoplasm is filled with contractile material (Figure 2I) and most cell organelles, such as nuclei and mitochondria, are confined in peripheral regions of the fibres. The contractile material consists of thin and thick filaments closely apposed, and in longitudinal sections do not reveal any sarcomeric organisation (Figure 2J). However, occasionally in transverse sections the thick filaments appear surrounded by thin filaments with the arrangement recalling that of the striated muscle (Figure 2K, inset). Dense bodies are recognisable in longitudinal sections along the fibre, representing regions to which thin and thick filaments bind. The disposition of these dense bodies is not random, however it was not possible to establish if they are distributed according a specific pattern (Figure 2J).

Fibres are covered by fuzzy material forming a thin basal lamina. In some cases, contiguous fibres present their sarcolemma closely apposed to each other and the extra-cellular material is no longer recognisable. Nervous fibres contact single muscle cells or penetrate between apposed fibres and form neuromuscular junctions (Figure 2K), which have been previously described as acetylcholinesterase (AChE) positive [64].

Heart

The heart of *B. schlosseri* is located in the ventral mantle and extends between the posterior limit of the endostyle and the stomach. It is in form of a curved double walled tube of external pericardium and internal myocardium, connected to each other at the level of the longitudinal rafe. The myocardium is responsible for the reversible, helicoidal contraction that drives blood movement. Phalloidin staining allows us to recognise muscle fibres at the myocardium level, organised in a dense network of transverse thin bundles. At the ultrastructural level (Figure 2L) the myocardic cells appear polarised, with the contractile material organised in striated myofibrils close to the cardiac lumen. The sarcomeric distribution and the ratio 1:2 of thick to thin filaments recalls the striated musculature of the larva [65]. In many sections it is possible to see a deeper layer of myofibrils oriented in a right angle with respect the superficial one. ISH for the localisation of *BsMA2* transcripts show signal at the myocardial level, localised between stomach and branchial sac (Figure 2M). No *BsTnT-c* expression was found in the heart of the adult zooid (Figure 2N).

Musculature differentiation during the blastogenetic cycle

Body-wall

We investigated the differentiation of unstriated muscles during the entire blastogenetic cycle, beginning from the appearance of a budlet to the adult stage and zooid regression. Results from phalloidin, TEM and ISH experiments allowed us to follow in detail the musculature modifications throughout each developmental stage (summarised in Figure 4A-L). Antisense RNA probes designed against *BsMA2* and *BsTnT-c* mRNAs provided similar results.

In the early phases of bud development, no phalloidin signal was detected. Signal then began to be recognisable in the form of a diffuse fluorescence throughout the whole bud, but no discrete muscle fibres were distinguishable. At the same time, the first evidence of the diffuse expression of *BsMA2* and *BsTnT-c* transcripts appeared just before the formation of a new blastogenetic generation from the body-wall of bud (stage 6). Both probes produce

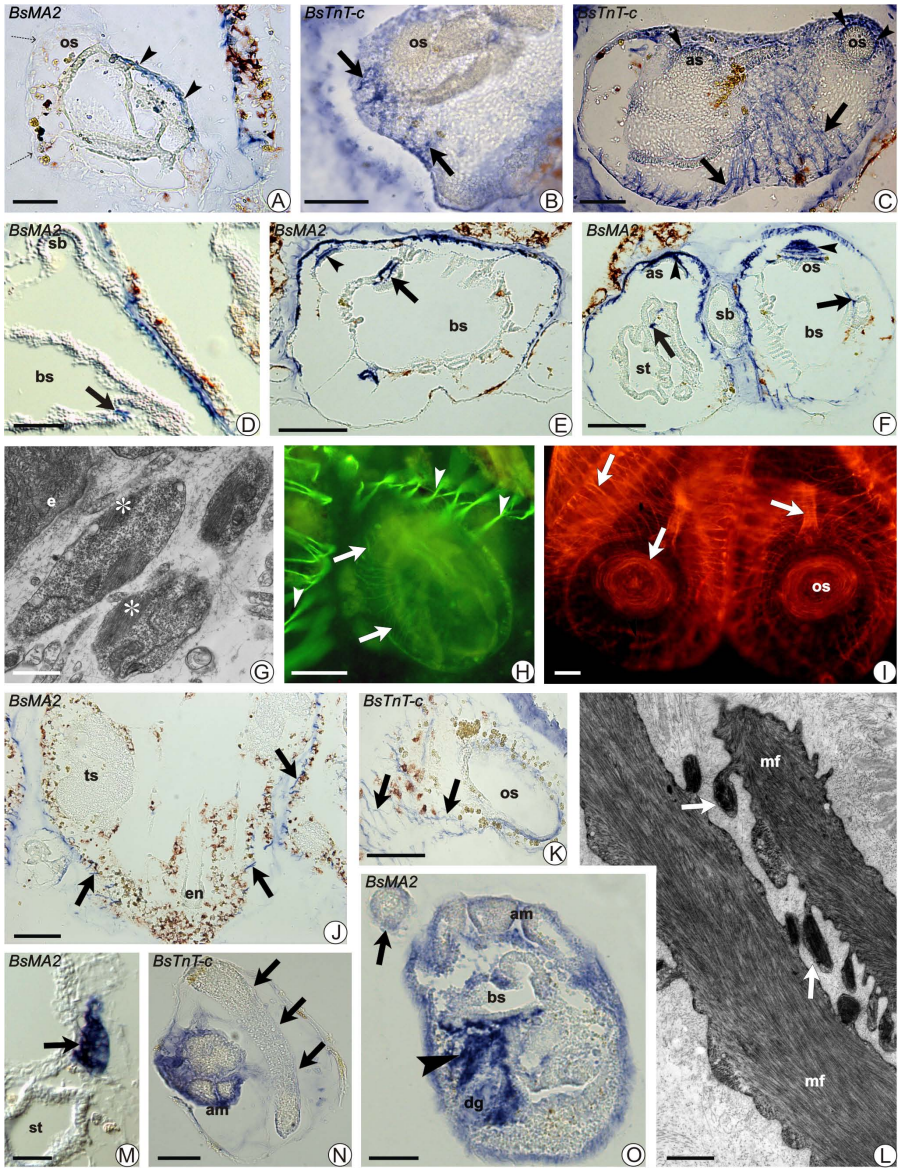

Figure 4

Modifications of the musculature during the blastogenetic cycle. Bud development (A-I; M), take-over (J-L), and larval phases (N, O), shown by: ISH on sections (A-F; J; K; M-O), phalloidin -FITC (H), -TRITC (I), and TEM (L). **A)** Stage 6; signal in the intersiphonal region (*BsMA2*; arrowheads). (os), oral siphon. Dotted arrows: epidermis. Scale bar = 50 μm. **B)** Stage 7; myoblasts (arrows) around the rudiment oforal siphon (os). Scale bar = 50 μm. **C-F)** Stage 8; mantle fibres between oral (os) and atrial (as) siphons (C, ISH for *BsTnT-c*). Fibres run along the dorsal lamina (arrows, E, F) and through the recto-oesophageal trabecula (arrows, D, F). Arrowheads (C, E, F): fibres around the siphons. (bs), branchial sac;(st), stomach; (sb), secondary bud. Scale bar = 50 μm (C, D); scale bar = 0.1 mm (E, F). **G)** Myoblasts adhere to mantle epithelia (e). Asterisks: contractile material. Scale bar = 1.2 μm. **H)** Stage 8; phalloidin -FITC evidences thin mantle fibres (arrows) and muscle bundles in the adult (arrowheads). Scale bar = 0.1 mm. **I)** Two zooids approaching the opening of oral siphons (os). Arrows: muscle fibres. Scale bar = 0.1 mm. **J, K)** Zooids during regression. A decrease (compare Figures 2D-H) in the expression level of *BsMA2* (J) and *BsTnT-c* (K) is recognisable. Fibres (arrows) assume an irregular aspect. Testis (ts; J) is not marked. (os), oral siphon; (en), endostyle. Scale bar = 0.1 mm. **L)** During regression, muscle fibres (mf)form cytoplasmic protrusions. Arrows: organelles in degeneration. Scale bar = 0.8 μm. **M)** The heart (arrow) of bud gives a signal only with *BsMA2*. (st), stomach. Scale bar = 25 μm. **N, O)** Early larvae. In the striated caudal muscles (arrows) no signal for *BsTnT-c* (N) and *BsMA2* (O) expression. ISH of *BsMA2* labels mesenchymal cells (arrowheads). Tunic is around ampullae (am) and cephalenteron and stains non-specifically. Scale bar = 50 μm.

a diffuse signal, labelling a localised region between oral and atrial siphon and staining cells probably representing mesenchymal cells differentiating into myoblasts (Figures 4A-B). These cells begin to organise to form bundles of fibres; the siphons are in form of rudiments as epidermal thickenings. In the next stage, the body-wall musculature generates a network of fibres (Figure 4C) and signs of gene expression are observable in fibres that run along the dorsal lamina and through the recto-oesophageal trabecula (Figures 4D-F). The presence of differentiating myoblasts has been confirmed with TEM: they appear as circulating cells, which adhere and group to the mantle epithelia close to the developing siphons and are characterised by contractile material in their cytoplasm (Figure 4G).

Subsequently, the heart begins to beat and organogenesis progresses. Thin, discrete, apparently disorganised muscle fibres start to be recognisable with phalloidin (Figure 4H) and, approaching the opening of the siphon, the muscle fibres become thicker and reach the definitive regular organisation, extending laterally to envelope the rest of the body (Figure 4I). At this stage, the fibres that run around the velum and the pericoronal bands are particularly evident, as seen on ISH sections using both *BsMA2* and *BsTnT-c* probes (not shown).

During takeover, the primary buds open their siphons, replacing the adult zooids, which are contracting to the centre of the system and are gradually reabsorbed. The regressing muscle fibres become more irregular and show decreased level in expression for both *BsMA2* and *BsTnT-c* transcripts, as compared to the filtering zooids (Figures 4J-K). The contraction of fibres leads to the formation of cytoplasmic protrusions along the contractile material, which contain degenerating organelles (Figure 4L). The contractile material condenses to form a rigid structure, the paracrystalline body [66]. As with the other zooid tissues, the muscle cells are phagocytised by macrophages and digested in intracellular vacuoles.

Heart

Our observations agree with a previous report on heart development [65]. Briefly, in the buds of *B. schlosseri* the heart originates from a ventral vesicle, which forms from mesenchymal cells that invaginate along the dorsal lamina to form the myocardium (stage 4). The first regular heart beat characterises the transition of bud to stage 8, from which point a strong signal of *BsMA2* expression is first recognisable (Figure 4M), limited to the cytoplasm of cardiac cells in the developing myocardium. This is maintained until zooid regression.

In situ *hybridisation in larval muscle*

Antisense RNA probes for *BsMA2* and *BsTnT-c* were tested in late embryos and larvae in order to verify if the two genes were expressed in musculature also during embryogenesis. Sections containing both the cephalenteron and tail of specimens at different stage show that transcripts of *BsTnT-c* are never detectable (Figure 4N). Also transcripts of *BsMA2* are not detectable at the level of the caudal striated muscle. However, the *BsMA2* probe gives strong signal at the oral siphon level where it labels mesenchymal cells, some of them dispersed in the branchial area, but most aggregated around the ectoderm of the rudiment of oral siphon (Figure 4O).

Discussion

Previous research has shown that the unstriated muscle of adult ascidians possesses intermediate features between the striated and smooth muscles of vertebrates; it has multinucleate cells [17] and a contractile regulatory system based on the Tn/Tm apparatus similar to vertebrate striated muscle [15,16], but also lacks sarcomeric periodicity and regular spatial organisation of myofilaments, similar to vertebrate smooth muscle. From a developmental point of view, it is interesting to note that unstriated muscle differentiation in ascidians is associated with the formation of sessile zooids that occurs through metamorphic events, in the oozooid, or asexual reproduction in all the blastozooids.

During their life cycle ascidians also develop striated muscle in the tail of the free-swimming larvae and in the myocardium of adults. This has typical characteristics of the vertebrate striated muscles, such as the arrangement and the ratio of the myofilaments in the myofibrils (see [13,67]). The study of the different musculatures during the complete cycle of a colonial ascidian can be of interest from developmental and evolutionary perspectives, especially considering that the tunicates are the closest group (taxon) to vertebrates [68]. In this light, our study on *B. schlosseri* muscle allows us to better analyse the development and organisation of this system. In particular, we aimed to characterise two main genes (actin and TnT), whose expression patterns were investigated in the larva and during the life cycle of the blastozooids forming the colony. Moreover, our data contribute to a better understanding of the evolution and maintenance of the different muscle types in the chordate group.

Actins

Our analyses confirm that actin genes are extremely well conserved in metazoans, with most variability confined to N-terminal region, that remains the most distinct feature amongst different actin isoforms and is exposed on the surface of the protein monomers [69]. CAs and MAs are distinguishable by the presence of residues at specific positions, and by a series of acidic amino acids involved in the interaction with myosin in the muscular actins [70].

Some ascidians, such as *C. intestinalis* [34] and *Molgula oculata* [GenBank: AAC28358, AAC28356], are known to

possess different CA genes; accordingly, it is possible that *B. schlosseri* possesses other genes coding for CAs.

As demonstrated by our ISH experiments, *BsMA2* is expressed in both unstriated and cardiac musculature of *B. schlosseri* blastozooids and in the presumptive adult muscle, but not in the striated musculature of the larva.

The alignment of the amino acid sequences shows that ascidian larval and adult MAs are very similar to the MAs of vertebrates. The two different ascidian MAs are well resolved from each other and belong to a well-defined group of chordate MAs. This suggests there was a single common ancestral gene in the chordate common ancestor from which evolved all the different MAs of the phylum.

The intron pattern of *BsMA2* could be found in other ascidian MA2s and the position of the first intron seems to be conserved from vertebrate to echinoderm actin genes, apart for ascidian larval and amphioxus muscle forms (additional file 2). All the examined tunicate muscle actins do not exhibit the specific intron at position 328/329 which characterises the vertebrate forms, and it could be hypothesised that this intron was acquired during vertebrate evolution.

Our analysis on actin intron-exon organisation fits Kusakabe and collaborators' [35] depiction of a conserved deuterostome actin intron pattern, some of which are also present in protostomes (which have between zero and seven introns).

The intron positions of *BsCA1* share the same pattern found in other ascidian CAs, such as *HrCA1* (additional file 2). Two ascidian introns (150 and 204) are shared with the vertebrate muscle actins, but not with the cytoplasmic actins.

Troponin T

The most probable scenario pictured by our analysis, considering animal phylogeny [68,71,72], predicts an ancestral TnT gene in the bilaterian common ancestor from which protostome and deuterostome TnTs evolved. In the deuterostome lineage, ascidian and vertebrate TnT isoforms evolved separately from an ancestral chordate TnT gene. The troponin T genes of vertebrates are normally involved in several splicing phenomena that result in a number of isoforms characterising different tissues or developmental stages. Our phylogenetic analysis confirms that the vertebrate TnT gene family arose by gene duplications within the vertebrate lineage and, at least in vertebrates, there is a similarity between TnT isoforms of the same muscle type in different species greater than between isoforms of different muscle types in the same species [34,73]. This "tissue-specific TnT isoforms homology" hypothesis could be also extended to ascidians as *BsTnT-c* is closely related to the adult isoform of *H. roretzi*, but more information is needed from other tunicate species to confirm this.

It has been shown that one TnT gene encodes for a specific larval and another for a body-wall muscle form in *H. roretzi*, while in *C. intestinalis* one gene codes for three isoforms, which are expressed respectively in the larva, heart and adult body-wall muscle [34,60]. In our study, we found that the expression of the *BsTnT-c* transcript is detected only in the body-wall musculature of zooids, without any signal at the myocardial level. We hypothesise that *B. schlosseri* possesses a different isoform expressed only in the heart muscle and probably the same situation is present in *H. roretzi*, in which only a form was isolated from the body-wall muscle [60].

General Morphology

The study with phalloidin was successful in revealing the general organisation of the body-wall muscle in the blastozooids of *B. schlosseri* and, interestingly, a strict correspondence was found between the time of appearance and morphology of the muscle and the expression of the two investigated genes.

The muscle system of *B. schlosseri* follows the general organisation reported in other ascidians (see [67]). As expected, muscles concentrate in the mantle around the siphons where they are organised in a net of circular and longitudinal bands that are extended mainly along the dorso-lateral mantle. No muscle was observed in the branchia and gut, where food movement is caused by ciliary beating [74]. However, two bands run along the dorsal lamina penetrating the recto-oesophageal trabecula to reach the atrial siphon. They take part in the general contraction of the body. Tentacles of the oral siphon lack musculature and their movement depends on blood pressure. They expose the coronal organ with mechanosensory cells participating in the regulation of muscle activity to control the water flow through the body [63,75]. The general layout of the muscle innervation, described in detail in *B. schlosseri* buds [76], has shown that motor axons run out from cell bodies in the brain to the developing muscles of the zooid. However, excitation can extend to contiguous zooids and it was proposed that coordination of cardiac and body-wall muscle contractions in the zooids of the same colony can be achieved by electric impulses propagated through epithelial cells lining the body and the blood vessels in the tunic [77]. Heart beating begins early in the bud, before differentiation of the other organs [65] and continues also during take-over and regression of organs, in order to guarantee blood circulation for the distribution of tissue residuals in the entire colony.

With our original protocol for ISH on sections of *B. schlosseri* colonies and larvae, we recognised the structures expressing *BsMA2* and *BsTnT-c*. At the same time these structures were analysed by means of cytochemical and ultrastructural techniques. This integrated study on muscle organisation allowed us to characterise the series of events for muscle appearance, differentiation and regression during the entire blastogenetic cycle and to recognise several critical differences between unstriated muscle and striated cardiac and larval musculature. During differentiation, we found that the mRNAs for *BsMA2* and *BsTnT-c* were synthesised by cells a short time before their translation into proteins and that the first myoblasts could be revealed by different techniques (fluorescence, TEM, ISH) in the mantle around the rudiment of siphons. Phalloidin gave a diffuse light signal, whereas TEM recognised differentiating myoblasts among mesenchymal cells adhering to epithelia, thanks to the appearance of aggregating myofilaments in their cytoplasm. This recalls what Sugino et al. [78] observed in the siphons of the buds of another stolidobranch, *Simplegma reptans*. We showed that, in *B. schlosseri*, the probes for *BsMA2* and *BsTnT-c* stained earlier and exactly the differentiating cells, in agreement with the idea that the probes specifically localise expressed mRNAs, whereas TEM and phalloidin recognise actin after polymerisation. Thus, the signal of phalloidin marks specifically the muscle only when a great number of thin filaments form fibres. Differently, when the zooids approached regression and shrank, muscle activity (with the exception of the heart) decreased markedly and stopped. In correspondence to these events, as previously reported by Burighel and Schiavinato [66], we showed that the disorganisation of muscle was accompanied by morphological alteration of cells with formation of cytoplasmic protrusions containing organelles. At the same time the two investigated muscle genes underwent a progressive reduction of transcript levels, as revealed by the decrease of the intensity of their expression signal with ISH.

Notably, both the probes do not label the striated muscle of the larva. This could suggest that different isoforms were expressed in the larval caudal muscle. However, a strong signal was recognised in the larva, due to the differentiating unstriated muscle in the rudiment of the siphon. In the solitary ascidian *C. intestinalis* no signal at this level was detected possibly due to a heterochronic difference in siphon development, because the embryonic life of *C. intestinalis* extends for 18 h, while the *B. schlosseri* embryo develops for 5 days in the atrial cavity of mother, thus its larva has more developed adult structures [67].

In cardiac, striated in the larval tail and unstriated in the adult body-wall muscle types of *B. schlosseri* we have found, respectively, three different combinations of the MA and TnT expression: BsMA2$^+$/BsTnT-c$^-$, BsMA2$^-$/BsTnT-c$^-$ and BsMA2$^+$/BsTnT-c$^+$. This indicates that the three ascidian muscle types differ not only "ultrastructurally", but also in the combinations of the subtype of the molecules that compose them.

Conclusion

Common and divergent pathways in alternative developmental processes are an intriguing issue in evolutionary and developmental biology research (see [38] for review in ascidians), and this work adds an element in this field as our data indicate a putative common pathway between embryogenesis and blastogenesis in unstriated adult body-wall muscle of ascidians, which also displays a similar organisation in both solitary and colonial ascidians [see also [67]].

Our data agree with the idea that the smooth muscle of vertebrates does not derive directly from the unstriated muscle of ascidians, but from a striated muscle possessed by the ancestor of vertebrates [24]. Indeed, the body-wall muscle of ascidians possesses intermediate aspects between striated (e.g. multinucleate fibres, a troponin regulatory system and expression of MyoD-like transcription factors, nicotinic-type acetylcholine receptors-cholinergic) and smooth (absence of sarcomeric organisation) muscle of vertebrates [[10,20] and [23]]. This supports the idea that it derived from the striated muscle of the chordate ancestor, as an adaptation to the sessile life-style which requires slow contractions for fine regulation of water flow throughout the body and extended, rapid retraction (till 50% of length) of the body for defensive activities [24,67].

Tunicates show high muscle plasticity in that, besides the three kinds of muscles described in ascidians, they can also form other muscle types. Among thaliaceans (except for pyrosomids that possess an unstriated muscle similar to body-wall muscle of ascidians), doliolids and salps show unusual muscle bands encircling their bodies. Both taxa lack a T system, but salps have multinucleated striated muscle endowed with an extensive sarcoplasmic reticulum [79,80], whereas doliolids, capable of extremely rapid movements, possess obliquely striated muscle with no or scarce sarcoplasmic reticulum [81].

Moreover, the appendicularian *Oikopleura longicauda* has a typical caudal striated muscle with specific characters: muscle cell differentiation proceeds throughout a first mononucleated phase, (recalling the definitive larval muscle of ascidians), then followed by division of the nuclei and formation of a multinucleated musculature, in contrast with cell fusion that typically characterises vertebrate skeletal muscle [82,83]. In addition, at the molecular level, the actin sequence of appendicularians possesses intermediate features between the two ascidian types [82].

The characteristics and plasticity of tunicate muscle, possibly derived from an original striated muscle, together with the position in phylogenetic tree of actin and troponin ascidian genes, agree with the recent view that not cephalochordates, but ascidians are the sister group of vertebrates [68]. At the same time, in the light of the actual debate on the sessile or motile nature of chordate ancestor [84], all the above considerations agree with the idea that a motile animal possessing the genetic machinery for differentiation of the typical chordate striated muscle was the common chordate ancestor, from which the tunicates originated and evolved their variety of muscles.

Authors' contributions

VD and FG designed the study and drafted the manuscript; VD performed the analysis of genomic sequences; VD, FG, CS identified, analysed and cloned transcripts, and performed ISH; SMS, PB and LM participated in the design of the study and helped draft the manuscript, SMS and FG conducted the phylogenetic analyses; PB and LM performed histochemistry, ultrastructure and helped with analysis and interpretations of ISH. All authors read and approved the final manuscript.

Additional material

Additional file 1

***Figure S1**. Table reassuming the primers used in PCR reactions, as described in the text.*
Click here for file
[http://www.biomedcentral.com/content/supplementary/1471-213X-9-48-S1.pdf]

Additional file 2

***Figure S2**. Intron positions in protein-coding region of* BsMA2 *and* BsCA1 *and actin genes of other organisms.*
Click here for file
[http://www.biomedcentral.com/content/supplementary/1471-213X-9-48-S2.pdf]

Additional file 3

***Figure S3**. Molecular phylogenetic analysis of the actin protein family.*
Click here for file
[http://www.biomedcentral.com/content/supplementary/1471-213X-9-48-S3.pdf]

Additional file 4

***Figure S4**. Comparison at specific amino acid positions of actins from different organisms.*
Click here for file
[http://www.biomedcentral.com/content/supplementary/1471-213X-9-48-S4.pdf]

Additional file 5

***Figure S5**. Alignment of 65 complete amino acid sequences of muscle and cytoplasmatic actins from metazoans.*
Click here for file
[http://www.biomedcentral.com/content/supplementary/1471-213X-9-48-S5.pdf]

Additional file 6

***Figure S6**. The N-termini of cytoplasmic and muscle actins of various species.*
Click here for file
[http://www.biomedcentral.com/content/supplementary/1471-213X-9-48-S6.pdf]

Additional file 7

***Figure S7**. Alignment of troponin T sequences.*
Click here for file
[http://www.biomedcentral.com/content/supplementary/1471-213X-9-48-S7.pdf]

Additional file 8

***Figure S8**. Pairwise scores calculated between TnTs of some deuterostomes compared to a rabbit fast skeletal muscle form.*
Click here for file
[http://www.biomedcentral.com/content/supplementary/1471-213X-9-48-S8.pdf]

Acknowledgements

The authors wish to thank M. Del Favero for technical help, and Marine Genomics Europe for the production and subsequent sequencing of the cDNA library clones at Max Planck Institute for Molecular Genetics. SMS acknowledges the support of the Royal Society and BBSRC. This study was founded by grants from the Ministero della Università e Ricerca Scientifica e Tecnologica and by the Università degli Studi di Padova to L. M. and P. B.

References

1. Satoh N: *Developmental biology of ascidians* New York: Cambridge University Press; 1994.
2. Ceresa Castellani L, Camatini M, Lora Lamia Donin C: **Aspetti ultrastrutturali della muscolatura di ascidia.** *Ist Lomb Rend Sc B* 1972, **106:**59-72.
3. Schiaffino S, Burighel P, Nunzi MG: **Involution of the caudal musculature during metamorphosis in the ascidian, *Botryllus schlosseri*.** *Cell Tissue Res* 1974, **153:**293-305.
4. Schiaffino S, Nunzi MG, Burighel P: **T system in ascidian muscle: organization of the sarcotubular system in the caudal muscle cells of *Botryllus schlosseri* tadpole larvae.** *Tissue Cell* 1976, **8:**101-110.
5. Nishida H, Satoh N: **Cell lineage analysis in ascidian embryos by intracellular injection of a tracer enzyme. I. Up to the eight-cell stage.** *Dev Biol* 1983, **99:**382-394.
6. Meedel TH, Crowther RJ, Whittaker JR: **Determinative properties of muscle lineages in ascidian embryos.** *Development* 1987, **100:**245-260.
7. Hudson C, Yasuo H: **Similarity and diversity in mechanisms of muscle fate induction between ascidian species.** *Biol Cell* 2008, **100:**265-277.
8. Nishida H: **Determinative mechanisms in secondary muscle lineages of ascidian embryos: development of muscle-specific features in isolated muscle progenitor cells.** *Development* 1990, **108:**559-568.
9. Passamaneck YJ, Di Gregorio A: ***Ciona intestinalis* : chordate development made simple.** *Dev Dyn* 2005, **233:**1-19.
10. Meedel TH, Chang P, Yasuo H: **Muscle development in *Ciona intestinalis* requires the b-HLH myogenic regulatory factor gene *Ci-MRF*.** *Dev Biol* 2007, **302:**333-344.
11. Hirano T, Nishida H: **Developmental fates of larval tissues after metamorphosis in ascidian *Halocynthia roretzi*. I. Origin of mesodermal tissues of the juvenile.** *Dev Biol* 1997, **192:**199-210.
12. Davidson B, Levine M: **Evolutionary origins of the vertebrate heart: Specification of the cardiac lineage in *Ciona intestinalis*.** *Proc Natl Acad Sci USA* 2003, **100:**11469-11473.

13. Meedel TH: **Development of ascidian muscles and their evolutionary relationship to other chordate muscle types.** In *Reproductive Biology of Invertebrates: Progress in Developmental Biology Volume VIII*. Edited by: Collier JR, Adiyodi KG, Adiyodi RG. New York: John Wiley and Sons; 1998:305-330.
14. Whittaker JR: **Determination of alkaline phosphatase expression in endodermal cell lineages of an ascidian embryo.** *Biol Bull* 1990, **178:**222-230.
15. Toyota N, Obinata T, Terakado K: **Isolation of troponin-tropomyosin-containing thin filaments from ascidian smooth muscle.** *Comp Biochem Physiol* 1979, **62B:**433-441.
16. Endo T, Obinata T: **Troponin and its components from ascidian smooth muscle.** *J Biochem* 1981, **89:**1599-1608.
17. Shinohara Y, Konishi K: **Ultrastructure of the body-wall muscle of the ascidian *Halocynthia roretzi* : smooth muscle cell with multiple nuclei.** *J Exp Zool* 1982, **221:**137-142.
18. Takagi T, Konishi K: **Amino acid sequence of troponin C obtained from ascidian (*Halocynthia roretzi*) body wall muscle.** *J Biochem* 1983, **94:**1753-1760.
19. Terakado K, Obinata T: **Structure of multinucleated smooth-muscle cells of the ascidian *Halocynthia roretzi*.** *Cell Tissue Res* 1987, **247:**85-94.
20. Florey E: **Cholinergic neurons in tunicates: an appraisal of the evidence.** *Comp Biochem Physiol* 1967, **22:**617-627.
21. Mendes EG, Zingales BS: **Pharmacological studies on the invertebrate non-striated muscles. II. The tunicate siphon muscles.** *Comp Gen Pharmacol* 1972, **3:**261-270.
22. Kobzar GT, Shelkovnikov SA: **The muscle chemoreceptors of the ascidian *Halocynthia aurantium*.** *Comp Biochem Physiol C* 1985, **80:**395-400.
23. Nevitt G, Gilly WF: **Morphological and physiological properties of non-striated muscle from the tunicate, *Ciona intestinalis* : parallels with vertebrate skeletal muscle.** *Tissue Cell* 1986, **18:**341-360.
24. Meedel TH, Hastings KE: **Striated muscle-type tropomyosin in a chordate smooth muscle, ascidian body-wall muscle.** *J Biol Chem* 1993, **268:**6755-6764.
25. Tomlinson CR, Beach RL, Jeffery WR: **Differential expression of a muscle actin gene in muscle cell lineages of ascidian embryos.** *Development* 1987, **101:**751-765.
26. Beach RL, Jeffery WR: **Temporal and spatial expression ofa cytoskeletal actin gene in the ascidian *Styela clava*.** *Dev Genet* 1990, **11:**2-14.
27. Beach RL, Jeffery WR: **Multiple actin genes encoding the same alpha-muscle isoform are expressed during ascidian development.** *Dev Biol* 1992, **151:**55-66.
28. Kusakabe T, Makabe KW, Satoh N: **Tunicate muscle actin genes. Structure and organization as a gene cluster.** *J Mol Biol* 1992, **227:**955-960.
29. Kusakabe T, Hikosaka A, Satoh N: **Coexpression and promoter function in two muscle actin gene complexes of different structural organization in the ascidian *Halocynthia roretzi*.** *Dev Biol* 1995, **169:**461-472.
30. Kusakabe T, Swalla BJ, Satoh N, Jeffery WR: **Mechanism of an evolutionary change in muscle cell differentiation in ascidians with different modes of development.** *Dev Biol* 1996, **174:**379-392.
31. Kovilur S, Jacobson JW, Beach RL, Jeffery WR, Tomlinson CR: **Evolution of the chordate muscle actin gene.** *J Mol Evol* 1993, **36:**361-368.
32. Swalla BJ, White ME, Zhou J, Jeffery WR: **Heterochronic expression of an adult muscle actin gene during ascidian larval development.** *Dev Genet* 1994, **15:**51-63.
33. Araki I, Tagawa K, Kusakabe T, Satoh N: **Predominant expression of a cytoskeletal actin gene in mesenchyme cells during embryogenesisof the ascidian *Halocynthia roretzi*.** *Dev Growth Differ* 1996, **38:**401-411.
34. Chiba S, Awazu S, Itoh M, Chin-Bow ST, Satoh N, Satou Y, Hastings KE: **A genomewide survey of developmentally relevant genes in *Ciona intestinalis*. IX. Genes for muscle structural proteins.** *Dev Genes Evol* 2003, **213:**291-302.
35. Kusakabe T, Araki I, Satoh N, Jeffery WR: **Evolution ofchordate actin genes: evidence from genomic organization and amino acid sequences.** *J Mol Evol* 1997, **44:**289-298.
36. Lehman W, Szent-Györgyi AG: **Regulation of muscular contraction. Distribution of actin control and myosin control in the animal kingdom.** *J Gen Physiol* 1975, **66:**1-30.
37. Gordon AM, Homsher E, Regnier M: **Regulation of contraction in striated muscle.** *Physiol Rev* 2000, **80:**853-924.
38. Manni L, Burighel P: **Common and divergent pathways in alternative developmental processes of ascidians.** *Bioessays* 2006, **28:**902-912.
39. Sabbadin A: **Osservazioni sullo sviluppo, l'accrescimento e la riproduzione di *Botryllus schlosseri* (Pallas), in condizioni di laboratorio.** *Boll Zool* 1955, **22:**243-265.
40. Manni L, Zaniolo G, Cima F, Burighel P, Ballarin L: ***Botryllus schlosseri* : a model ascidian for the study of asexual reproduction.** *Dev Dyn* 2007, **236:**335-352.
41. Gasparini F, Franchi N, Spolaore B, Ballarin L: **Novel rhamnose-binding lectins from the colonial ascidian *Botryllus schlosseri*.** *Dev Comp Immunol* 2008, **32:**1177-1191.
42. Wilbur WJ, Lipman DJ: **Rapid similarity searches of nucleic acid and protein data banks.** *Proc Natl Acad Sci USA* 1983, **80:**726-730.
43. Myers EW, Miller W: **Optimal alignments in linear space.** *Comput Appl Biosci* 1988, **4:**11-17.
44. Larkin MA, Blackshields G, Brown NP, Chenna R, McGettigan PA, McWilliam H, Valentin F, Wallace IM, Wilm A, Lopez R, Thompson JD, Gibson TJ, Higgins DG: **Clustal W and Clustal X version 2.0.** *Bioinformatics* 2007, **23:**2947-2948.
45. Huelsenbeck JP, Ronquist F: **MRBAYES: Bayesian inference of phylogenetic trees.** *Bioinformatics* 2001, **17:**754-755.
46. Ronquist F, Huelsenbeck JP: **MrBayes 3: Bayesian phylogenetic inference under mixed models.** *Bioinformatics* 2003, **19:**1572-1574.
47. Page RD: **TreeView: an application to display phylogenetic trees on personal computers.** *Comput Appl Biosci* 1996, **12:**357-358.
48. Blom N, Sicheritz-Pontén T, Gupta R, Gammeltoft S, Brunak S: **Prediction of post-translational glycosylation and phosphorylation of proteins from the amino acid sequence.** *Proteomics* 2004, **4:**1633-1649.
49. Kiemer L, Bendtsen JD, Blom N: **NetAcet: prediction of N-terminal acetylation sites.** *Bioinformatics* 2005, **21:**1269-1270.
50. Wheelan SJ, Church DM, Ostell JM: **Spidey: a tool for mRNA-to-genomic alignments.** *Genome Res* 2001, **11:**1952-1957.
51. Vandekerckhove J, Weber K: **Mammalian cytoplasmic actins are the products of at least two genes and differ in primary structure in at least 25 identified positions from skeletal muscle actins.** *Proc Natl Acad Sci USA* 1978, **75:**1106-1110.
52. Vandekerckhove J, Weber K: **The complete amino acid sequence of actins from bovine aorta, bovine heart, bovine fast skeletal muscle, and rabbit slow skeletal muscle. A protein-chemical analysis of muscle actin differentiation.** *Differentiation* 1979, **4(3):**123-133.
53. Khalturin K, Becker M, Rinkevich B, Bosch TC: **Urochordates and the origin of natural killer cells: identification of a CD94/NKR-P1-related receptor in blood cells of *Botryllus*.** *Proc Natl Acad Sci USA* 2003, **100:**622-627.
54. Perry SV: **Troponin T: genetics, properties and function.** *J Muscle Res Cell Motil* 1998, **19:**575-602.
55. Pearlstone JR, Johnson P, Carpenter MR, Smillie LB: **Primary structure of rabbit skeletal muscle troponin-T. Sequence determination of the NH2-terminal fragment CB3 and the complete sequence of troponin-T.** *J Biol Chem* 1977, **252:**983-989.
56. Risnik VV, Gusev NB: **Some properties of the nucleotide-binding site of troponin T kinase-casein kinase type II from skeletal muscle.** *Biochim Biophys Acta* 1984, **790:**108-116.
57. Krebs EG, Eisenman RN, Kuenzel EA, Litchfield DW, Lozeman FJ, Lüscher B, Sommercorn J: **Casein kinase II as a potentially important enzyme concerned with signal transduction.** *Cold Spring Harb Symp Quant Biol* 1988, **53:**77-84.
58. Jackson P, Amphlett GW, Perry SV: **The primary structure of troponin T and the interaction with tropomyosin.** *Biochem J* 1975, **151:**85-97.
59. Pearlstone JR, Smillie LB: **The binding site of skeletal alpha-tropomyosin on troponin-T.** *Can J Biochem* 1977, **55:**1032-1038.
60. Endo T, Matsumoto K, Hama T, Ohtsuka Y, Katsura G, Obinata T: **Distinct troponin T genes are expressed in embryonic/larval tail striated muscle and adult body wall smooth muscle of ascidian.** *J Biol Chem* 1996, **271:**27855-27862.
61. Blumenschein TM, Tripet BP, Hodges RS, Sykes BD: **Mapping the interacting regions between troponins T and C. Binding of**

TnT and TnI peptides to TnC and NMR mapping of the TnT-binding site on TnC. *J Biol Chem* 2001, **276:**36606-36612.
62. Tanokura M, Tawada Y, Ono A, Ohtsuki I: **Chymotryptic subfragments of troponin T from rabbit skeletal muscle. Interaction with tropomyosin, troponin I and troponin C.** *J Biochem* 1983, **93:**331-337.
63. Burighel P, Lane NJ, Gasparini F, Tiozzo S, Zaniolo G, Carnevali MD, Manni L: **Novel, secondary sensory cell organ in ascidians: in search of the ancestor of the vertebrate lateral line.** *J Comp Neurol* 2003, **46:**236-249.
64. Burighel P, Sorrentino M, Zaniolo G, Thorndyke MC, Manni L: **The peripheral nervous system of an ascidian, *Botryllus schlosseri*, as revealed by cholinesterase activity.** *Invertebr Biol* 2001, **120:**185-198.
65. Nunzi MG, Burighel P, Schiaffino S: **Muscle cell differentiation in the ascidian heart.** *Dev Biol* 1979, **68:**371-380.
66. Burighel P, Schiavinato A: **Degenerative regression of the digestive tract in the colonial ascidian *Botryllus schlosseri* (Pallas).** *Cell Tissue Res* 1984, **235:**309-318.
67. Burighel P, Cloney RA: **Urochordata: Ascidiacea.** In *Microscopic anatomy of invertebrates Volume 15*. Edited by: Harrison FW, Ruppert EE. New York: Wiley- Liss, Inc; 1997:221-347.
68. Delsuc F, Tsagkogeorga G, Lartillot N, Philippe H: **Additional molecular support for the new chordate phylogeny.** *Genesis* 2008, **46:**592-604.
69. Lorenz M, Popp D, Holmes KC: **Refinement of the F-actin model against X-ray fiber diffraction data by the use of a directed mutation algorithm.** *J Mol Biol* 1993, **234:**826-836.
70. Schröder RR, Manstein DJ, Jahn W, Holden H, Rayment I, Holmes KC, Spudich JA: **Three-dimensional atomic model of F-actin decorated with *Dictyostelium* myosin S1.** *Nature* 1993, **364:**171-174.
71. Swalla BJ, Smith AB: **Deciphering deuterostome phylogeny: molecular, morphological and palaeontological perspectives.** *Philos Trans R Soc Lond B Biol Sci* 2008, **363:**1557-1568.
72. Dunn CW, Hejnol A, Matus DQ, Pang K, Browne WE, Smith SA, Seaver E, Rouse GW, Obst M, Edgecombe GD, Sørensen MV, Haddock SH, Schmidt-Rhaesa A, Okusu A, Kristensen RM, Wheeler WC, Martindale MQ, Giribet G: **Broad phylogenomic sampling improves resolution of the animal tree of life.** *Nature* 2008, **452:**745-749.
73. MacLean DW, Meedel TH, Hastings KE: **Tissue-specific alternative splicing of ascidian troponin I isoforms. Redesign of a protein isoform-generating mechanism during chordate evolution.** *J Biol Chem* 1997, **272:**32115-32120.
74. Burighel P: **Sviluppo e differenziamento del tubo digerente nel blastozooide dell'ascidia coloniale *Botryllus schlosseri* (Pallas).** *Boll Zool* 1970, **37:**177-192.
75. Manni L, Mackie GO, Caicci F, Zaniolo G, Burighel P: **Coronal organ of ascidians and the evolutionary significance of secondary sensory cells in chordates.** *J Comp Neurol* 2006, **495:**363-373.
76. Zaniolo G, Lane NJ, Burighel P, Manni L: **Development of the motor nervous system in ascidians.** *J Comp Neurol* 2002, **443:**124-135.
77. Mackie GO, Singla CL: **Coordination of compound ascidians by epithelial conduction in the colonial blood vessels.** *Biol Bull* 1983, **165:**209-220.
78. Sugino YM, Matsumura M, Kawamura K: **Body muscle-cell differentiation from coelomic stem cells in colonial tunicates.** *Zoolog Sci* 2007, **24:**542-546.
79. Bone Q, Ryan KP: **The structure and innervation of thelocomotor muscles of salps (Tunicata: Thaliacea).** *J mar biolAss UK* 1973, **53:**873-883.
80. Toselli PA, Harbison GR: **The fine structure of developing locomotor muscles of the pelagic tunicate, *Cyclosalpa affinis* (Thaliacea: Salpidae).** *Tissue Cell* 1977, **9:**137-156.
81. Bone Q, Ryan KP: **On the structure and innervation of themuscle bands of *Doliolum* (Tunicata: Cyclomyaria).** *Proc R Soc Lond B Biol Sci* 1974, **187:**315-327.
82. Nishino A, Satou Y, Morisawa M, Satoh N: **Muscle actingenes and muscle cells in the appendicularian, *Oikopleura longicauda* : phylogenetic relationships among muscle tissues in the urochordates.** *J Exp Zool* 2000, **288:**135-150.
83. Fenaux R: **Anatomy and functional morphology of the Appendicularia.** In *The biology of pelagic tunicates* Edited by: Bone Q. New York: Oxford University Press; 1998:25-34.
84. Stach T, Winter J, Bouquet JM, Chourrout D, Schnabel R: **Embryology of a planktonic tunicate reveals traces of sessility.** *Proc Natl Acad Sci USA* 2008, **105:**7229-7234.

CONCLUDING REMARKS

The aim of our research was to investigate the development and evolution of mechanisms underlying the formation of structures playing a pivotal role in the vertebrate evolution and radiation.

Our analysis took origin from the actual discussion about the presence of ectodermal placodal-like territories in ascidians, analysing tissue and cell types that could derive from them. Particularly, the study was addressed to various aspects, comprising molecular and cytological mechanisms involved in the differentiation of tissues in embryo and bud.

In the first paper, it is described the papillae differentiation in the larva of *B. schlosseri*. We followed their organisation during each embryonic stage until their regression (see contribution A, Caicci *et al*., 2010). Two types of sensory cells compose the papillae: primary sensory neurons (papillary neurons) accompanied by their parietal cells and RTENs (Rostral Trunk Epidermal Neurons). Our results evidence the existence of an anterior epidermal thickening (rostral placode) from which the sensory component of the papillae originate. Moreover, our analyses evidenced the presence of 'papillary ganglia', whose presence is of current importance if deriving from regions similar to neural crests/placodes. However, in *B. schlosseri* this structure does not possess the characteristics of a vertebrate peripheral ganglion and consequently, we proposed to assume a new classification model.

In our study, we also extended this investigation to these other transitory regions. In particular, we focused the attention on those features that share common characters with cells deriving from the vertebrate placodes, such as the hair cells that were found in several ascidian species constituting the secondary sensory cells of the coronal organ in the oral siphon (Burighel *et al*., 2003). We evidenced that coronal cells display great variability between the species, even if a fundamental organisation characterising the two orders is recognisable, suggesting that the presence of secondary sensory cells represent a plesiomorphic condition in ascidians, possibly inherited from the ancestor common to ascidians and vertebrates (see contribution B, Burighel *et al*., 2008 and contribution C, Caicci *et al*., 2010b).

Focusing on the placodes evolution in chordates, these territories derive from ectodermal regions yet defined by specific genes pattern during the ascidian embryogenesis, in contrast to the situation evidenced in cephalochordates (Kozmik *et al*., 2007). We characterised members of the molecular networks, involved in the induction and specification of placodes, during the different stages of the blastogenetic cycle of *B. schlosseri* (see contribution D, Degasperi *et al*., 2010). Moreover, we were able to show that not only common morphogenetic

processes are recognisable between blastogenesis/embryogenesis, but also that there is co-optation of the transcription factors regulating for these. Orthologs of vertebrate placodal genes are expressed in regions subjected to movements such as evagination/invagination, epithelial fusion and delamination. These regions differentiate into a variety of cell types, including primary and secondary sensory cells, secreting cells and neurons. The presence of homologous territories to vertebrate placodes suggests that ascidians possess organised networks of transcription factors differentiating specific ectodermic and non-neural cells supporting sensory structures. In vertebrates, placode-derived tissues and cells display an elevated complexity, probably acquired thanks to the recruitment of new genes after the genome duplication events characterising the vertebrate lineage (Schlosser, 2008).

The placodal genes expression in ascidians provides us new insights on the evolution of these molecular pathways, as discussed in the contribution D (Degasperi *et al*., 2010). The availability of the colonial ascidian *B. schlosseri* allowed us to study the placodal genes during the blastogenetic cycle. Our data support the view that the co-option of these genes regards different processes - such as siphon formation and stigmata differentiation - as discovered in vertebrates, where members of the *Pax-Six-Eya-Dach* pathway are recruited in the regulation of the myogenesis (Heanue *et al*., 1999).

To understand how this happens could give new cues on the mechanisms that control the cyclical asexual reproduction in *B. schlosseri*, a process that can be also interpreted as the highest expression of the regenerative potential. The peribranchial wall reveals intense expression of *Six1/2*, *Eya* and *FoxI* starting from the early stages of its differentiation. An open question is how these genes are reactivated during the first phases of blastogenesis. At the moment, there are no evidences if an external inductive signal activates the process, or if there is an internal clock triggering the process. It is also discussed if the regions involved in bud formation are maintained in a quiescent undifferentiated status of multipotentiality, or if arise from a differentiated epithelium subsequently subjected to transdifferentiation. In any case, despite the two different views the bud, which derives from somatic cells, is early constituted of undifferentiated cells that undergo proliferation and differentiation revealing in specific domains molecular-cytological potentiality of the neural placodes.

The plasticity of bud regeneration is also appreciable during the formation of the body-wall musculature, where the unstriated fibres are reabsorbed and reformed after each zooid regression. In this case, our data reveal that a pivotal role is played by circulating mesenchymal cells, able to express muscle-specific transcripts and aggregate to form muscle fibres, in a modality completely different to the larval muscle formation (see contribution E, Degasperi *et al*., 2009).

In conclusion, the interpretation of the mechanisms underlying the

development of tunicates is critical to understand the evolution of key features driving the vertebrate radiation. We carry out for the first time a molecular and morphologic study in order to characterise the muscle differentiation during the blastogenetic cycle. In particular, our results revealed that this structure, despite formed by genes that are the most conserved in nature, displays an exceptional plasticity, as also demonstrated for the nervous system development. Both musculature and nervous system played a key role in the vertebrate radiation and despite the extensive genome reduction in tunicates, the interpretation of their adaptational roots could help to understand how these crucial evolutive processes are triggered.

REFERENCES

Baker C.V., Bronner-Fraser M. 1997. The origins of the neural crest. Part II: an evolutionary perspective. *Mech. Dev.* 69: 13-29.

Bassham S., Postlethwait J.H. 2005. The evolutionary history of placodes: a molecular genetic investigation of the larvacean urochordate *Oikopleura dioica*. *Development* 132: 4259-4272.

Berrill, N.J. 1955. The origin of vertebrates. Oxford: Claredon Press, p. 257.

Bone Q., Ryan K.P. 1974. On the structure and innervation of the muscle bands of *Doliolum* (Tunicata: Cyclomyaria). *Proc. R. Soc. Lond. B Biol. Sci.* 187: 315-327.

Bone Q., Marshall N.B., Blaxter J.H.S. 1995. Sensory systems and communication. In: Bone Q., Marshall N.B., Blaxter J.H.S., editors. Biology of fishes. Glasgow: Blackie Academic & Professional. p. 219-262.

Burighel P., Lane N.J., Gasparini F., Tiozzo S., Zaniolo G., Carnevali M.D., Manni L. 2003. Novel, secondary sensory cell organ in ascidians: in search of the ancestor of the vertebrate lateral line. *J. Comp. Neurol.* 461: 236-49. Erratum in: 2003, *J. Comp. Neurol.* 464: 114.

Cañestro C., Yokoi H., Postlethwait J.H. 2007. Evolutionary developmental biology and genomics. *Nat. Rev. Genet.* 8: 932-942.

Ceresa Castellani L., Camatini M., Lora Lamia Donin C. 1972. Aspetti ultrastrutturali della muscolatura di ascidia. *Ist. Lomb. Rend. Sc. B* 106: 59-72.

Chea H.K., Wright C.V., Swalla B.J. 2005. Nodal signaling and the evolution of deuterostome gastrulation. *Dev. Dyn.* 234: 269-278.

Dehal P., Satou Y., Campbell R.K., *et al*. 2002. The draft genome of *Ciona intestinalis*: insights into chordate and vertebrate origins. *Science* 298: 2157-2167.

Delsuc F., Tsagkogeorga G., Lartillot N., Philippe H. 2008. Additional molecular support for the new chordate phylogeny. *Genesis* 46: 592-604.

Endo T., Obinata T. 1981. Troponin and its components from ascidian smooth muscle. *J. Biochem.* 89: 1599-1608.

Hall B.K. 2009. The neural crest and neural crest cells in vertebrate development and evolution. New York: Springer Science + Business Media.

Heanue T.A., Reshef R., Davis R.J., Mardon G., Oliver G., Tomarev S., Lassar A.B., Tabin C.J. 1999. Synergistic regulation of vertebrate muscle development by *Dach2*, *Eya2* and *Six1*, homologs of genes required for *Drosophila* eye formation. *Genes Dev.* 13: 3231-3243.

Holland L.Z. 2009. Chordate roots of the vertebrate nervous system: expanding

the molecular toolkit. *Nat. Rev. Neurosci.* 10: 736-746.

Holland P.W, Garcia-Fernàndez J., Williams N.A., Sidow A. 1994. Gene duplications and the origins of vertebrate development. *Dev. Suppl.* 125-133.

Jeffery W.R., Strickler A.G., Yamamoto Y. 2004. Migratory neural crest-like cells form body pigmentation in a urochordate embryo. *Nature* 431: 696-699.

Jeffery W.R., Chiba T., Krajka F.R., Deyts C., Satoh N., Joly J.S. 2008. Trunk lateral cells are neural crest-like cells in the ascidian *Ciona intestinalis*: insights into the ancestry and evolution of the neural crest. *Dev. Biol.* 324: 152-160.

Katz M.J. 1983. Comparative anatomy of the tunicate tadpole, *Ciona intestinalis*. *Biol. Bull.* 164: 1–27.

Kozmik Z., Holland N.D., Kreslova J., Oliveri D., Schubert M., Jonasova K., Holland L.Z., Pestarino M., Benes V., Candiani S. 2007. *Pax-Six-Eya-Dach* network during amphioxus development: conservation *in vitro* but context specificity *in vivo*. *Dev. Biol.* 306: 143-159.

Manni L., Burighel P. 2006. Common and divergent pathways in alternative developmental processes of ascidians. *Bioessays* 28: 902-912.

Manni L., Lane N.J., Joly J.S., Gasparini F., Tiozzo S., Caicci F., Zaniolo G., Burighel P. 2004. Neurogenic and non-neurogenic placodes in ascidians. *J. Exp. Zool. B Mol. Dev. Evol.* 302: 483-504.

Manni L., Agnoletto A., Zaniolo G., Burighel P. 2005. Stomodeal and neurohypophysial placodes in *Ciona intestinalis*: insights into the origin of the pituitary gland. *J. Exp. Zool. B Mol. Dev. Evol.* 304: 324-339.

Manni L., Zaniolo G., Cima F., Burighel P., Ballarin L. 2007. *Botryllus schlosseri*: a model ascidian for the study of asexual reproduction. *Dev. Dyn.* 236: 335-352.

Mazet F., Hutt J.A., Milloz J., Millard J., Graham A., Shimeld S.M. 2005. Molecular evidence from *Ciona intestinalis* for the evolutionary origin of vertebrate sensory placodes. *Dev. Biol.* 282: 494-508.

Meedel T.H., Hastings K.E. 1993. Striated muscle-type tropomyosin in a chordate smooth muscle, ascidian body-wall muscle. *J. Biol. Chem.* 268: 6755-6764.

Meulemans D., Bronner-Fraser M. 2004. Gene-regulatory interactions in neural crest evolution and development. *Dev. Cell.* 7: 291-299.

Morales A.V., Barbas J.A., Nieto M.A. 2005. How to become neural crest: from segregation to delamination. *Semin. Cell. Dev. Biol.* 16: 655-662.

Nevitt G., Gilly W.F. 1986. Morphological and physiological properties of non-striated muscle from the tunicate, *Ciona intestinalis*: parallels with vertebrate skeletal muscle. *Tissue Cell.* 1986, 18:341-360.

Nicol D., Meinertzhagen I.A. 1991. Cell counts and maps in the larval central nervous system of the ascidian *Ciona intestinalis* (L.). *J. Comp. Neurol.* 309: 415-429.

Northcutt R.G., Gans C. 1983. The genesis of neural crest and epidermal placodes: a reinterpretation of vertebrate origins. *Q. Rev. Biol.* 58: 1-28.

Satoh N. 1994. Developmental biology of ascidians. Cambridge, New York, Melbourne: Cambridge Univ. Press.

Satoh N. 2003. The ascidian tadpole larva: comparative molecular development and genomics. *Nat. Rev. Genet.* 4: 285-295.

Schiaffino S., Burighel P., Nunzi M.G. 1974. Involution of the caudal musculature during metamorphosis in the ascidian, *Botryllus schlosseri*. *Cell. Tissue Res.* 153: 293-305.

Schiaffino S., Nunzi M.G., Burighel P. 1976. T system in ascidian muscle: organization of the sarcotubular system in the caudal muscle cells of *Botryllus schlosseri* tadpole larvae. *Tissue Cell.* 8: 101-110.

Schlosser G. 2008. Do vertebrate neural crest and cranial placodes have a common evolutionary origin? *Bioessays* 30: 659-672.

Shimeld S.M., Holland P.W. 2000. Vertebrate innovations. *Proc. Natl. Acad. Sci. U.S.A.* 97: 4449-4452.

Shinohara Y., Konishi K. 1982. Ultrastructure of the body-wall muscle of the ascidian *Halocynthia roretzi*: smooth muscle cell with multiple nuclei. *J. Exp. Zool.* 221: 137-142.

Swalla B.J., Smith A.B. 2008. Deciphering deuterostome phylogeny: molecular, morphological and palaeontological perspectives. *Philos. Trans. R. Soc. Lond. B Biol. Sci.* 363: 1557-1568.

Terakado K., Obinata T. 1987. Structure of multinucleated smooth- muscle cells of the ascidian *Halocynthia roretzi*. *Cell. Tissue Res.* 247: 85-94.

Toyota N., Obinata T., Terakado K. 1979. Isolation of troponin-tropomyosin-containing thin filaments from ascidian smooth muscle. *Comp. Biochem. Physiol*. 62B: 433-441.

CONFERENCES

Caicci F., Zaniolo G., Burighel P., **Degasperi V.**, Gasparini F., Manni L. 2009. Differenziamento delle papille e dei neuroni sensoriali rostrali nella larva di un'ascidia. *70° Congresso Nazionale dell'Unione Zoologica Italiana (UZI)*. Rapallo, 21-24 Settembre.

Gasparini F., **Degasperi V.**, Ruffoni E., Burighel P., Manni L. 2009. Characterization of a MuSashI-like transcript in a colonial chordate, phylogenetic analysis of the protein group and differential expression patterns in sexual versus asexual development. *12th Congress of the European Society for Evolutionary Biology (ESEB)*, Torino, 24-29 August.

Degasperi V., Shimeld S.M., Gasparini F., Manni L, Burighel P. 2009. Gene expression during body muscle differentiation in the colonial ascidian *Botryllus schlosseri*. *5th International Tunicate Meeting*, Okinawa (Japan), 21-25 June.

Caicci F., Zaniolo G., **Degasperi V.**, Gasparini F., Burighel P., Manni L. 2009. Differentiation of rostral sensory neurons in the larva of the ascidia *Botryllus schlosseri*. *5th International Tunicate Meeting*, Okinawa (Japan), 21-25 June.

Degasperi V., Shimeld S.M., Gasparini F., Manni L., Burighel P. 2009. Gene expression during body muscle differentiation in ascidian (Tunicata) and the evolution of muscle in chordates. *PhD and Post-Doc Day*, Padova, 3 Aprile.

Gasparini F., Shimeld S.M., **Degasperi V.**, Manni L., Zaniolo G., Caicci F., Burighel P. 2008. Alternative development pathways in ascidians and aspect of chordate evolution. *1st International Congress on Invertebrate Morphology,* Copenhagen (Denmark), 17–21 August.

Degasperi V., Shimeld S.M., Gasparini F., Manni L., Burighel P. 2008. Gene expression during body muscle differentiation in ascidians (Tunicata) and the evolution of muscle in chordates. *Euro Evo Devo,* Ghent (Belgium), 29 July – 1 August.

Degasperi V., Gasparini F., Manni L., Burighel P. 2008. The adult musculature in *Botryllus schlosseri*: differentiation and gene expression. *II Incontro degli Ascidiologi Italiani,* Palermo (Italia), 30 Giugno – 1 Luglio.

Gasparini F., Burighel P., **Degasperi V.**, Manni L., Franchi N., Ballarin L. 2008. MGE contribution to the colonial ascidian *B. schlosseri* genomic studies: insight into immunobiology and muscle development. *Marine Genomics Europe Final General Assembly,* Faro (Portugal), 13–16 May.

Burighel P., Caicci F., Zaniolo G., Gasparini F., **Degasperi V.**, Manni L. 2007. Does hair cell differentiation predate the Vertebrate appearance? *5th European Conference on Comparative Neurobiology,* Paris (France), 25–28 April.

Caicci F., Manni L., **Degasperi V.**, Zaniolo G., Gasparini F. 2007. La comparsa delle cellule capellute precede l'origine dei vertebrati? *68° Congresso UZI,* Lecce, 24–27 Settembre.

Manni L., Caicci F., Gasparini F., **Degasperi V.**, Zaniolo G., Burighel P. 2007. Chordate mechanoreceptors and origin of vertebrate hair cells. *8th International Congress of Vertebrate Morphology,* Paris, 16–21 July.

Manni L., Zaniolo G., Ballarin L., Cima F., **Degasperi V.**, Caicci F., Gasparini F., Burighel P. 2007. The colonial ascidian *Botryllus schlosseri*, model for developmental and evolutionary studies. *4th International Tunicate Meeting,* Villefranche-sur-Mer, 23–27 June.

COURSES AND PERIODS IN OTHER LABORATORIES

University of Oxford. 2009. Visitor in the laboratory of Evolution and Developmental

Mechanisms (Department of Zoology). Supervisor: Dr. Sebastian M. Shimeld. 6-19 Settembre.

MGE Summer Course - Marine Evolutionary & Ecological Genomics. 2008. Station Biologique de Roscoff (France), 16–27 June.

Selfish Genes and Individual Fitness Course. PhD School in Biosciences, University of Padova, Italy.

Scientific English Course. PhD School in Biosciences, University of Padova, Italy.

Critical Reading. PhD School in Biosciences, University of Padova, Italy

Electronic Microscopy Course. PhD School in Biosciences, University of Padova, Italy.

MGE Training Course - Bioinformatics III. 2007. Advanced bioinformatics for analyzing eukaryotic genomes. Ghent University (Belgium), 7–11 May.

DIDACTIC

Co-tutor:

- Antonio A. Socci, Corso di Laurea in Biologia (A.A. 2008-2009), Università degli Studi di Padova: "Espressione del gene *FoxI* in *Botryllus schlosseri*".
- Eleonora Vianello, Corso di Laurea in Biologia (A.A. 2008-2009), Università degli Studi di Padova: "Analisi dell'espressione di un gene placodale in *Botryllus schlosseri*".
- Cecilia A. Brunello, Corso di Laurea in Biologia (A.A. 2008-2009), Università degli Studi di Padova: "Reazione di immunoistochimica sul fosfoistone H3 in zebrafish".
- Diletta Trojan, Corso di Laurea in Biologia (A.A. 2008-2009), Università degli Studi di Padova: "Evidenziazione tramite l'immunoistochimica del fosfoistone H3 in zebrafish".

Co-relatore:

- Chiara Sinigaglia, Corso di Laurea Specialistica in Biologia Evoluzionistica (A.A. 2007–2008), Università degli Studi di Padova: "Citodifferenziamento del muscolo in un'ascidia coloniale: aspetti molecolari e considerazioni evolutive".

Didattica di supporto:

- "Biologia dello sviluppo" della Laurea in Biologia, Università degli Studi di Padova, Ottobre – Dicembre 2008 e 2009, 25 ore.
- "Biologia dello sviluppo" della Laurea Magistrale in Scienze della Natura, Università degli Studi di Padova, Ottobre – Dicembre 2006-2009, 25 ore.
- "Organizzazione e diversità degli animali 2" della Laurea in Biologia, Università degli Studi di Padova, Febbriaio – Marzo 2007, 25 ore.